The role of endocytosis for pathogenic development of the corn smut fungus *Ustilago maydis*

Dissertation

zur

Erlangung des Doktorgrades

der Naturwissenschaften

(Dr. rer. nat.)

dem Fachbereich Biologie
der Philipps Universität Marburg
vorgelegt von

Uta Fuchs
aus Radebeul

Marburg / Lahn 2006

Vom Fachbereich Biologie der Philipps Universität Marburg als Dissertation angenommen am 25. 8. 2006.

Erstgutachter: Prof. Dr. Gero Steinberg

Zweitgutachter: Prof. Dr. Michael Bölker

Tag der mündlichen Prüfung 1. 9. 2006

The research pertaining this thesis was carried out from October 2003 until June 2006 at the Department of Organismic Interactions at the Max-Planck-Institute for Terrestrial Microbiology Marburg, Germany, under supervision of Prof. Dr. Gero Steinberg.

Parts of this thesis are published in:

Fuchs, U., and Steinberg, G. (2005). Endocytosis in the plant-pathogenic fungus *Ustilago maydis*. Protoplasma *226*, 75-80.

Fuchs, U., Hause, G., Schuchardt, I. and G. Steinberg (2006): Endocytosis is essential for pathogenic development in the corn smut fungus *Ustilago maydis*. Plant Cell 18 (8) 2066-2081.

Erklärung

Ich versichere, dass ich meine Dissertation mit dem Titel ”The role of endocytosis for pathogenic development of the corn smut fungus *Ustilago maydis*“ selbständig, ohne unerlaubte Hilfe angefertigt und mich dabei keiner anderen als der von mir ausdrücklich bezeichneten Quellen und Hilfen bedient habe.

Diese Dissertation wurde in der jetzigen oder einer ähnlichen Form noch bei keiner anderen Hochschule eingereicht und hat noch keinen sonstigen Prüfungszwecken gedient.

_____	_____
Ort, Datum	Uta Fuchs

Summary

It has long been established that fungal growth and pathogenic development are supported by exocytosis. However, the role of endocytosis during these growth processes has not been elucidated yet. It was the aim of the present study to use the temperature-sensitive mutant of the endocytic t-SNARE Yup1, to analyse the importance of endocytosis for fungal growth and pathogenic development in *Ustilago maydis*.

U. maydis is a basidiomycete fungus that infects maize plants and causes the formation of tumors in the corncob and other parts of the plant. Pathogenic development is initiated by pheromone recognition of compatible haploid partner cells. *Yup1*^{ts} cells are defective in pheromone recognition and do not initiate the subsequent mating reaction. Key player for pheromone recognition is the G-protein coupled pheromone receptor Pra1. In the absence of pheromone, biologically active Pra1-GFP is constitutively endocytosed from the plasma membrane and degraded in the vacuole. After pheromone ligand binding, growth of conjugation hyphae is initiated and Pra1-GFP localises to the tip of conjugation hyphae while in *yup1*^{ts} cells, Pra1-GFP accumulates in small endocytic vesicles, which are no longer able to fuse with early endosomes.

These findings suggest a role for Yup1 on early endosomes at the intersection of incoming endocytic vesicles and the degradation pathway as well as a putative recycling pathway. Therefore recycling and degradation of Pra1 are inhibited in *yup1*^{ts} cells. In an independent experiment it was found that wild-type Pra1-GFP is recycled. Thus it is thought that Pra1-GFP is depleted from the plasma membrane due to malfunction of Yup1. The recycling deficiency of Pra1-GFP in *yup1*^{ts} results in the defect in pheromone perception. Interestingly, increased expression of Pra1-GFP can rescue this perception defect.

However, even the restored partner recognition could not resolve the subsequent mating defects identified for cell-cell fusion, while filamentous growth, formation of appressoria and plant infection which follow cell-cell fusion, are only affected to a small extend. Interestingly, the tumors that are formed in the maize plant after *Ustilago*

infection are empty, indicating a lack of teliospore formation in the absence of *yup1*-mediated endocytosis. Independently, germination of teliospores is reduced and the promycelium shows morphological alterations in *yup1*^{ts} cells. Endocytosed cargos responsible for these phenotypes have not been determined so far. First indications point to an involvement of chitin synthases. One of their representatives, the myosin chitin synthase 1 (Mcs1) was shown to be endocytosed in a *yup1*-mediated fashion.

The presented results are supported by the analysis of the *U. maydis* genome, which reveals the presence of components commonly discussed to mediate endocytosis. Taken together the results clearly proof the existence and the importance of endocytosis for growth and virulence in the filamentous fungus *U. maydis*.

Zusammenfassung

Das Wachstum und die pathogene Entwicklung von Pilzen werden durch Exozytose unterstützt während die Rolle der Endozytose für diese Vorgänge weitgehend unbekannt ist. Ziel der vorliegenden Arbeit war es, mit Hilfe der temperatursensitiven endozytotischen t-SNARE Mutante Yup1, den Einfluss von Endozytose auf pilzliches Wachstum und Pathogenität in *Ustilago maydis* zu untersuchen.

U. maydis, ein Vertreter der Gruppe der Basidiomyceten, ist der Erreger des Maisbeulenbrandes. Die pathogene Entwicklung des Pilzes wird eingeleitet, wenn zwei kompatible haploide Zellen aufeinandertreffen und sich über einen Pheromon-erkennungsmechanismus wahrnehmen. Zellen der *Yup1*^{ts} Mutante sind nicht in der Lage den Partner zu finden und eine Paarungsreaktion zu vollziehen. Der G-Protein gekoppelte Pheromonrezeptor Pra1 ist eine der Schlüsselkomponenten für diesen Vorgang. Es wurde gefunden, dass biologisch aktives Pra1, fusioniert mit dem grünfluoreszierenden Protein GFP (Pra1-GFP), in der Abwesenheit von Pheromon konstitutiv von der Plasmamembran endozytiert und in der Vakuole degradiert wird. Nachdem Pheromon als Ligand von Pra1-Rezeptor gebunden wurde, bilden sich Konjugationshyphen an deren Spitze Pra1-GFP lokalisiert. In *yup1*^{ts} Zellen akkumuliert Pra1-GFP in primär-endozytotischen Vesikeln, welche nicht länger dazu in der Lage sind, mit frühen Endosomen zu fusionieren.

Diese Ergebnisse legen nahe, dass Yup1 eine Funktion an frühen Endosomen besitzt, die die Schnittstelle zwischen den hereinkommenden primär-endozytotischen Vesikeln und dem Abbauweg sowie einem möglichen Weg der Molekül- Wiederverwertung der Zelle bildet. Sowohl die Wiederverwertung als auch der Abbau von Pra1-GFP sind deshalb in *yup1*^{ts} Zellen nicht funktional. In einem unabhängigen Experiment konnte nachgewiesen werden, dass Pra1 unter natürlichen Bedingungen wiederverwertet wird. Es wird deshalb angenommen, dass Pra1-GFP durch die gestörte Funktion von Yup1 von der Plasmamembran dezimiert wird. Ein Defekt in der Pra1 Wiederverwertung ist schließlich sehr wahrscheinlich dafür verantwortlich, dass *yup1*^{ts} Zellen kein Pheromon perzipieren können. Interessanter Weise kann eine Überexpression von Pra1-GFP diesen Defekt wiederausgleichen.

Die wiederhergestellte Partnererkennung ist jedoch nicht ausreichend, um Defekte zu überbrücken, die während der nachfolgenden Paarungsreaktion in der Abwesenheit von Endozytose auftreten. Während dessen sind das filamentöse Wachstum, die Bildung von Appressorien and die Pflanzeninfektion, die sich an die Zell-Zellfusion anschließen, in der *yup1*^{ts} Mutante nur zu einem kleinen Teil beeinträchtigt. Die Gallen, die nach der Pilzinfektion mit *yup1*^{ts} Zellen von der Maispflanze gebildet werden, enthalten allerdings keine Teliosporen. Unabhängig davon ist die Auskeimung der Teliosporen verringert und das sich bildende Promyzel zeigt morphologische Defekte. Mögliche Komponenten, die für diese Phänotypen verantwortlich sind, wurden noch nicht identifiziert. Es gibt jedoch Hinweise darauf, dass Chitinsynthasen involviert sind. Für einen Vertreter dieser Gruppe, die Myosin-Chitinsynthase 1 (Mcs1), konnte eine *yup1*- abhängige Endozytose nachgewiesen werden.

Die vorgestellten Resultate werden durch *U. maydis* Genomanalysen unterstützt. Sie zeigen, dass allgemein bekannte Proteine des Endozytoseapparates vorhanden sind, Zusammengefasst weisen die Ergebnisse dieser Arbeit darauf hin, dass Endozytose in Pilzen existiert und eine große Relevanz für das Wachstum und die pathogene Entwicklung des filamentösen Pilzes *U. maydis* hat.

Glossary

a2 (mfa2)	*Ustilago* mating pheromone mfa2
Aa	amino acids
α -Tub	alpha tubulin
Amp	ampicillin
a. u.	arbitrary units
ble^R	phleomycin-resistance cassette
bp	base pair
cbx-Locus	gene locus of the Iron-Sulphur subunit of the Succinate-dehydrogenase from *Ustilago maydis*
cbx^R	carboxin-resistance cassette
CM	complete medium
C-terminal	carboxy-terminal
ddH_2O	doubled distilled water
DIC	Differential Interference Contrast
DMSO	Dimethylsulfoxide
DNA	deoxyribonucleic acid
dNTP	deoxyribonucleotide
dpi	days post infection
EDTA	Ethylendiamintetraacetic acid
EE	early endosome
eGFP	enhanced green fluorescent protein
EGTA	Ethylene-bis(oxyethylenenitrilo)tetraacetic acid
EtOH	Ethanol
f. c.	final concentration
GFP	green fluorescent protein
GTP	guanosine 5´-triphosphate
h	hour
hyg^R	Hygromycin-resistance cassette
kDa	Kilo Dalton
Lat A	Latrunculin A (Actin-inhibitor)
LE	Late Endosome
mA	milliampere
Mcs1 (*mcs1*)	Myosin chitin synthase 1 of *Ustilago maydis*
Mfa1 (a1)	mating factor encoded by the a1 allele of *Ustilago maydis*
Mfa2 (a2)	mating factor encoded by the a2 allele of *Ustilago maydis*
min	minute
ml	milliliter
mM	milimolar
MT	microtubule
nat^R	Nourseothricin-resistance cassette
nt	nucleotide
N-terminal	amino-terminal

OD	optical density
ON	over night
otef-Promoter	promoter of the translation elongation factor 1 of *U. maydis*
ORF	open reading frame
PCR	Polymerase-Chain Reaction
PEV	primary endocytic vesicles
PIPES	Piperazin-N-N'-bis-(2-ethansulfonat)
Pra1	pheromone receptor encoded by the a1 allele of *Ustilago maydis*
Pra2	pheromone receptor encoded by the a2 allele of *Ustilago maydis*
RFP	red fluorescent protein
RT	room temperature
sec	second
SNARE	soluble *N*-ethylmaleimide-sensitive factor (NSF) accessory protein receptor
t-SNARE	SNARE of the target membrane
UARS	*Ustilago maydis* autonomously replicating sequence
µl	microliter
µm	micrometer
rpm	rotation per minute
URA	uracil
UTR	untranslated Region
vec	vector
wt	wildtype
w/v	weight per volume
Vam7	Vacuolar morphogenesis gene 7 of *Saccharomyces cerevisiae*
WGA	wheat germ agglutinin
Yup1	early endosomal t-SNARE 1 of *Ustilago maydis*
$yup1^{ts}$	temperature-sensitive allele of the endosomal t-SNARE Yup1

Table of content

1 Introduction

Endocytosis is a cellular process that allows the eukaryotic cell to take up extra-cellular compounds and to internalise plasma membrane components and receptor-associated ligands. Primarily, endocytosis provides the means to maintain cellular homeostasis by recovery of protein and lipid components, which have been inserted into the plasma membrane by secretion. Furthermore, activities that involve the transmission of metabolic and proliferative signals, the uptake of nutrients and the regulated interaction with the surrounding environment are facilitated by endocytosis (Mellman, 1996).

1.1 Receptor mediated endocytosis

There are several mechanisms for internalisation of molecules and their delivery to various intracellular destinations. One very well understood endocytic process is the receptor-mediated ligand endocytosis, a process that is largely analogous between animal systems and the well-studied yeast model *Saccharomyces cerevisiae* (reviewed in Geli and Riezman, 1998).

In general two distinct modes of receptor-mediated endocytosis are known: a ligand-independent, constitutive uptake mode as well as a ligand-dependent mode. The trans-membrane bound G-protein coupled pheromone receptors Ste2p and Ste3p of *S. cerevisiae* have been studied as an example of these two processes. Here, constitutive endocytosis is rapid and the receptors are directly delivered to the vacuole after a short surface residency (Davis et al., 1993; Roth and Davis, 1996; Roth et al., 1998; Roth and Davis, 2000). During constitutive pheromone receptor endocytosis receptor internalisation is triggered by ubiquitin, which is added to the surface localised receptor and serves as internalisation signal (Roth and Davis, 1996; Roth et al., 1998; Roth and Davis, 2000). Ligand-induced pheromone receptor endocytosis on the other hand takes place after binding of the yeast mating pheromone. A specific internalisation signal encoded by the receptor, is exposed after ligand binding and subsequently induces receptor-ligand internalisation (Chen and Davis, 2000). In higher

eukaryotic systems especially the ligand-induced mode of receptor endocytosis is described. Prominent examples for this mode are the epidermal growth factor receptor (EGFR), the low density lipoprotein receptor (LDLR) and the transferrin receptor (summarized in Mellman, 1996).

In both the ligand-independent and the ligand-dependent endocytic pathway, internalisation of the receptor alone or the receptor-ligand complexes occurs by their clustering into specific plasma membrane domains (Anderson et al., 1977; Goldstein et al., 1979; Maxfield and McGraw, 2004). One such membrane domain are eisosomes that have been described very recently as static sites of endocytosis in *S. cerevisiae* (Walther et al., 2006). Following the clustering, internalisation of the components requires the interplay between a large number of different proteins (summarized in D'Hondt et al., 2000). The initial steps of endocytosis are actin dependent and result in budding of most often clathrin-coated, membrane bound vesicles (= primary endocytic vesicles, PEV) into the cytoplasm (Kaksonen et al., 2003; Huckaba et al., 2004; Lakadamyali et al., 2006; Toshima et al., 2006). The vesicles, which contain the receptor complexes, subsequently loose their clathrin coat (Bonifacino and Lippincott-Schwartz, 2003) and become part of the endosomal pathway by fusion with each other and with the early endosomes (EE). In the mammalian system, EE form a sorting compartment that contains two populations of organelles with distinct mobility and maturation kinetics: (1) the sorting endosomes and (2) the endocytic recycling compartment (Sheff et al., 1999; Lakadamyali et al., 2006). They represent the first intersection between the recycling and the degradative pathways and mediate appropriate targeting of molecules (Fig. 1). However, in the yeast model, early endosomes have not been distinguished into a sorting and a recycling compartment (Prescianotto-Baschong and Riezman, 1998; Mulholland et al., 1999; Pelham, 2002).

Ligands dissociate from their receptors due to the acidic environment of the sorting endosome (Mukherjee et al., 1997). As a consequence of sorting endosome maturation, the ligands and a subset of membrane proteins migrate to multivesicular bodies and subsequently turn to become late endosomes (LE) (Katzmann et al., 2002). They are finally converted to lysosomes/vacuoles by their fusion with hydrolase-bearing transport vesicles from the trans Golgi network (Geuze et al., 1985; Geuze et al., 1988). Proteins, such as a chimeric form of furin, can also directly cycle form the

plasma membrane via late endosomes to the Golgi and back to the plasma membrane (Mallet and Maxfield, 1999).

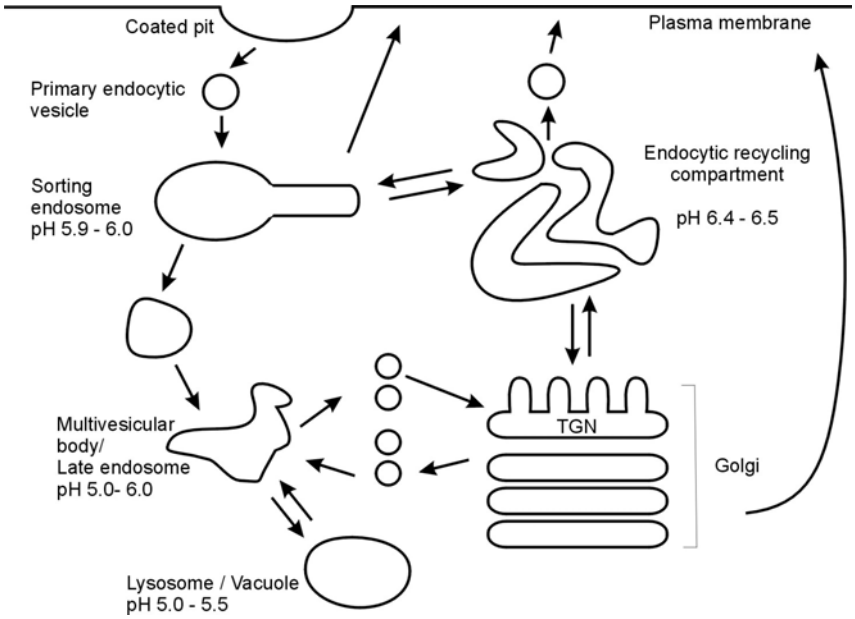

Figure 1. Endocytosis and endocytic recycling pathways in higher eukaryotes.

Routes taken by the endocytosed cargo are delineated by arrows, detailed information on the pathways are given in the text. The illustration was modified from Maxfield and McGraw, 2004).

In higher eukaryotic systems, the transport of the different organelles in the endocytic pathway depends on the microtubule cytoskeleton (Aniento et al., 1993), (Lakadamyali et al., 2006). The delivery of membrane proteins to late endosomes requires specific targeting information such as ubiquitylation. This has been described for signalling receptors and additionally represents a way to terminate signalling and to make the cells unresponsive to the specific stimulus (Katzmann et al., 2002). This overall pathway describes the main routes of molecules, but it needs to be noted that sorting mechanisms are not 100% efficient and that all compartments are dynamic which means that no molecules will be permanently resident of a compartment (Maxfield and McGraw, 2004).

1.2 Endocytic receptor recycling

While ligands are degraded in the lysosome/vacuole, receptors dissociate from their ligand and can directly be routed back to the plasma membrane or delivered to the long-lived, microtubule-dependent endocytic recycling compartment before their return to the plasma membrane (Hopkins, 1983; Yamashiro et al., 1984). It is thought that such a recycling of components is essential to maintain the proper composition of various organelles and for the return of molecules with essential functions at the appropriate compartments. In addition, recycling of receptors allows the receptor protein to participate in multiple rounds of ligand binding and internalisation (Ciechanover et al., 1983; Goldstein et al., 1985). Recycling may also be used for resensitation, in case of the β_2-adrenergic receptor, uncoupling of the heterotrimeric G protein, dephosphorylation and subsequent return to the plasma membrane restore the original responsiveness of the receptor (von Zastrow and Kobilka, 1992).

It has been suggested that the mode of receptor recycling seems to be a default route. Unless the receptor bears a cytoplasmic signal that directs its sorting to LE, it is returned to the plasma membrane via the endosomal recycling compartment. Recycling receptors concentrate in specific domains of sorting endosomes suggesting for the interaction of a specific sorting signal with an endosome-associated adaptor complex (Geuze et al., 1987). Alternatively, the recycling tubules represent domains that concentrate the receptor in an adaptor independent fashion (summarized by Mellman, 1996). Some receptors like the epidermal growth factor receptor await a mixed outcome with some of the receptor being reused and some being degraded in the lysosome (Jiansong Xie, 2004).

1.3 Regulation and specificity of endocytosis

Several groups of proteins are required to confer specificity and regulation during endocytic sorting and membrane trafficking. **S**oluble ***N***-ethylmaleimide-sensitive factor (NSF) **a**ccessory protein **re**ceptors [SNAREs] play a crucial role in intracellular membrane fusion (Rothman, 1994). They are related membrane-anchored proteins that contain a coiled-coiled domain the so-called “SNARE” motif. The SNARE motif becomes part of a four helix bundle formed by SNAREs of the **v**esicle (= v-SNARE)

and the **t**arget (= t-SNARE) membranes. This interaction is thought to draw the membranes into close apposition and initiate membrane fusion (Sutton et al., 1998; Jahn and Sudhof, 1999).

The majority of membrane-traffic components in the endocytic pathway recognize the correct organelle by binding to either specific lipids, such as phosphoinositides, or to activated forms of RabGTPases (summarized by Behnia and Munro, 2005). Both lipids and GTPases provide each organelle with a unique identity that will be recognized by the many proteins that act on its cytosolic surface. Most important among the lipids are the phosphoinositides. They are forms of phosphatidylinositol (PtdIns) with phosphate attached by specific kinases to the 3,4 or 5 positions of the inositol ring (summarized by Niggli, 2005). PtdIns(3)P, for example, is present on EE and is recognized by a broad range of peripheral membrane proteins with a FYVE or Phox (PX) domain (Ellson et al., 2002; Stenmark et al., 2002; Gillooly et al., 2003).

RabGTPases are key regulators of endocytic vesicle generation and vesicle transport between different sub-cellular compartments in the eukaryotic cell. They mediate vesicle budding from the donor membrane, movement to as well as tethering and docking with the acceptor membrane and subsequent fusion of the two vesicle membranes. RabGTPases cycle between an inactive GDP bound and an active GTP bound form (Vetter and Wittinghofer, 2001). One of the endocytic Rab proteins, Rab5, mediates fusion and fission of early endosomes (Bucci et al., 1992) as well as their transport along microtubules (Nielsen et al., 1999) Two other Rab proteins, Rab4 and Rab11, are responsible for the regulation of endocytic recycling from the sorting endosome and the endocytic recycling compartment, respectively (Van Der Sluijs et al., 1991; Mohrmann and van der Sluijs, 1999; Sönnichsen et al., 2000; Wilcke et al., 2000). Rab7 specifically locates to late endosomes (Rink et al., 2005) while Rab9 mediates transport from LE to the Golgi (Lombardi et al., 1993; Riederer et al., 1994).

1.4 Endocytosis in filamentous fungi

As described above, endocytosis is a common cellular pathway among eukaryotes with conserved mechanisms between mammalian systems and the fungal yeast model *S. cerevisiae* (Geli and Riezman, 1998). Despite the great importance of filamentous fungi and structural similarities to higher mammalian systems such as the neuron, the

existence of endocytosis in this group of organisms has long been a matter of debate (Read and Kalkman, 2003).

Filamentous fungi are widespread and ancient species that include symbiontic and benefical species as well as animal and plant parasites. They invade substrates, including the host tissue, by directed invasive growth. Fungal hyphae expand at their apex which is similar to tip-growing plant cells, such as pollen tubes or root hairs (Geitmann and Emons, 2000; Hepler et al., 2001). This filamentous growth is supported by polarized exocytosis at the hyphal tip (Gow, 1995a). An accumulation of membranous organelles, the so-called Spitzenkörper (Reinhard, 1892; Girbardt, 1957) that might consist of secretory vesicles (Bartnicki-Garcia et al., 1995) is present at the growth region. However, hyphal tips can expand at rates up to 18.5 µm min^{-1} (Carlile and Watkinson, 1994) and it has long been speculated that this rapid polarized growth requires the endocytic uptake and recycling of wall-components, such as synthetic enzymes (Wessels, 1986).

The first indications for endocytosis in filamentous fungi came from the work of Hoffmann and Mendgen (1998) and Steinberg and co-workers (Steinberg et al., 1998), who could demonstrate that the endocytic marker dyes FM 4-64 and Lucifer Yellow are taken up into the plant pathogenic fungi *Uromyces fabae* and *Ustilago maydis*, respectively. Similar studies in other fungal species have suggested that endocytosis is a common process in filamentous fungi such as *Magnaporthe grisea*, *Neurospora crassa* and *Aspergillus nidulans* (Cole et al., 1998; Fischer-Parton et al., 2000; Atkinson et al., 2002; Read and Kalkman, 2003; Penalva, 2005). Contradictory to the results above, ultrastructural and lightmicroscopy techniques applied by Torralba and Heath (2002) did not reveal any indications for endocytosis in *N. crassa*. However, first genomic evidence for endocytosis was provided by studies in *U. maydis* where it could be shown that conditional mutants defective in the uptake of components into early endosomes show a heavily altered morphology (Wedlich-Söldner et al., 2000). Higuchi et al. (2006), who studied the internalisation and transport of the eGFP-fused plasma membrane bound purine transporter AoUapC in *Aspergillus oryzae*, further supported the existence of endocytosis in filamentous fungi.

In the meantime screening the published fungal genomes for homologues of proteins involved in yeast endocytosis became a powerful tool to support the existence of endocytosis in filamentous fungi. Based on numerous studies it had been suggested

that about 2 % of the *S. cerevisiae* genome consist of genes that mediate endocytosis, which again points towards the significance of this basic cellular process (D'Hondt et al., 2000). (Read and Kalkman (2003) did an extensive search for proteins involved in endocytosis in the recently published genomic sequence of *N. crassa* and concluded that essentially all important components of the endocytic machinery are present in this filamentous fungus. The advantage of a fully sequenced and accessible genome also applies to the phytopathogenic fungus *Ustilago maydis* for which a similar analysis was carried out (Fuchs and Steinberg, 2005 and see below).

1.5 The corn smut fungus *Ustilago maydis*

Ustilago maydis, a basidiomycete fungus, is a ubiquitous corn pathogen. The phytopathogenic fungus infects maize plants and causes tumor formation on the leaves, the stem and in the corncob of the plants. The tumors appear smutty and darkened due to the vast amount of black teliospores produced by the fungus, which are the infectious progeny.

During its lifecycle *U. maydis* exists in three different, morphologically distinct growth forms: (1) yeast-like, haploid sporidia (2) conjugation hyphae and (3) dikaryotic filaments that are the result of conjugation hyphae fusion (Snetselaar et al., 1996). For pathogenic development to occur two compatible haploid sporidia (such as cells with mating type *a1b1* and *a2b2*) have to recognize each other by a pheromone (mfa1/2) – pheromone receptor (Pra1/Pra2) system (Fig.2) on the plant surface (Bölker et al., 1992). In response to the mating pheromone the cells initiate a mating reaction. The mating reaction includes the signal transmission from the ligand bound pheromone receptor to components of the mitogen-activated protein kinase (MAPK) pathway (summarized by Kahmann and Kämper, 2004). The cell cycle is arrested (Garcia-Muse et al., 2003) and conjugation hyphae that grow towards the partner cell along a pheromone gradient, are formed (Spellig et al., 1994; Snetselaar et al., 1996). These conjugation hyphae fuse and as a result an infectious dikaryotic filament develops (Snetselaar et al., 1996), which is able to penetrate the maize plant on the surface. After growth and proliferation of the dikaryotic fungal mycelium within the plant, the characteristic tumors are formed. Subsequently, sporogenic hyphae that have developed within the tumor give rise to diploid teliospores. The teliospores are

released once the tumor breaks open. Teliospore germination then includes meiotic division, which originates the production of the haploid sporida (summarized in Banuett and Herskowitz, 1996).

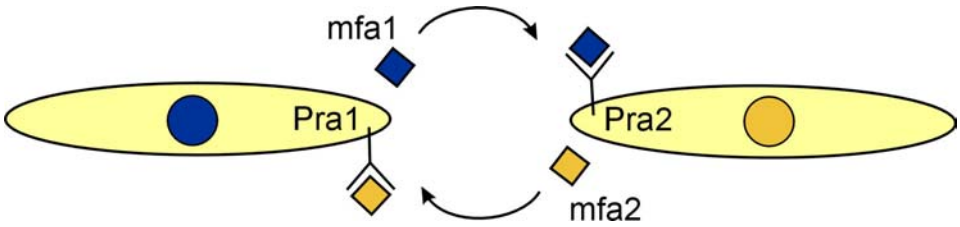

Figure 2. Pheromone-pheromone receptor recognition in *U. maydis.*

Two compatible haploid sporidia can initiate a mating reaction. The pheromone receptor Pra1 of one partner recognises the mfa2 pheromone of the other. In turn Pra2 expressed by the mating partner recognises mfa1. Subsequently, growth towards the partner is initiated and is followed by cell-cell fusion.

Over the last decades *U. maydis* became a valuable model organism for molecular biology studies in cell signalling and cell biology. Several different molecular techniques have been established for the analysis of gene function, which allows the study of essential cellular processes in this fungus (summarized by Bölker, 2001; Kahmann and Kämper, 2004). Due to a short generation time, the easy cultivation methods in axenic culture and the lifecycle of only three weeks *U. maydis* allows a thorough molecular analysis. Importantly, the different growth forms of *U. maydis* that do not require the plant environment (stages prior plant penetration) can be adequately analysed under laboratory conditions. The whole *Ustilago* genome sequence is now publicly available (http://www.broad.mit.edu/annotation/genome/ustilago_maydis/Home.html) and is currently annotated and investigated (Kämper et al., in preparation).

U. maydis has especially proven to be an excellent model for studies of the microtubule cytoskeleton. Microtubules and microtubule- dependent transport processes are essential for polar growth of *U. maydis* (Steinberg et al., 1998; Steinberg et al., 2001; Wedlich-Söldner et al., 2002). Furthermore, it could be shown that active endosome transport is mediated by the microtubule cytoskeleton and depends on the action of kinesin-3 and cytoplasmic dynein (Wedlich-Söldner et al., 2002). Additionally, it has been suggested that a dynein loading zone for retrograde endosome transport

exists at the hyphal tip of growing filaments (Lenz et al., 2006). Yup1, a t-SNARE that resides on the bidirectionally moving endosomes was determined to be responsible for membrane turnover and recycling at this growth region (Wedlich-Söldner et al., 2000).

It was the aim of the present study, to use the temperature-sensitive *yup1* mutant to further extend the knowledge about endocytosis in the filamentous fungus *U. maydis*. The main emphasis in this respect was (1) to provide further evidence for endocytosis on a molecular level, (2) to elucidate the role of endocytosis for pathogenic development of *U. maydis* and (3) to identify endocytic cargoes that are essential for growth and pathogenicity of *U. maydis*.

2 Results

2.1 Endocytosis in *Ustilago maydis*

In order to gain further evidence for endocytosis I analysed the genome of *U. maydis* for components of the endocytic machinery (Fuchs and Steinberg, 2005). I used a two-way blast search analysis for which I chose reference proteins that have been identified as requirements for endocytosis in the related yeast *S. cerevisae* (D'Hondt et al., 2000; Munn, 2000). The protein sequences were first blasted against the *U. maydis* genome and the obtained homologues were confirmed by reblasting them against the yeast genome database. The retrieved proteins are listed in Table 1. In addition, I could identify FYVE domain containing proteins that are specifically associated with EE (Table 2). For some of those proteins a closer homology existed to the appropriate human protein with which a similar blast analysis was done.

The *Ustilago* genome also encodes for small RabGTPases that are known to regulate membrane traffic within eukaryotic cells (Mohrmann and van der Sluijs, 1999). As most of the characterisation of these Rab proteins was done in mammalian systems I additionally attempted a blast search with the human (Hs) Rabs against the *Ustilago* genome (Table 1 displays Rab5 homologues of yeast proteins and Table 3 displays Rab homologues of the human proteins). Two Rab5-like proteins, which share 55% sequence identity, were identified in *U. maydis*. However, a Rab4-like protein could only be identified by blast analysis with the human Rab4 while a homologue of Rab4 was not present in *S. cerevisiae* or any other *Ascomycete*. The overall phylogenetic relation of the yeast, human and Ustilago Rab proteins is summarized in Figure 3.

The predicted *U. maydis* (Um) Rab4 shows 65% identity to HsRab4. Both proteins contain a specific C-terminal region. This region is absent from the closest yeast relative, Ypt31, implied in secretion and vesicle traffic (Jedd et al., 1997) (Figure 4). Blast search with the Rab4 specific C-terminal region of *U. maydis*, retrieved only other Rab4 proteins indicating the specificity of this region (Figure 5). Using this approach, a Rab4-like protein of *Schizosaccharomyces pombe* was identified that had less homology in the overall protein structure, which was the reason for negative results in

the earlier blast searches. However, the functional implication of the Rab4-specific region remains to be elucidated.

Table 1. Important components of the endocytic machinery in *Saccharomyces cerevisiae* (S.c.) and their homologues in *Ustilago maydis* (U.m.).

(modified and updated from Fuchs and Steinberg, 2005)

Protein	Type of protein	U. maydis protein	E-value (U.m. blast against S.c.)	E-value (S.c. blast against U.m.)
Act1p/ End7p	Actin	UM06217	2.0e-185	2.0e-185
Arp2p	actin-related protein	UM05405	1.7e-149	1.7e-149
		UM11265	1.2e-139	1.8e-45
Chc1p	Clathrin heavy chain	UM03921	0.0	0.0
Clc1p	Clathrin light chain	UM01316	1.4e-17	1.4e-17
Cmd1p	Calmodulin	UM03910	1.4e-47	1.5e-47
End3p	EH domain-containing protein	No hits		
End4/Sla2p	Talin	UM00582	1.3e-78	1.3e-78
End5p/Vrp1p	Proline-rich protein verprolin	UM10566	1.4e-21	1.7e-21
		UM10422	2.9e-20	6.1e-21
End6p/Rvs161p	BAR adaptor protein	UM05283	4.1e-66	4.2e-66
Rvs167		UM01748	1.4e-51	1.4e-51
End8p/Lcb1p	Ceramide biosynthesis	UM03515	2.1e-85	2.2e-85
End9p/Arc35p	Arp complex subunit	UM11479	1.8e-49	1.8e-49
End11p/Erg2p	ergosterol biosynthesis enzyme	UM01934	6.9e-48	7.1e-48
Ent1p	Epsin-like	UM03598	2.0e-48	2.1e-48
Ent2p	Epsin-like	UM03598	1.6e-66	1.6e-66
Inp51p	Synaptojanin-like	UM02595	3.7e-103	3.9e-103
Inp52p	Synaptojanin-like	UM02595	1.2e-161	1.3e-161
		UM06317	2.6e-38	2.6e-38
Inp53p	Synaptojanin-like	UM02595	3.9e-154	4.0e-154
Myo5p	Type I myosin	UM11115	0.0	0.0
Pan1p	EH domain-containing protein	UM11804	1.3e-40	1.4e-40
Sac6p	fimbrin	UM04768	2.6e-218	2.7e-218
Ypt51p/Vps21	Rab5-like	UM10615	3.2e-59	3.3e-59
		UM02485	4.6e-51	4.7e-51
Ypt52p	Rab5-like	UM10615	3.6e-35	3.8e-51
		UM02485	3.7e-51	3.7e-35
Ypt53p	Rab5-like	UM10615	7.7e-49	7.9e-49
		UM02485	3.7e-42	3.7e-42

Proteins with a commonly discussed role in endocytosis were selected. Both *S.c.* and *U.m* sequences were obtained from MIPS (http://mips.gsf.de/projects/fungi) and blasted against each other's database applying dual blast.

Table 2. FYVE-domain containing proteins in *U. maydis* and their homologues in *Homo sapiens* (marked by *) and *Saccharomyces cerevisiae* (marked by ¶)

(modified and updated from Fuchs and Steinberg, 2005)

name	type/function	*U. maydis* protein	E- value
Rabenosyn-5*	Rab5 effector	UM01215	1e-19
Fgd6*	GEF-protein	UM10152 (=UmDon1)	6e-18
Pkk2*	Protein kinase	UM02100	9e-20
Fab1¶	PI(3)P 5-kinase	UM10465	2e-85
Vps27¶	Vacuolar protein sorting	UM03862	6e-48

Table 3. Rab proteins in human endocytosis and their homologues in *U. maydis*

(modified and updated from Fuchs and Steinberg, 2005)

Name	Type/function	*U. maydis* protein	E- value
Rab4	GTP-binding protein	UM01735	4e-73
Rab5	GTP-binding protein	UM10615 + UM02485	2e-50/4e-62
Rab7	GTP-binding protein	UM05511	1e-27
Rab11	GTP-binding protein	UM01651	3e-85

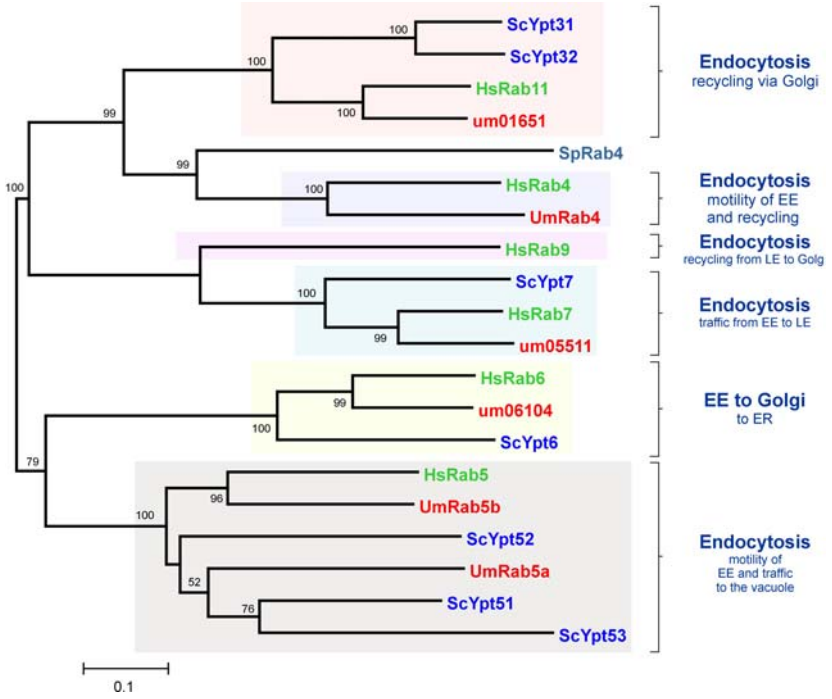

Figure 3. Phylogenetic dendrogram summarizing the relationship between Rab proteins of *S. cerevisiae, H. sapiens and U. maydis*

Protein sequences were downloaded from public databases (http://www.ncbi.nlm.nih.gov/entrez/query.fcgi) and aligned with ClustalX (Thompson et al., 1997). Phylogenetic dendrograms were constructed using the minimum evolution method (MEGA version 2.1; (Kumar et al., 2001) with a nearest neighbor joining tree as starting point and 1000 Bootstrap replicates. (Modified and updated from Fuchs and Steinberg, 2005).

Figure 4. Sequence comparison of Rab4 sequences

Protein sequences of human Rab4 (HsRab4), Rab4 of *U. maydis* (UmRab4) and the closest relative of *S. cerevisiae* Ypt31 (ScYpt31) were aligned by ClustalX (Thompson et al., 1997). The blue marked amino acids are identical among the proteins. The P-loop is the GTP binding pocket. The Rab4 specific domain was identified by sequence comparison. (Modified and updated from Fuchs and Steinberg, 2005).

Figure 5. Sequence comparison of Rab4 specifc domains

Specific C-terminal sequences of *Homo sapiens* (Hs), *Gallus gallus* (Gg), *Danio rerio* (Dr), *Drosophila melanogaster* and *Schizosaccharomyces pombe* (Sp) and *Ustilago maydis* (Um) were aligned by ClustalX (Thompson et al., 1997). The green marked amino acids resemble identical amino acids among the protein sequences.

Based on these results it is very likely that endocytosis and associated recycling pathways exist in *U. maydis*. All identified components await further characterisation for a function in endocytosis of *U. maydis*.

2.1.1 The t-SNARE Yup1 colocalises with Rab4 and Rab5

In a previous study Yup1 was identified as an early endosomal t-SNARE protein required for functional endocytosis in *Ustilago maydis* (Wedlich-Söldner et al., 2000). However, this was solely based on the use of the endocytic marker dye FM4-64 (Vida and Emr, 1995) that colocalised with Yup1-GFP on EE (Wedlich-Söldner et al., 2000).

In order to further strengthen this conclusion, three strains were generated that contained Yup1, fused to a double tag of red fluorescent protein (RFP_2) and a fusion of GFP with the previously identified early endosomal markers Rab4 or Rab5 (see above) respectively (strains $FB1G_3Rab4Yup1R_2$, $FB2GRab5aYup1R_2$ and $FB2GRab5b Yup1R_2$). In line with the previous observations, Yup1 and each Rab protein colocalised (Fig. 6 and Fig. 7). For Rab5a and Rab5b comigration with Yup1 was observed on small moving dots (Rab5a: 94.8%, n=94 Yup1-carrying endosomes, Fig. 6A lower panel; Rab5b: 82.3 %, n=96 Yup1-carrying endosomes) but not on vacuoles (Fig. 6A, arrow). Colocalisation of Yup1 and Rab4 was also observed on the vacuole (data not shown). As these GTPases are characteristic for EE these results add strong support to our conclusion that Yup1 acts on EE in *U. maydis*. The additional role of Rab4 on vacuoles cannot yet be explained and needs further elucidation.

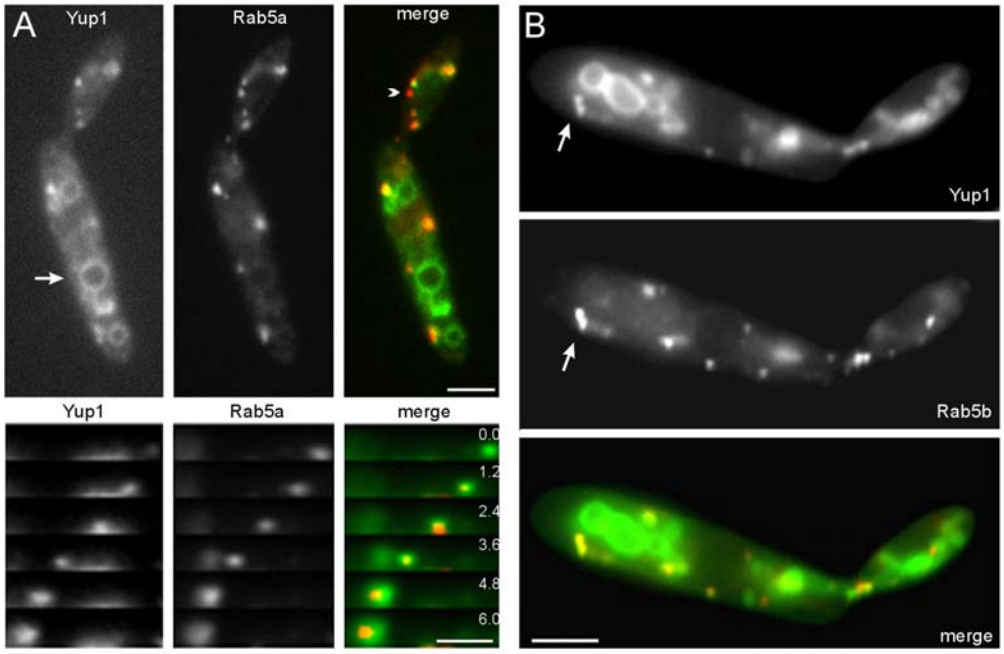

Figure 6. Colocalisation of Yup1 with Rab5a and Rab5b.

(A) Colocalisation and Co-movement (lower panel) of Yup1 (false coloured in green) with the early endosomal marker Rab5a (false coloured in red) resulting in a light yellow colour in the merged image. Arrow indicates localisation of Yup1 on the vacuole. Elapsed time is given in seconds. Bar: 3 µm (top) and 1 µm lower panel. (B) Colocalisation of Yup1 (false coloured in green) with the early endosomal marker Rab5b (false coloured in red) resulting in a yellow colour in the merged image. Arrow indicates significant colocalisation pattern. Bar: 3 µm. (Images acquired by I. Schuchardt, Figure in cooperation with G. Steinberg).

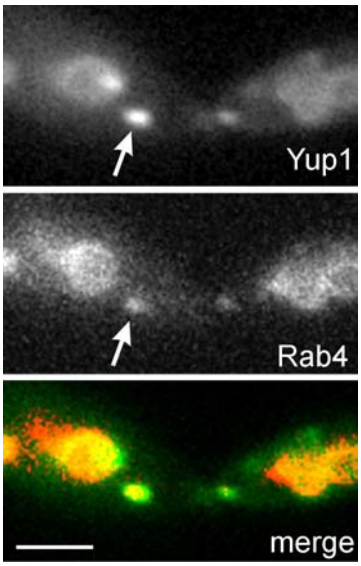

Figure 7. Colocalisation of Yup1 with Rab4

Colocalisation of Yup1 (false coloured in green) with the early endosomal marker Rab4 (false coloured in red) resulting in a light yellow colour in the merged image. Arrow indicates significant colocalisation. Bar: 2 µm (Figure in cooperation with G. Steinberg)

2.1.2 Yup1 has a function on early endosomes and vacuoles

In the course of the extended analysis of Yup1 on EE also an additional functional characterisation was attempted. It had been noted previously that Yup1 and the vacuolar t-SNARE Vam7p from *S. cerevisiae* (Wada and Anraku, 1992) share significant sequence similarity and a PX domain (Wedlich-Söldner et al., 2000). Furthermore, Yup1 also localises to the vacuolar tonoplast, which suggests a similar vacuolar function as for Vam7. To first exclude the possibility that the localisation on the tonoplast (Fig 6A, arrow) is due to an overexpression artefact of the ectopically integrated Yup1-GFP or –RFP fusion construct (Wedlich-Söldner et al., 2000) I constructed a strain which expressed the endogenous Yup1 protein fused to a double RFP tag (strain FB1Yup1R_2). However a similar localization pattern on EE and the vacuole was obtained with the endogenous construct (not shown).

To check whether Yup1 can substitute for Vam7p in homeotypic vacuolar fusion in *S. cerevisiae* (Wada and Anraku, 1992), I transformed the *vam7Δ* strain with a CEN6-plasmid containing the Yup1 gene under control of the *ura3* promoter. The resulting mutant grew slightly better (Fig. 8A; #3) compared to *vam7Δ* strain carrying the empty vector (Fig. 8A; #2), but was still reduced in growth compared to wild type transformed with empty vector (Fig. 8A, #1). Pulse chase experiments using FM4-64 in *vam7*Δ mutants and *vam7*Δ cells expressing *yup1* (Fig. 8B, "Δvam7" and "Δvam7+yup1") demonstrated that Yup1 is also able to partially rescue the defect in vacuole

fragmentation (Fig. 8B "*vam7*Δ"), which is typical for *vam7*Δ mutants (Wada and Anraku, 1992). In contrast, the *yup1*^{ts}-phenotype that results in inhibition of growth at 34°C (Wedlich-Söldner et al., 2000) could not be rescued by expression of *Vam7* (Fig. 8A; #4: wild type control with empty vector; #5: *yup1*^{ts} with empty vector; #6: *yup1*^{ts} + *VAM7*; for details see Materials and Methods).

Taken together, the t-SNARE Yup1 functions on EE as was confirmed by colocalisation with the EE-markers Rab4 and Rab5. Yup1 can complement for ScVam7 indicating additional functions in the course of the endocytic pathway.

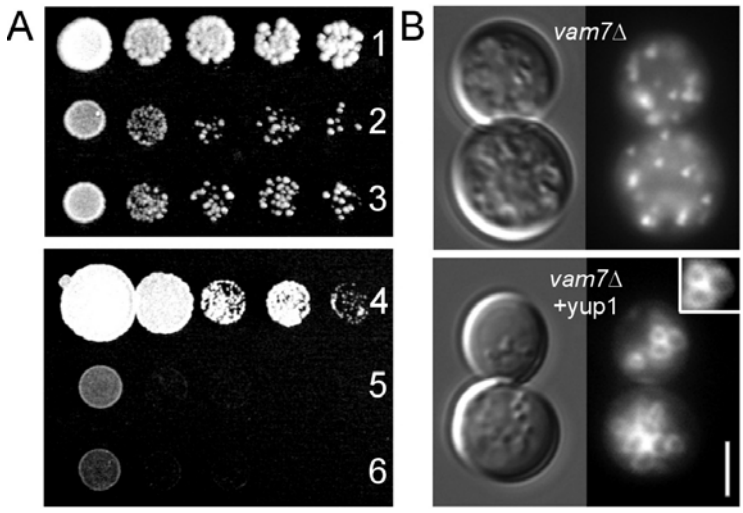

Figure 8. Functional relationship between UmYup1 and ScVam7

(A) Complementation of *S.c. vam7Δ* with Yup1. Cells were incubated at 28°C (1)-(3) and 34°C (4)-(5). (1) SEY6210+vector (2) *vam7Δ*+vector (3) *vam7Δ*+Yup1 (4) FB2+Vector (5) FB2yup1^{ts}+Vector (6) FB2yup1^{ts}+*VAM7*. (B) FM4-64 staining of *S.c. vam7Δ* and *S.c. vam7Δ* complemented with Yup1. Bar: 3 µm.

2.2 The role of endocytosis for *U. maydis* pathogenic development

After confirming the association of Yup1 with EE I used the temperature sensitive *yup1* mutant (Wedlich-Söldner et al., 2000) in order to determine the importance of endocytosis for pathogenicity. I infected 6 day old maize plants with a mixture of control strains FB1 and FB2, as well as the temperature sensitive endocytosis mutant strains FB1Yup1^{ts} and FB2Yup1^{ts}. Infected plants were incubated at both permissive temperature (22°C) and restrictive temperature (34°C), and tumor formation was monitored 14 days post infection. At 22°C infection symptoms were found at similar

rates in both wild-type and mutant infected plants (Fig.9A, “control”, 22°C;”yup1^{ts}, 22°C”; Fig. 9B). However, at restrictive conditions (34°C) *yup1*^{ts} mutant cells failed to induce symptoms, whereas almost normal infection was observed for plants infected with control strains (Fig. 9A, “control, 34°C”; “yup1^{ts}, 34°C”; Fig. 9B). Plant infection requires the formation of dikaryotic filaments, which can be monitored on charcoal containing agar plates. To further analyse the impaired virulence of *yup1*^{ts} strains, I performed these mating assays using strains FB1Yup1^{ts} and FB2Yup1^{ts}, as well as compatible control strains. At permissive temperatures both compatible control and *yup1*^{ts} cells fused to form a "fuzzy" and white colony consisting of dikaryotic filaments (Fig. 9C, upper panel). In contrast, at 34°C only the control cells formed fuzzy colonies, while *yup1*^{ts} mutants were unable to form dikaryotic hyphae (Fig. 9C, lower panel), suggesting that EE are required early in the infection process. However, a cross of a wild-type strain and a *yup1*^{ts} mutant strain was dominated by the wild-type phenotype and resulted in fuzzy filaments.

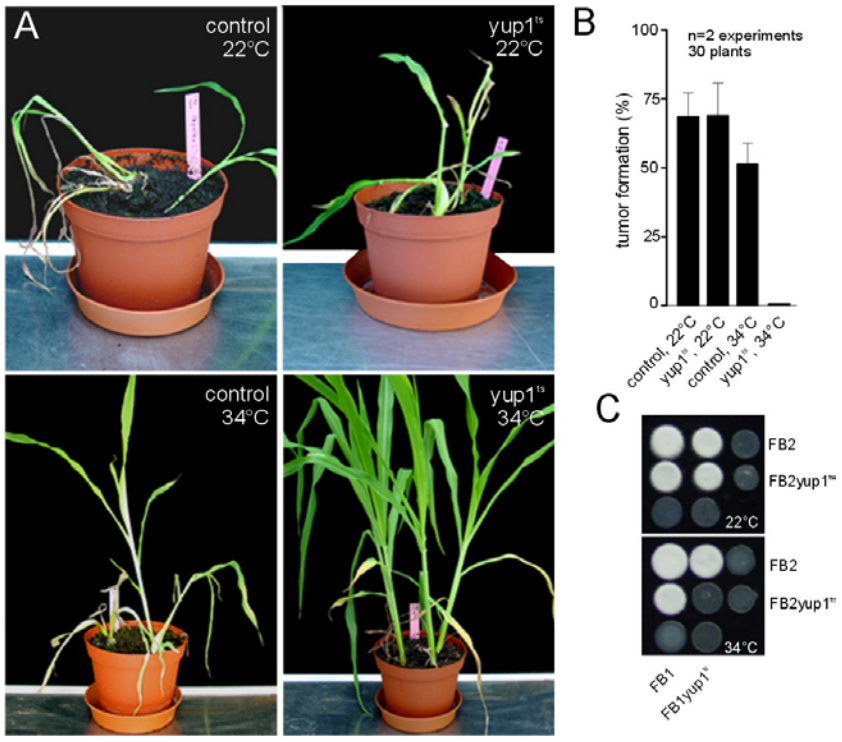

Figure 9. Characterisation of wild-type and conditional *yup1*^{ts} mutant strains in plant infection assays.

(A) Maize plants were infected with wild-type control strains and *yup1*^{ts} mutants at 22°C and 34°C and incubated for 14 days. (B) Quantification of tumor formation on infected maize plants at 22°C and 34°C. (C) Cross of control strains FB1 x FB2 and *yup1*^{ts} mutant strains FB1Yup1^{ts} x FB2Yup1^{ts} on charcoal-containing agar plates at 22°C and 34°C.

2.2.1 Pheromone perception is defective in *yup1*^{ts} mutants

As a prerequisite of mating, compatible cells have to recognize the mating partner pheromone, which triggers a signal cascade and finally leads to increased expression of their own pheromone and the formation of conjugation hyphae (Urban et al., 1996b). Our mating assays on *yup1*^{ts} mutants suggested that early endosome function is essential for the formation of dikaryotic filaments. Therefore, I tested whether growth of conjugation tubes is also mediated by this process. I mimicked the presence of a mating partner by the addition of synthetic pheromone (Spellig et al., 1994). After about 6 hours of incubation with synthetic pheromone at 22°C both wild-type and mutant cells had formed long conjugation filaments to similar extents (Fig. 10B). In the presence of pheromone conjugation hyphae were also formed in wild-type strains at 34°C (Fig. 10A, control, pheromone; 10B, control). However, pheromone did not induce the formation of conjugation hyphae in *yup1*^{ts} mutants at 34°C (Fig. 10A, 10B; pheromone, yup1^{ts}). Instead, mutant cells were thickened and showed the previously described abnormal morphology (Fig. 10A yup1^{ts}, phermone; Wedlich-Söldner et al., 2000). This raised the possibility that the absence of mating hyphae in *yup1*^{ts} mutants is due to a morphological defect.

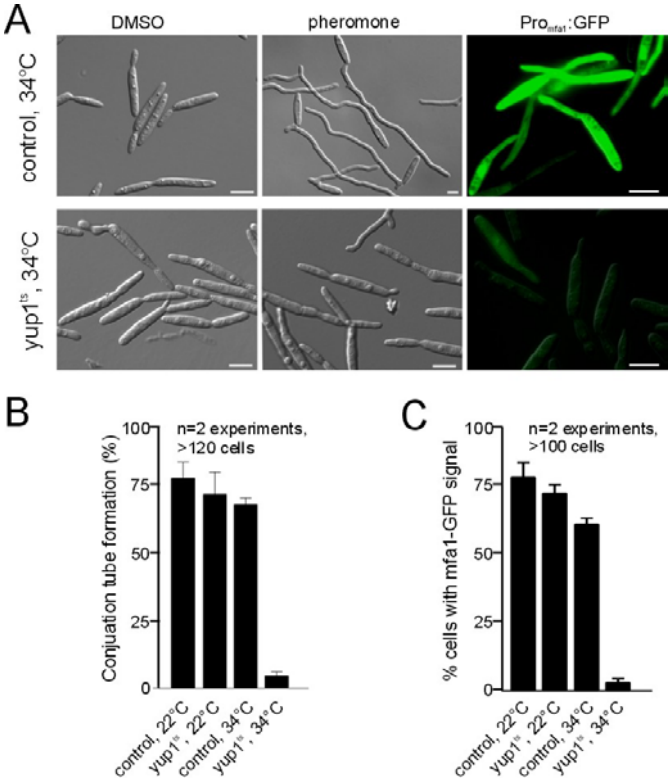

Figure 10. Formation of conjugation hyphae

(A) Filamentous growth and formation of conjugation hyphae was induced in strain FB1 and in FB1Yup1^{ts} at 34°C for at least 6 hours. DMSO was used as solvent control. Pheromone perception was visualized using the *mfa1* Promoter –GFP fusion construct as a reporter at 34°C. Both conjugation hyphae formation (B) and pheromone perception (C) were quantified at 22°C and 34°C. Bars: 5 µm

Alternatively, it was considered possible that the impaired formation of conjugation hyphae is a consequence of defects in pheromone sensing. Thus, I made use of a strain that expressed GFP under the control of the promoter of the mating pheromone gene (*mfa1*; strains FB1mG). In this strain, addition of external pheromone or the presence of a mating partner induces the expression of GFP, which is visible about two hours after pheromone addition (Spellig et al., 1996). Wild-type and *yup1*^{ts} mutant cells (strain FB1Yup1^{ts}mG) were able to perceive supplemented pheromone, as indicated by the cytoplasmic GFP signal at permissive temperature (Fig. 10C). A similar situation was found in wild-type cells at 34°C (Fig. 10A, Pro$_{mfa1}$:GFP, control; Fig. 10C). In contrast, mutant cells did not express GFP at 34°C (Fig. 10A, Pro$_{mfa1}$:GFP, Yup1^{ts}; Fig. 10C). Thus, it is most likely that early endosome function is required for pheromone perception and, consequently, for conjugation hyphae formation.

2.2.2 The pheromone receptor Pra1 is internalized via early endosomes

Pheromone perception in *U. maydis* wild-type strain FB1 requires the activity of the G-protein coupled pheromone receptor Pra1 (Bölker et al., 1992), which is predicted (see Materials and Methods) to contain seven transmembrane segments and shares an overall similarity of 45% with Ste3, one of the two pheromone receptors of *Saccharomyces cerevisiae*. Ste3 contains a signal sequence for constitutive endocytosis and ligand induced endocytosis (Chen and Davis, 2000) that is not present in Pra1. Nevertheless, it was considered that impaired endocytosis of Pra1 via Yup1-tagged endosomes is responsible for the reduced pheromone sensing of the *yup1^{ts}* mutant. Therefore, the green fluorescent protein (GFP) was fused to the C-terminus of the endogenous copy of Pra1 and observed its cellular distribution in strain FB1Pra1G. In non-stimulated yeast-like cells the receptor is only weakly expressed (Urban et al., 1996a) and consequently only faint signals of the Pra1-GFP fusion protein were observed in the plasma membrane (Fig. 11A1, inset), while most Pra1-GFP localised in the vacuoles (Fig. 11A1), where the receptor is most likely degraded.

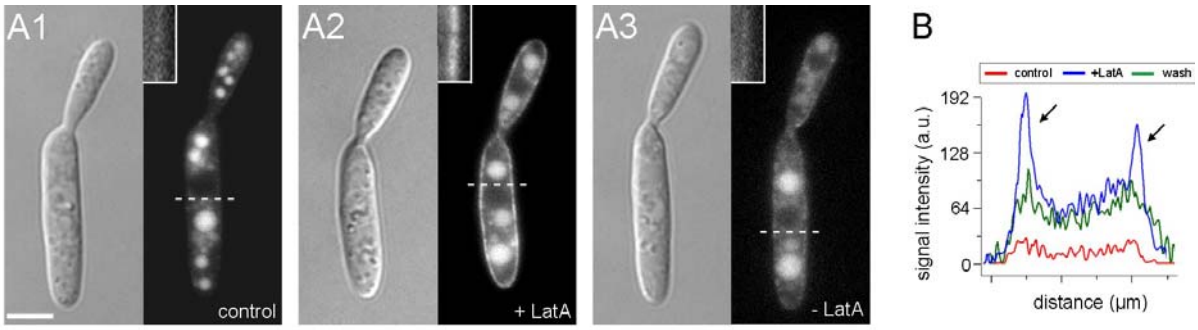

Figure 11. Localisation and constitutive endocytosis of Pra1-GFP in haploid sporidia.

(A) The strain FB1PraG was treated with 10 µM of the actin inhibitor Latrunculin A (A2) or with the solvent DMSO (A1) for 45 min before washout of LatA (A3). Insets highlight amounts of Pra1-GFP in the membrane. Bar: 3 µm. (B) Line scan analysis of Pra1-GFP signal intensities. Scanning lines are indicated in A. (Figure in cooperation with G. Steinberg).

However, disruption of F-actin by the inhibitor Latrunculin A enriched Pra1-GFP in the plasma membrane (Fig. 11A2, inset; Fig. 12A), and after washing-out the drug, the receptor disappeared from the cell surface (Fig. 11A3, inset; Fig. 12A). The increase in Pra1-GFP content in the plasma membrane is best illustrated by linescan analysis of the intensities of Pra1-GFP in the mother cell (Fig. 11B; scanning lines are indicated in Fig. 11A1-3). While only faint signals are detected in DMSO-treated control cells (Fig. 11B, red line), LatA treatment drastically increased the signal in the plasma membrane at the edge of the cell (Fig. 11B, blue lines, arrows), which decreased after removal of the drug (Fig. 11B, green line). Disruption of actin is known to inhibit the endocytic removal of receptors from the cell surface (Kaksonen et al., 2003), suggesting that the rise in Pra1-GFP after disruption of microfilaments is due to a defect in endocytic internalisation. After washing out LatA the excess of Pra1 is partially removed within the observation time. These results indicate that Pra1 is constitutively endocytosed in yeast-like cells of *U. maydis* in the absence of mating pheromone.

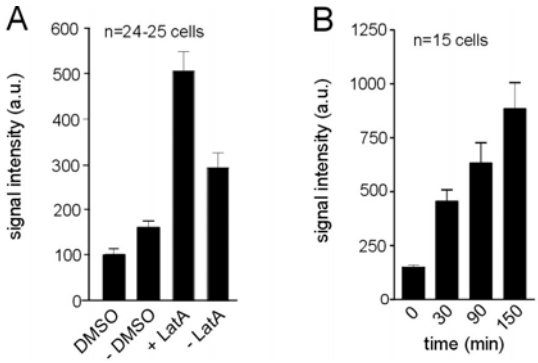

Figure 12. Signal intensities of Pra1-GFP at the plasma membrane after disruption of the actin cytoskeleton.

(A) Quantitative analysis of the intensity of Pra1-GFP in the tip of conjugation hyphae of strain FB1Pra1G in the presence/absence of LatA. (B) Analysis of Pra1-GFP signal intensities at the tip of conjugation hyphae at different time points after treatment with LatA.

After addition of pheromone, cells of strain FB1Pra1G formed conjugation hyphae (Fig. 13A, "DIC"), indicating that the Pra1-GFP fusion protein was fully functional. In these conjugation hyphae, Pra1-GFP localised to the plasma membrane in a cap-like fashion at the growing hyphal apex (Fig. 13; "Pra1-GFP", arrow head and right inset in merged image). In addition, Pra1-GFP accumulated in vacuoles that were stained with the vacuolar dye Celltracker ^{TM} Blue (Fig. 13; arrows and left inset in merged image).

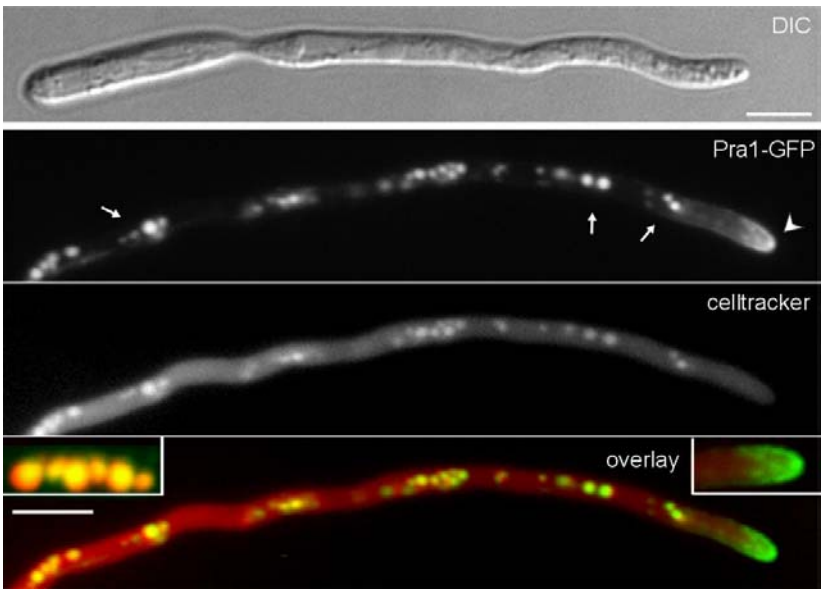

Figure 13. Localisation of Pra1-GFP in conjugation hyphae.

Incubation of yeast-like cells of strain FB1PraG with synthetic pheromone for 3 h induced the formation of conjugation hyphae (DIC). Pra1-GFP (green) localised to the tip of the hyphae (arrow head) where it forms an apical cap (overlay, right inset). In addition, Pra1-GFP localised in subapical organelles (Pra1-GFP, arrows) that co-stained with Celltracker blue (red; celltracker), indicating that they were vacuoles (overlay, left inset; colocalisation results in yellow). Bar: 5 µm.

Similar to yeast-like cells, disruption of F-actin in conjugation hyphae by 10µM LatA for up to 150 min led to a significant increase of Pra1-GFP in the plasma membrane at the tip region (Fig. 12B), indicating that internalisation of Pra1 is actin-dependent in conjugation hyphae as well, whereas the delivery of new receptor does not require the actin cytoskeleton.

To further elucidate the role of the pheromone receptor Pra1 I investigated the role of Pra1 beyond the initial pheromone stimulus. Cells expressing Pra1-GFP from the endogenous locus (FB1Pra1G) were pheromone treated for 3h and characteristic Pra1-GFP localisation was observed (Fig. 14A compare to Fig. 13). One set of cells

was further incubated with pheromone (Fig. 14B1) while in a second set of cells the compatible pheromone was washed out (Fig. 14C) before further incubation overnight. In the absence of pheromone cells reverted to the haploid growth form (Fig. 14C "-a2 ON"). Interestingly, an intense Pra1-GFP signal was still present in the plasma membrane of reverted haploid cells of FB1Pra1G, which can presently not be explained (98 % cells are haploid, n= 2 experiments, > 90 cells each). Control cells that received a continuous pheromone treatment at the same time grew filamentous (Fig. 14B1; 92.91 % cells filamentous n= 2 experiments, > 90 cells each) and Pra1-GFP still characteristically concentrated at the tip of the conjugation hyphae (Fig. 14B2). This indicates that a continuous pheromone stimulus is required for growth of conjugation hyphae and that Pra1 is continuously exposed at the hyphal tip during growth of conjugation hyphae.

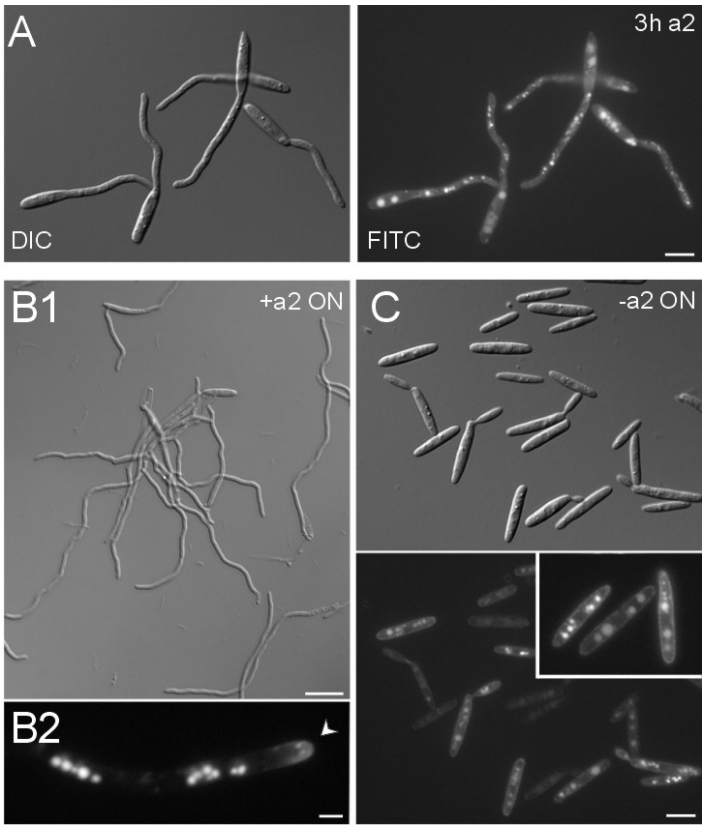

Figure 14. Long-term pheromone treatment of *U. maydis*.

Cells of FB1Pra1G were incubated with synthetic pheromone for 3 h to initiate pheromone perception and growth of conjugation hyphae. Subsequently pheromone was washed out (C) or cells were further incubated with pheromone (B1+ B2) over night. (B2) arrowhead points to Pra1-GFP cap that is still present after overnight pheromone treatment. (C) Inset shows enlargement of cells in which the pheromone was washed out. Bars: A, C = 5 µm; B1 = 10 µm, B2= 2 µm.

2.2.3 Endocytic recycling of Pra1 is impaired in the *yup1*^{ts} mutant

I next asked whether endocytosis of Pra1-GFP involves the Yup1-carrying EE. In order to gain support for this idea I constructed a strain expressing both Pra1-GFP and Yup1-RFP$_2$ (FB1Pra1GYup1R$_2$). After pheromone stimulation Pra1-GFP colocalised with Yup1RFP$_2$ and rapidly moved on EE (Fig. 15). The cap-like structure of Pra1-GFP at the hyphal tip was not involved in colocalisation.

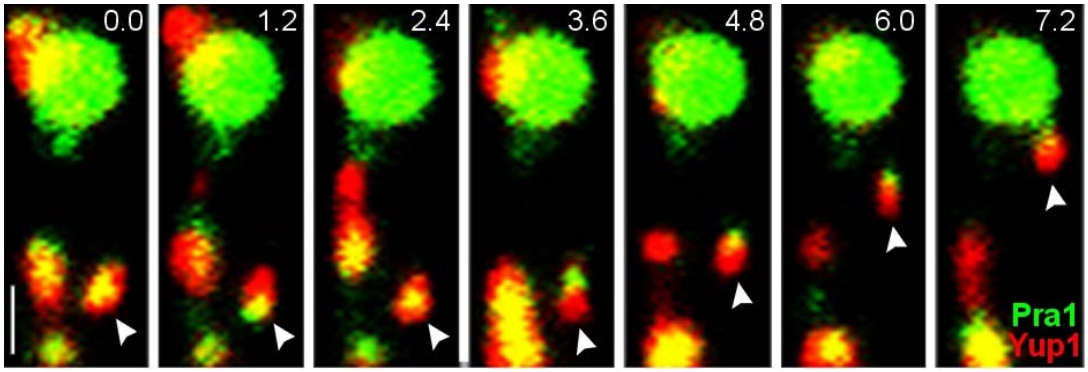

Figure 15. Colocalisation and Comigration of Yup1-RFP and Pra1-GFP.

Time-lapse series of Yup1RFP$_2$ (red) and Pra1GFP (green). Colocalisation is shown in yellow in the merged images. Arrows indicate moving EE. Time is given in seconds. Bar: 1 µm. (Image in cooperation with G. Steinberg)

To obtain further evidence for a role of EE in Pra1-GFP processing, control cells and *yup1*^{ts} mutants were stimulated with pheromone under permissive conditions for 2 h to initiate pheromone perception and subsequently were shifted to restrictive temperature for additional 2 h. While this treatment had no effect on the Pra1-GFP distribution of control hyphae (Fig 16A "control"), Pra1-GFP accumulated in *yup1*^{ts} mutant hyphae in small immobile dots within the cytoplasm (Fig. 16A, "yup1^{ts}", arrows), with most Pra1-GFP found in the hyphal tip (Fig. 16A, "yup1^{ts}", arrowhead).

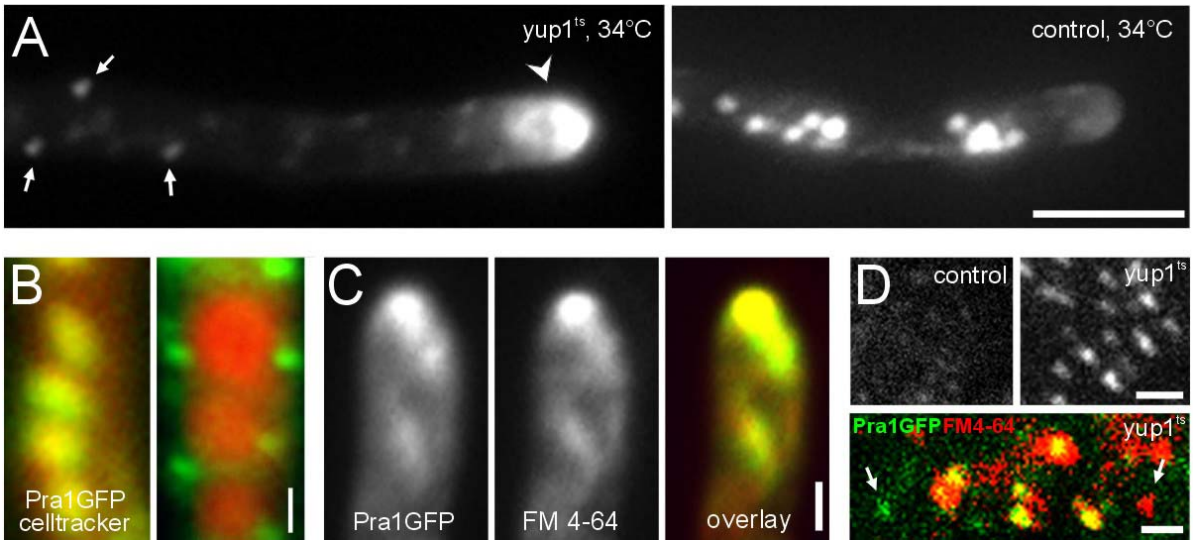

Figure 16. Localisation of Pra1-GFP in the *yup1*^{ts} mutant background .

(A) Localisation of Pra1-GFP in Strain FB1Yup1^{ts}Pra1G and the control strain FB1Pra1G that were stimulated with pheromone for 2 h at 22°C before shift to 34°C for 2 h. Arrows indicate Pra1-vesicles that are very likely clusters of primary endocytic vesicles. Arrowhead points to the accumulation of Pra1-GFP at the tip. Bar: 5 µm. (B) Colocalisation of vacuoles; stained with Celltracker-Blue; (red) and Pra1-GFP (green) in strains FB1Pra1G (control) and FB1Yup1^{ts}Pra1G at 34°C; colocalisation results in yellow. (C) Double labelling experiments in *yup1*^{ts} mutants demonstrate that Pra1-GFP (green) and endocytic membranes, stained with FM 4-64 (red) colocalised in the apical cytoplasm in *yup1*^{ts} cells. (D) Pra1-GFP containing vesicles obtained from the protein extracts of pheromone stimulated and shifted control strain and FB1Yup1^{ts}Pra1G at 34°C. The merged image shows vesicles isolated from FB1Yup1^{ts}Pra1G at 34°C simultaneously incubated with FM 4-64. B-D Bars: 1 µm.

In *yup1*^{ts} mutants, Pra1-GFP no longer colocalised with vacuoles that were stained with CellTracker^{TM} Blue (Fig. 9B "yup1^{ts}" compare to "control"), but accumulated in small aggregates that might represent clusters of primary endocytic vesicles at 34°C. Consistently, the apical Pra1-GFP cluster colocalised with the endocytic marker dye FM 4-64 that had been coincubated with the cells (Fig. 16C), suggesting that Pra1-GFP is internalised in *yup1*^{ts} mutant hyphae, but accumulates in small primary endocytic vesicles within the cytoplasm. This notion is supported by the fact that whole cell extracts of strain FB1Yup1^{ts}Pra1G contained numerous small Pra1-GFP carrying vesicles (Fig. 16D), which were mainly colocalising with FM4-64 (Fig, 9D, lower panel; colocalisation results in yellow). These vesicles were much less abundant in extracts of strain FB1PraG that had been treated in similar ways (Fig. 16D "control"), again indicating that primary endocytic vesicles accumulate in *yup1*^{ts} mutants due to the fusion defect at early endosomes. However it is important to note that these cell extracts also contain vesicles that carried either Pra1-GFP or were only stained with FM4-64 (Fig. 16D arrows). While the Pra1-GFP stained vesicles could be secretory

vesicles, the existence of endocytic transport vesicles that do not contain the pheromone-receptor argues for additional endocytic pathways for the uptake of the endocytic marker dye FM 4-64.

In order to get a more detailed insight into the defects of *yup1*^{ts} mutants I investigated the spatial relation between the plasma membrane and Pra1-GFP signals in the hyphal apex. Therefore, I simultaneously added FM4-64 and 0.5% formaldehyde to wild-type and *yup1*^{ts} conjugation hyphae that had been incubated at 34°C. This allowed the dye to incorporate into the plasma membrane but blocked further internalisation, while the GFP-tagged receptor was still detectable.

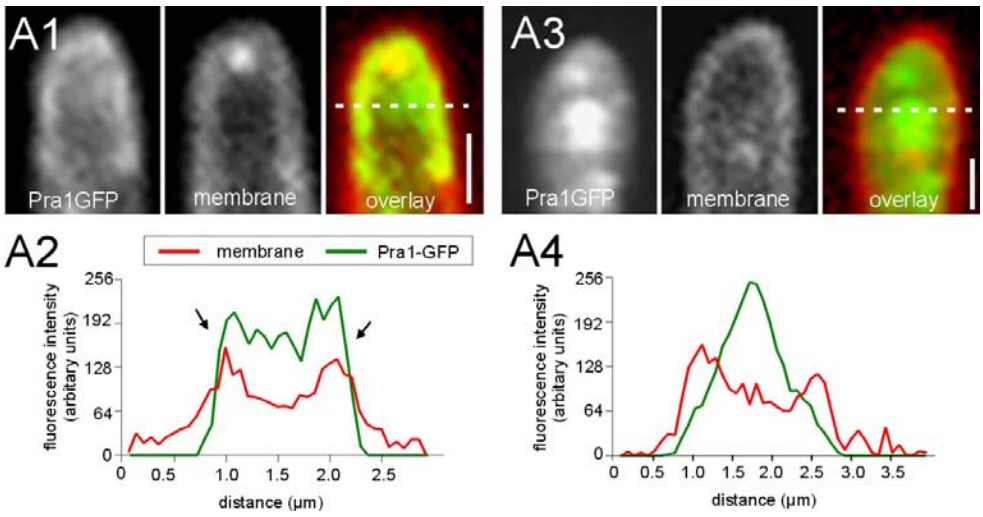

Figure 17. Analysis of Pra1-GFP localisation in the hyphal tip.

Analysis of localisation of Pra1-GFP (green) in respect to the plasma membrane (red) in control cells and *yup1*^{ts} mutant hyphae after incubation for 2h at 34°C. A line scan of the intensities demonstrates that FM4-64 and Pra1-GFP colocalised at the edges of the cell (A2, arrows; scanning line indicated in A1, overlay). In *yup1*^{ts} cells Pra1-GFP was depleted from the plasma membrane and accumulated within the cytoplasm in the hyphal tip (E3, E4). Bars: 1 µm.

In control cells Pra1-GFP colocalised with FM4-64 in the plasma membrane at the hyphal apex (Fig. 17A1), which is nicely illustrated by linescan analysis of the signal intensities of Pra1-GFP and FM-4-64 (Fig. 17A2; scanning line indicated in A1). In contrast, in *yup1*^{ts} mutants Pra1-GFP was depleted from the plasma membrane, but accumulated in the apical cytoplasm (Fig. 17A3, A4). Immuno-gold labeling of Pra1-GFP, done by G. Hause (University of Halle), confirmed that the receptor located in the cell periphery in control hyphae at 34°C as was detected using anti-GFP antibodies

(Fig. 18A, arrows). The majority of receptor molecules in the *yup1*^{ts} mutant hyphae was found within the cytoplasm (Fig. 18B, arrows).

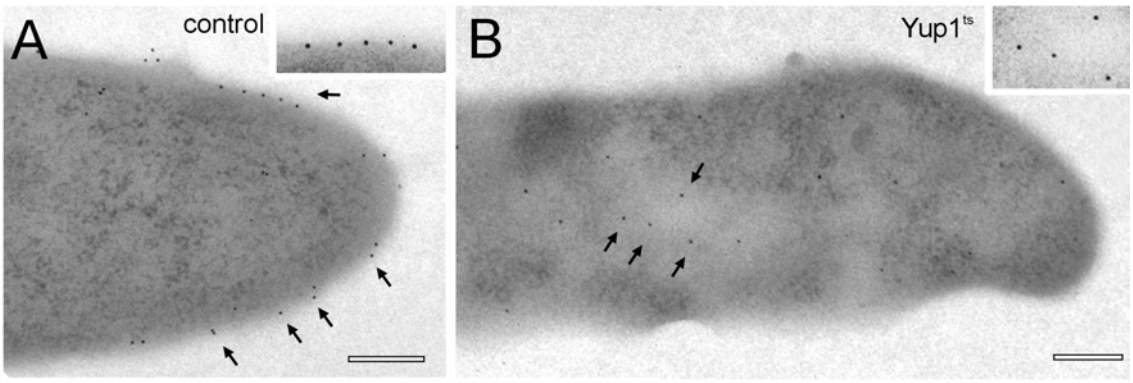

Figure 18. Electronmicroscopy studies of Pra1-GFP localisation in *yup1*^{ts} cells.

Immunolocalisation of Pra1-GFP in control (A) and *yup1*^{ts} mutant cells (B). Arrows indicated localisation of Pra1-GFP, insets give details of localisation pattern. Bars: 0.5 µm. Immunogoldlabelling and EM were done by Dr. Gerd Hause, University of Halle, Germany.

2.2.4 Recycling of the pheromone receptor

The results described so far indicated that the uptake of Pra1-GFP into EE is required to maintain enough active receptor in the plasma membrane, suggesting that the receptor is recycled to the surface for additional rounds of pheromone binding. I next attempted to gain more direct evidence for Pra1 recycling in conjugation hyphae of *U. maydis*. In a first set of control experiments, I confirmed that 100 µg/ml cycloheximide for 45 min fully inhibit protein biosynthesis in *Ustilago maydis* (Fig.19). Therefore I used cells of strain FB2rGTub1 that contain an additional copy of GFP-αtubulin that is expressed under the control of the *crg*-promoter which is blocked in glucose-containing medium (Bottin et al., 1996). Consequently, no GFP-labeled microtubules were visible (Fig. 19A1). Shifting these cells for 120 min to arabinose-containing medium induced the expression of GFP-αtubulin and MTs became visible (Fig. 19A2, "Ara"). In contrast, no GFP-αtubulin was detected after 120 min growth in arabinose-containing medium when supplemented with 100 µg/ml cycloheximide for the last 45 min (Fig. 19A3; "Ara + cyclo"). This strongly indicated that 45 min of 100 µg/ml cycloheximide treatment completely abolished protein synthesis, including that of GFP-αtubulin in *U. maydis*.

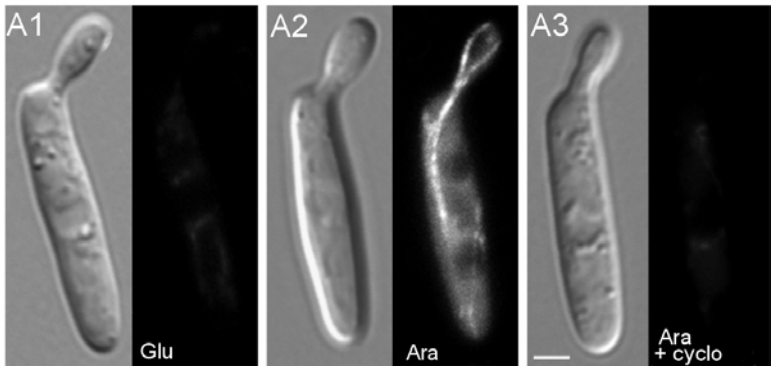

Figure 19. Cycloheximide treatment in *U. maydis.*

In control experiments the effect of cycloheximide on protein synthesis was investigated using strain FB2rGTub1 that contains an additional copy of α-tubulin fused to GFP (GFP-Tub1, (Steinberg et al., 2001) under the control of the inducible *crg*-promoter. In this strain no GFP-labelled microtubules were detected in glucose-containing medium (A1), but expression of GFP-Tub1 was induced after shift to arabinose-containing medium for at least 2 h (A2). When FB2rGTub1 was grown in arabinose-containing medium for 75 min and cycloheximide was added for additional 45 min protein biosynthesis was blocked and GFP-αtubulin was not synthesized. Bar: 2 µm.

Next, I incubated conjugation hyphae of strain FB1Pra1G with or without cycloheximide for 45 min. The block of protein synthesis led to a drastic decrease in Pra1-GFP signal intensity in the plasma membrane (Fig. 20A "control" and "+cyclo"; Fig. 20B), which demonstrates that synthesis and secretion of new receptor was the major source for the exposed receptor. When this treatment was followed by additional 120 min incubation in DMSO/cycloheximide the amount of Pra1-GFP further decreased and intensively stained vacuoles appeared (Fig. 20A "DMSO + cyclo"; Fig 20B,). In contrast, 120 min of cycloheximide treatment in combination with LatA led to a significant increase of Pra1-GFP in the plasma membrane (Fig. 20A "LatA + cyclo"; Fig. 20B; P=0.0001). This increase, under our artificial conditions where synthesis of new receptor and initial endocytic uptake is blocked, indicates that a significant amount of Pra1-GFP is stored in the endocytic pathway and recycles back to the plasma membrane and EE.

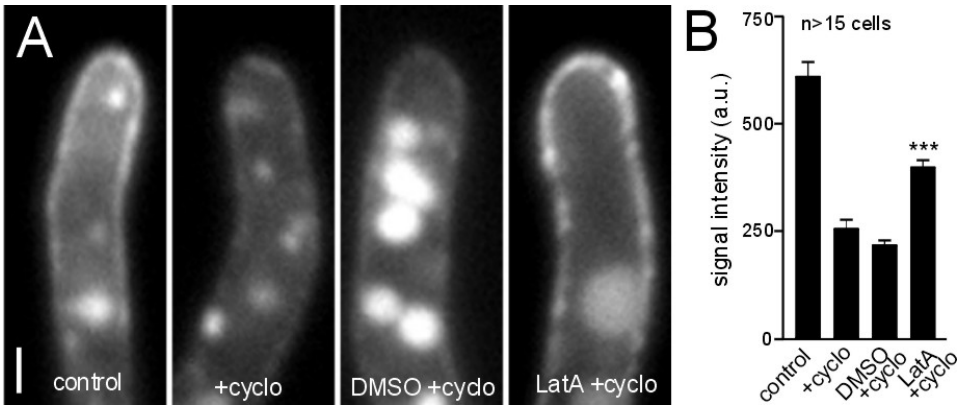

Figure 20. Quantitative analysis of Pra1-GFP recycling.

(A) Pra1-GFP signals in the tip of conjugation hyphae. Cells were treated with water (control) or cycloheximide (+cyclo) for 45 min. Hyphae were incubated for additional 120 min with Latrunculin A/cycloheximide or DMSO/cycloheximide . (B) Quantitative analysis of corresponding Pra1-GFP signals in (A) (LatA/+cyclo; *** : P<0.0001). Bar: 1 µm.

2.2.5 Constitutive expression of Pra1 restores pheromone perception

Our results indicated that *yup1*^{ts} mutants are defective in receptor recycling and that the pheromone receptor accumulates in the cytoplasm, which decreases the amount of exposed Pra1 on the cell surface. To test whether reduced amounts of Pra1-GFP are indeed responsible for the perception defects in *yup1*^{ts} mutants, I increased the amount of receptor by expression of Pra1-GFP under the control of the strong *otef*-promoter (strain FB1Yup1^{ts}oPraG). Western analysis confirmed that receptor protein levels were ~10-fold increased in the mutant strain at both 22°C and 34°C (Fig. 21A), and most Pra1-GFP was concentrated in the plasma membrane (Fig. 21B, "oPra1G", inset), whereas Pra1-GFP was almost invisible in the control strain FB1Yup1^{ts}Pra1G at 22°C (Fig. 21B, “control”).

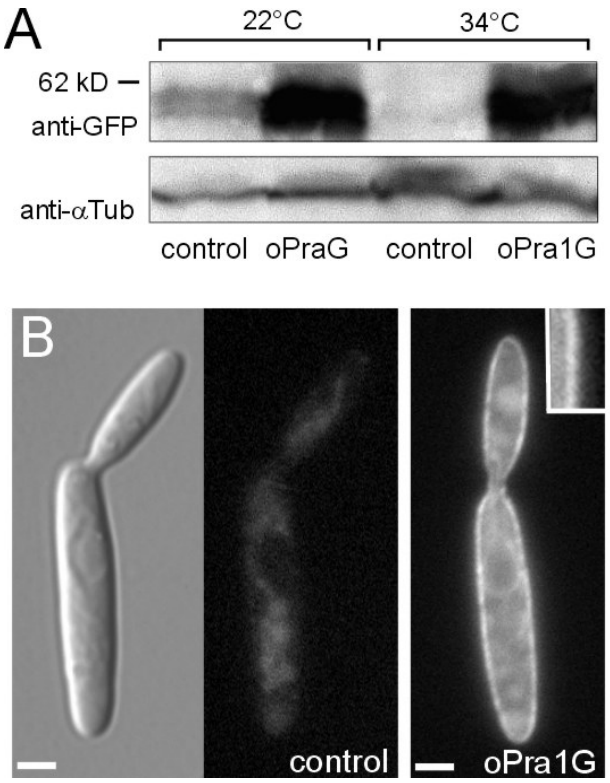

Figure 21. Complementation of *yup1*^{ts} mutants with constitutively expressed Pra1-GFP.

(A) Western blot showing levels of Pra1GFP in cell extracts of the *yup1*^{ts} mutant background at native levels and Pra1-GFP expressed under the control of the constitutive *otef*-promotor. (B) Localization of Pra1-GFP in *yup1*^{ts} (FB1Yup1^{ts}PraG) and with additional expression of Pra1GFP under the constitutive *otef*-promotor (FB1Yup1^{ts}oPra1GFP) at 22°C. High expression of Pra1-GFP increased the amount of receptor in the plasma membrane (inset). Bar: 2 µm.

In order to monitor the ability to perceive pheromone, I next integrated the red fluorescent protein under the control of the *mfa1*-promoter into this mutant. After 2 h at 34°C this strain (FB1Yup1^{ts}mRoPraG) showed a morphology defect (Fig. 22A, "DMSO") that was characteristic of mutants impaired in early endosome function (Wedlich-Söldner et al., 2000). Under these conditions Pra1-GFP clustered in cytoplasmic accumulation near the growth region (Fig. 22A, "Pra1-GFP", inset) that were reminiscent of the cytoplasmic Pra1-GFP cluster in *yup1*^{ts} conjugation hyphae (see Fig. 16A). In addition, Pra1-GFP was still localised to the plasma membrane, indicating that endocytosis is not able to remove the high excess of constitutively expressed Pra1-GFP from the surface (Fig, 22A; "Pra1-GFP", inset). Consistent with the notion, that a lack of receptor is responsible for the defect in pheromone perception, treatment with synthetic pheromone now induced expression of red fluorescent protein (Fig. 22C, "pheromone", 22B, "yup1^{ts}oPra1G"). In contrast, but consistently with the results described above, pheromone treatment induced RFP expression only in a very minor fraction of mutant cells when Pra1-GFP was expressed under its native *pra1*-promoter in the *yup1*^{ts} background (Fig. 22B, "yup1^{ts}"; strain FB1Yup1^{ts}mRPraG).

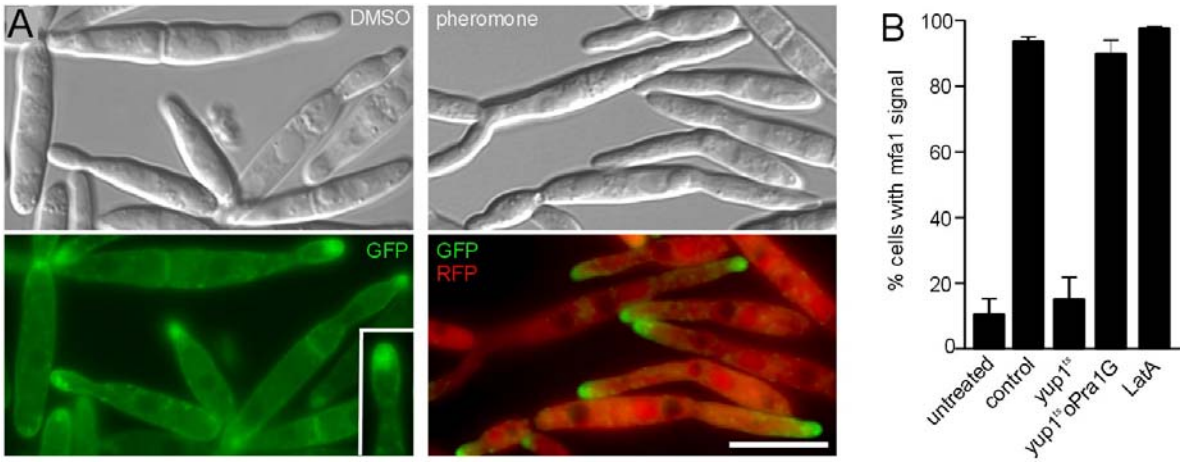

Figure 22. Pheromone treatment in complemented *yup1*^{ts} mutants.

(A) Strain FB1Yup1^{ts}mRoPraG was grown at 34°C and stimulated with synthetic pheromone or DMSO as control. Bar: 10 µm. (B) Quantification of the response to synthetic pheromone of control and *yup1*^{ts} cells treated with synthetic pheromone or synthetic pheromone and LatA. Bars represent the percentage of cells that show *mfa*-promoter induced RFP expression.

These results demonstrate that high levels of the pheromone receptor restore the defect in pheromone perception. Finally, we tested whether the initial steps of endocytosis of Pra1-GFP are required for pheromone perception. Therefore we disrupted F-actin in strain FB1mG with 10 µM LatA for 45 min and added synthetic pheromone/LatA to these cells. In these cells the pheromone induced the *mfa1*-promoter, as indicated by GFP expression (Fig. 22B, "LatA") confirming similar results of *S. cerevisiae* (Rohrer et al., 1993). This suggests that the initial steps of receptor internalisation are not needed for detection of the mating partner. Taken together these results strongly support the notion that recycling via EE is required to maintain steady state levels of the receptor at the cellular surface during the initial step of pheromone perception.

2.2.6 Endocytosis is essential for cell-cell fusion

Restored pheromone perception in FB1yup1^{ts}oPra1 (Fig. 23A; "yup1^{ts}") led to the formation of short and irregular conjugation hyphae in the presence of synthetic pheromone (Fig. 23A; compare to strain FB1oPra1, "control"). I next asked whether these conjugation hyphae are able to orient themselves in a gradient of pheromone and mediate cell-cell fusion. Therefore, I spotted compatible strains that expressed

cytoplasmic GFP or RFP across from each other on water agar slides at 34°C. In these confrontation assays, control cells (strains FB1oPra1_G and FB2oPra2_R) formed long filaments that grew towards the partner and fused, which resulted in a faint yellow colour in the merged image due to the mix of the cytoplasmic GFP and RFP (Fig. 23B, "control", arrow indicating the site of fusion; asterisk marks nuclei).

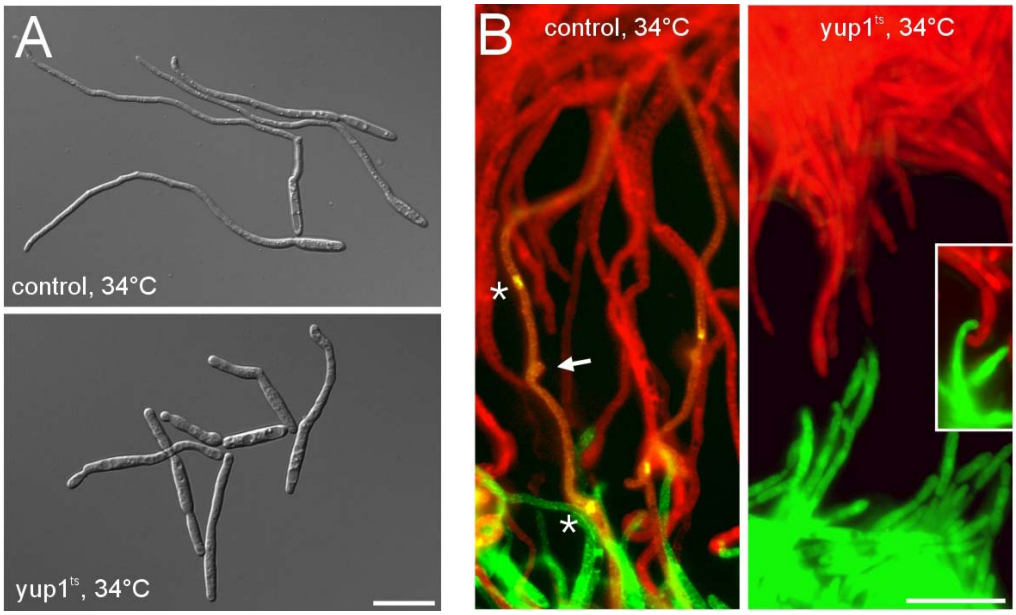

Figure 23. Mating and fusion ability of the *yup1*^{ts} mutant constitutively expressing *Pra1.*

(A) Conjugation hypha formation of wild-type and *yup1*^{ts} cells expressing otefPra1 with synthetic pheromone to analyse the ability to form conjugation hyhae. (B) Confrontation assay of mating partners expressing otef Pra as well as cytoplasmic GFP or RFP. Asterisks in the control indicate the nuclei in the haploid conjugation hyphae. Their fusion site to form the dikaryotic filament is marked by the arrow. Fused hyphae express both GFP and RFP resulting in yellow. *yup1*^{ts} cells did not fuse (inset). Bars: 10 µm.

Cells of the compatible *yup1*^{ts} mutants (FB1Yup1^{ts}oPra1_G and FB2Yup1^{ts}oPra2_R) grew towards the mating partner (Fig. 23B, "yup1^{ts}"; inset), but were unable to bridge large distances (not shown). However, under these conditions, no cell-cell fusion was detected in the *yup1*^{ts} mutants, suggesting that endocytosis might be required during this step. In agreement with this, a mixture of these compatible *yup1*^{ts} mutants did not form a "fuzzy" white colony and only rarely yellow dikaryotic cells were found at 34°C (Fig. 24A, "yup1^{ts}"; top right inset shows colony appearance, fusion). This was in striking contrast to control experiments (Fig. 24, "control"). Cell-cell fusion did not increase in *yup1*^{ts} cells even after 3.5 days at 34°C (Fig. 24A, "yup1^{ts}"; lower right

inset), indicating that endocytosis is essential for cell-cell fusion during early pathogenic development.

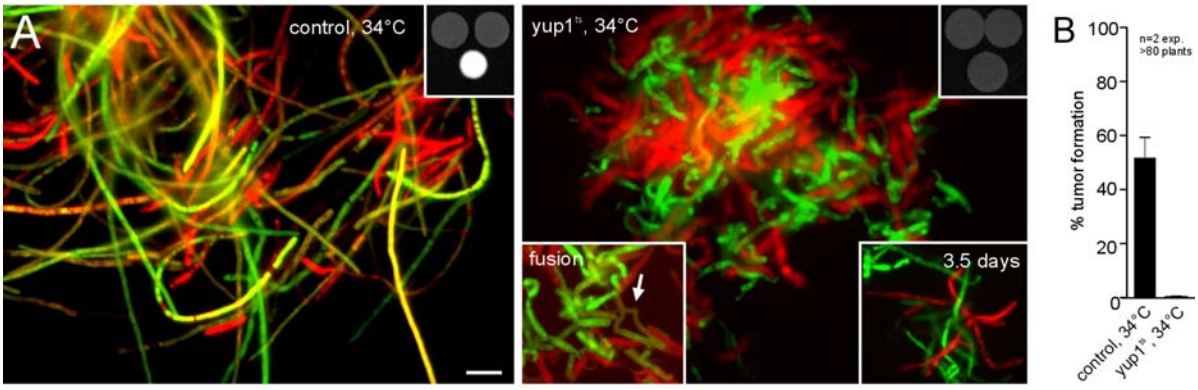

Figure 24. Assay for fusion of GFP or RFP labelled mating partners on charcoal plates.

Fused hyphae express both RFP and GFP resulting in a yellow colour after spotting a mixture of compatible cells on charcoal plates (strains FB1oPra1_G and FB2oPra2_R as a control and FB1Yup1^{ts}oPra1_G and FB2Yup1^{ts}oPra2_R). Top insets show the overall colony morphology. Lower left panel in *yup1*^{ts} shows a rare fusion event of mutant cells indicated by the arrow. Lower right inset depicts hyphae that have been incubated for 3.5 days. Bar: 10 µm. (B) Quantification of tumor formation after plant infection with FB1oPra1 x FB2oPra2 as control and the compatible mutants FB1Yup1^{ts}oPra1 x FB2Yup1^{ts}oPra2 for 14 days at 34°C.

Consequently, in plant infection assays, using the strains that constitutively express Pra1/Pra2, no symptoms were seen after infection with compatible *yup1*^{ts} cells at 34°C (Fig. 24B). Taken together, these results demonstrate that endocytosis is essential for mating in *U. maydis*.

2.2.7 Plant colonization is only slightly effected in *yup1*^{ts}cells

Next I analysed the importance of endocytosis in later stages of pathogenic development. I inoculated plants with compatible wild type strains (FB1 and FB2) and *yup1*^{ts} mutants (FB1Yup1^{ts} and FB2Yup1^{ts}) at permissive temperature and allowed them to complete the mating reaction, before shifting them to higher temperature (see Material and Methods). Under these conditions, *yup1*^{ts} mutants formed thicker and more irregularly shaped hyphae (Fig. 25A; cell wall stained with calcofluor white; compare "yup1^{ts}" to "control"), which were nevertheless able to form appressoria (Fig. 25A, insets) and entered the plant at restrictive temperature (Fig. 25B). Further time

course experiments covering the first 7 days did not reveal any significant differences between control hyphae and *yup1*^{ts} mutant hyphae inside the plant tissue (Fig. 25B), although *yup1*^{ts} cells appeared slightly thicker and were sometimes slower in colonization of the host. Consequently, *yup1*^{ts} infected plants that were incubated for 3 days at 22°C before shift to restrictive temperature showed tumor formation, albeit at reduced rates (Fig. 25C). Interestingly, tumors in these *yup1*^{ts} mutant infected plants were only observed at the stem and not in higher parts of the plant (not shown). However, these tumors did not contain any teliospores even after 19 days post infection (Fig. 25D; Fig. 25E), although fungal material was detected in the tumors of plants infected with *yup1*^{ts} mutant strains (Fig. 25E; compare to "control"). In summary this indicates that endocytosis is less important for growth within the plant but is essential for the formation of teliospores.

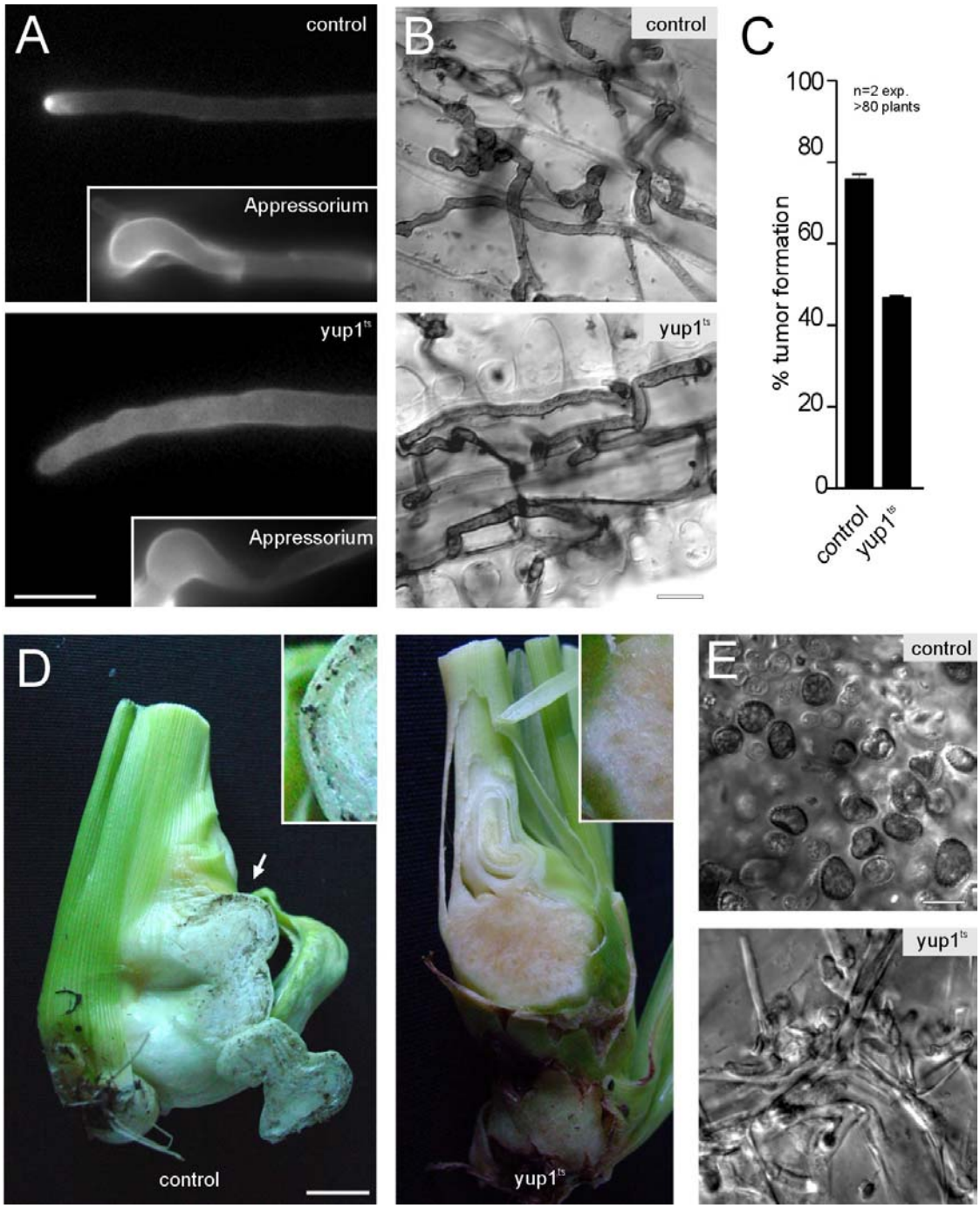

Figure 25. Analysis of *yup1*^{ts} mutants *in planta*.

(A) Control hyphae and *yup1*^{ts} hyphae stained with calcofluor after incubation at 22°C for 14h and subsequent shift to 34°C. Appressoria that penetrate the plant surface are formed by control and *yup1*^{ts} hyphae (insets). Bar: 5 µm. (B) Images of Chlorazole Black E stained control and *yup1*^{ts} hyphae after 1 day of incubation at 22°C and subsequent shift to 34°C for 1-2 days. Bar: 10 µm. (C) Quantitative analysis of tumor formation in plants infected with control strains and *yup1*^{ts} strains and incubation at 22°C for 3 days and subsequent shift to 34°C for a total of 14 dpi. (D) Whole plant tumor of infected plants were harvested 3 weeks post infection. Wild-type tumors contain black teliospores that form at the edge of the tumor (control, inset). In contrast *yup1*^{ts} tumors are devoid of teliospores in the center as well as at the edge of the tumor (yup1^{ts}). Bar: 1 cm. (E) Higher magnification of tumor tissue confirmed the presence of teliospores in wild-type tumors (control) while teliospores were absent in *yup1*^{ts} tumors and only hyphal fragments were visible (yup1^{ts}). Bar: 10 µm.

2.2.8 Teliospore germination is mediated by Yup1

Finally, I investigated the ability of *yup1*^{ts} mutants to germinate from teliospores generated at 22°C. Both wildtype and *yup1*^{ts} teliospores germinated after ~24h at 22°C on CM-G containing agar layers (Fig. 26A, 22°C and Fig. 26B). However germination rates of *yup1*^{ts} teliospores were greatly reduced at 34°C (Fig. 26A, 34°C, compare "yup1^{ts}" and "control"; 26C) and only slowly increased after prolonged incubation for 3 days (Fig. 26A, 34°C, "yup1^{ts}+").

In those cases where *yup1*^{ts} teliospores managed to germinate, the promycelium showed morphological alterations compared to wild type (Fig. 26D). Thus, Yup1-mediated endocytosis participates in teliospore germination and functional impairment of endocytosis leads to a reduced germination rate.

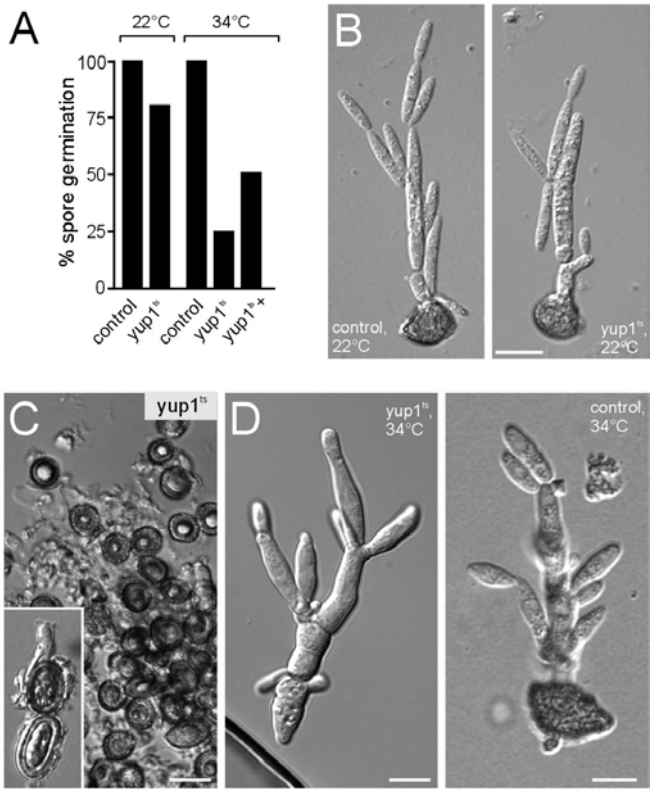

Figure 26. Teliospore germination.

Quantification of teliospore germination at permissive temperature 22°C and restrictive temperature 34°C for control and *yup1*^{ts} spores. At 34°C germination of *yup1*^{ts} teliospores is greatly impaired and only slightly increases after incubation (yup1^{ts}+) for 3 days. Germination of control teliospores is set to 100%. (B) Images of control and *yup1*^{ts} teliospores germinated at 22°C on CM-G containing agar-slides. Bar: 10 µm. (C+D) Images of control and *yup1*^{ts} teliospores germinated at 34°C.Yup1^{ts} spores after incubation of 1day at 34°C (inset) and 3 days. (D) When *yup1*^{ts} teliospores managed to germinate they again showed morphological alterations.(C3) Control teliospore germinated at 34°C after 1 day of incubation. Bars: 5 µm.

2.3 Additional components in the *yup1*-mediated endocytic pathway

One aspect of this work was to also identify cargos of the endocytic pathway. The results obtained so far indicate that surface proteins, such as the pheromone receptor Pra1 cycle between the plasma membrane and EE. It is known from the yeast *S. cereviaiae* that chitin synthases, which participate in wall formation, undergo endocytic recycling (Ziman et al., 1996). *Ustilago maydis* has eight chitin synthases that have different functions during development and pathogenic development of the fungus (Weber et al., 2006). One of them, the myosin chitin synthase 1 (Mcs1), is only required for pathogenicity (Weber et al., 2006). Previous results had indicated that Mcs1 locates to the active growth region (Weber et al., 2006) and is transported in a bi-directional fashion within the cell before it is degraded in the vacuole. This was the reason to anticipate that this chitin synthase must also be endocytosed.

To test this hypothesis Mcs1 was first localised tagging the protein with triple GFP at its N-terminus under control of the constitutive *otef*-Promoter (Spellig et al., 1996). In haploid sporidia GFP_3-Mcs1 localised to the newly emerging bud and was found in small particles and in the vacuole (Fig. 27A). Localisation at the growing bud was confirmed by a staining the newly synthesized chitin with wheat germ agglutinin (WGA) (Robin et al., 1986).

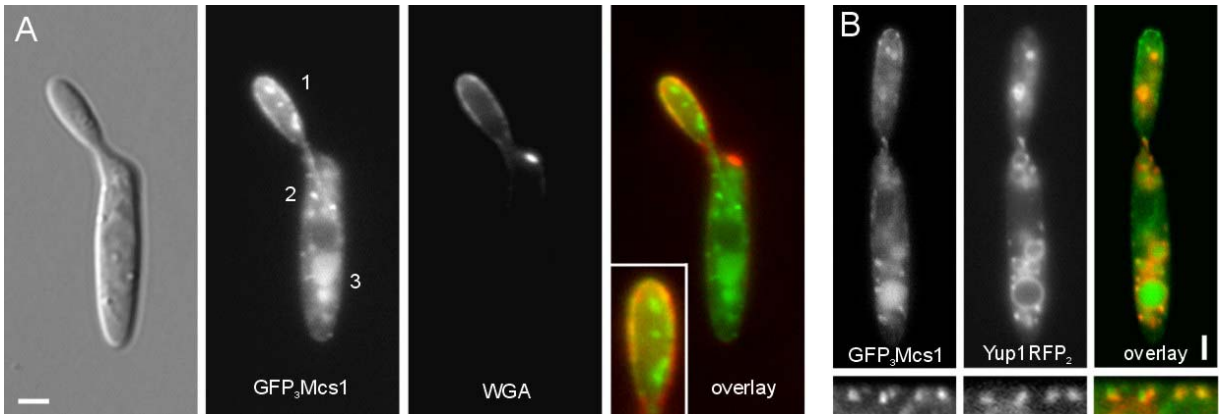

Figure 27. Localisation of Mcs1.

(A) GFP_3-Mcs1 localises to the new emerging bud (1) is seen in small particles (2) and is found in the vacuole (3). Localisation of Mcs1 (green) at the growing bud is confirmed by wheat-germ agglutinin staining (WGA, red) which results in a yellow colour in the overlay. (B) GFP_3-Mcs1 (green) is part of the endosomal pathway as is determined by colocalisation with the early endosomal marker Yup1-RFP (red). Colocalisation of both proteins results in a yellow colour in the overlay. Bar: 2 µm.

The GFP_3-Mcs1 fusion protein colocalised with RFP tagged-Yup1 in a strain that simultaneously expressed both proteins (FB1oGMcs1oYup1R) resulting in a yellow colour in the image overlay (Fig. 27B, overlay). In addition, GFP_3-Mcs1 co-localised with the endocytic marker dye FM4-64 (not shown). Therefore I next asked whether Mcs1 is endocytosed and whether endocytosis takes place in a *yup1*-dependent fashion. In analogy to the studies with Pra1, I blocked the initial steps of endocytosis (Kubler and Riezman, 1993) by inhibition of actin polymerisation with LatA. In the control cells GFP_3-Mcs1 localised to the tips of newly forming buds and was found in the vacuole (Fig. 28A+B, "+DMSO"). In contrast GFP_3-Mcs1 accumulated at the whole cell periphery of the Lat A treated cells (Figure 28A+B,"+ LatA"). The effect was reversible once Lat A was washed out (Fig. 28A+B,"- LatA"). This indicates that GFP_3-Mcs1 is constitutively endocytosed in *U. maydis*.

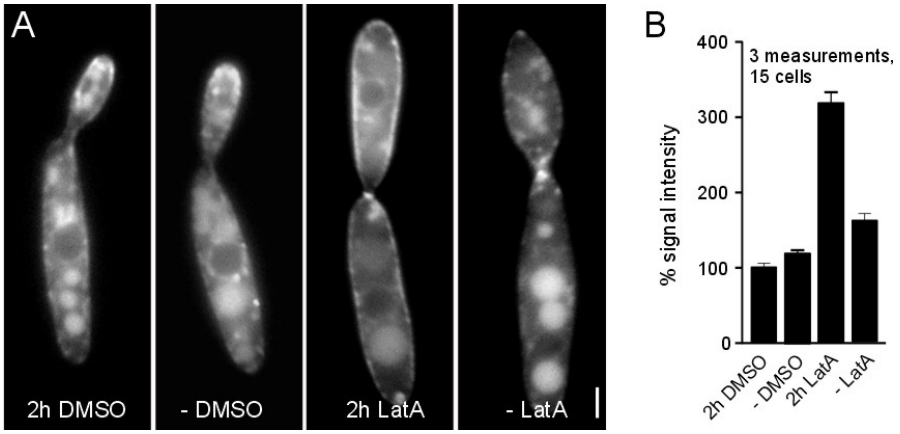

Figure 28. Block of GFP_3-Mcs1 endocytosis.

(A+B) Endocytosis of GFP_3-Mcs1 was blocked by LatA treatment for 2 h. Control cells were treated with DMSO. (B) Corresponding quantification of GFP_3-Mcs1 signals in (A) at three different points at the cell peripherie (excluding the normal localization sites at the bud peripherie). Bar: 2 µm.

To determine whether endocytosis of Mcs1 is a *yup1*-mediated process, I expressed GFP_3 –Mcs1 in a temperature sensitive Yup1 mutant (Wedlich-Söldner et al., 2000). (strain FB1yup1^{ts}oGFP_3-Mcs1) After incubation at restrictive conditions (6 h, 34°C) control cells showed a clear vacuolar localisation of GFP3-Mcs1, which was confirmed using the vacuolar stain CellTracker^{TM} Blue CMCA (false coloured in red) (Figure 29A, yellow colour in overlay). In contrast the GFP_3-Mcs1 signal could not be detected in the vacuole in *yup1*^{ts} cells that had also been incubated for 6 h at 34°C (Figure 29B, no

signal in GFP, results in red vs. yellow in overlay A). In addition some mutant cells showed a strong GFP signal from accumulation of GFP_3-Mcs1 at the bud tip in the cytoplasm (Figure 29B, GFP, inset) under restrictive conditions. Similarly to Pra1 accumulation in *yup1*^{ts} cells this could be the result from accumulation of putative primary endocytic vesicles that carry GFP_3-Mcs1. These results demonstrate that the primary internalisation of GFP_3-Mcs1 is actin-dependent and that Yup1 mediates subsequent endocytosis steps in *U. maydis*. However, these results are preliminary and should be confirmed using a GFP-Mcs1 fusion protein expressed from the endogenous locus.

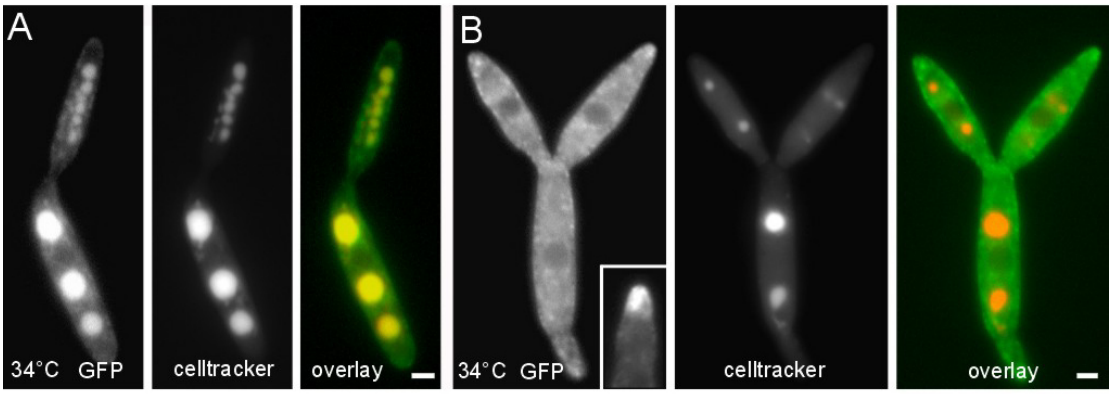

Figure 29. Distribution of GFP_3-Mcs1 in yup1^{ts} mutant cells.

(A) Control cells and (B) yup1^{ts} expressing GFP3-Mcs1 (green) were incubated at 34°C for 6h. Both samples were stained with celltracker blue (red) to label the vacuoles. Endocytosis and degradation of GFP3-Mcs1 in the vacuole results in a yellow colour in the overlay. Bars: 2 µm.

3 Discussion

3.1 Endocytosis in *U. maydis*

Endocytosis is a common process among eukaryotes with conserved mechanisms from yeast to animals (Geli and Riezman, 1998). It has long been controversial whether and to what extend endocytosis participates in growth and homeostasis of filamentous fungi (Read and Kalkman, 2003) while it is believed that it occurs in other tip-growing cells like pollen tubes (Camacho and Malho, 2003) and root hairs (Ovecka et al., 2005; Voigt et al., 2005). Growing evidence from different fungal species, including the one presented here in *U. maydis*, has changed this view and strongly indicates an essential role for endocytosis. Homologues of almost all commonly discussed components of the yeast endocytic machinery were identified by Blast analysis. Each of these yeast proteins had one or more significant homologues (E ≤1e-21) in the *Ustilago* genome. This is analogous to the findings of Read and Kalkman (2003), who followed a similar Blast approach in *N. crassa*. The genome analysis strongly suggests that *U. maydis* possesses the complex endocytic protein machinery (D'Hondt et al., 2000) required to conduct endocytosis. Nevertheless, it should be noted that proteins, such as actin, calmodulin and fimbrin do not exclusively participate in endocytosis but also perform other essential roles in the cell (Davis et al., 1986; Adams et al., 1991; Ayscough et al., 1997; Wu et al., 2001).

The RabGTPases involved in early endosomal sorting (summarized in Somsel Rodman and Wandinger-Ness, 2000) are also present in the *U. maydis* genome. Two homologues of Rab5 are encoded in the genome. This is comparable to *S. cerevisiae*, which also possesses multiple (three) Rab5-like proteins with diverse functions (Singer-Krüger et al., 1994) while in mammalian systems one Rab5 protein, Rab5a, is known and two isoforms with 85% homology, Rab5b and Rab5c, exist (Chavrier et al., 1992). It will have to be elucidated whether the *U. maydis* Rab5s are functionally redundant, which could be assumed from their similar localisation patterns, or whether they operate differently. The two Rab5 proteins alone have not been colocalized yet. Knock-out mutants of both Rab5 proteins are currently under construction to elucidate

their functional role in *U. maydis*. In addition, a homologue of Rab4 could be identified which does not seem to be conserved among ascomycete fungi but can be found in basidiomycetes. Rab4 mediates endocytic recycling and has been associated with microtubule-dependent endosome transport and regulation of molecular motors (Bielli et al., 2001; Bananis et al., 2003). Microtubule-dependent endosomal transport has also been described for *U. maydis* (Wedlich-Söldner et al., 2002) while it is not known in the ascomycete *S. cerevisiae*. The actual role of Rab4 in *U. maydis* will have to be elucidated.

3.2 The t-SNARE Yup1

Nevertheless, the presence of the whole endocytic machinery is not very surprising. It is in line since previous studies, using the temperature sensitive mutant of the endosomal t-SNARE Yup1, already suggested a function for endocytosis in the maintenance of cell morphology and regulated membrane turnover in *U. maydis* (Wedlich-Söldner et al., 2000). These findings also identified Yup1 as an important player for endocytosis in *U. maydis*.

Yup1 had been colocalised with the endocytic marker dye FM4-64 on bidirectionally moving EE (Wedlich-Söldner et al., 2000) but molecular evidence for a function on EE was missing. The existence of the early endosome specific RabGTPases, Rab4 and Rab5, in the *Ustilago* genome allowed a refined characterisation of the localisation for Yup1. Colocalisation of Yup1-RFP_2 and homologues of the early endosomal markers Rab4 (van der Sluijs et al., 1992) and Rab5 (Bucci et al., 1992; Pfeffer, 2001) suggested that it is indeed very likely that Yup1 functions as a t-SNARE on EE. However, it was obvious that in addition to colocalisation of the proteins, independent Rab-GFP signals were observed and Yup1-RFP also localised to the vacuole. The vacuolar localisation of Yup1-RFP is not an overexpression artefact but suggests for additional functions of Yup1. This is further supported by the results of complementation assays in the yeast *vam7* deletion mutant.

Vam7 is a SNARE protein of *S. cerevisiae* (Wada and Anraku, 1992; Ungermann and Wickner, 1998) that shares high homology with Yup1. Similarly to Yup1, Vam7 contains a t-SNARE- and a PX domain but functions in homeotypic vacuole fusion (Wada and Anraku, 1992; Sato et al., 1998) and fusion of vesicles with the vacuole (Sato et al., 1998), whereas Yup1 acts on EE (Wedlich-Söldner et al., 2000 and

above). Interestingly, substitution of *vam7Δ* with Yup1 complemented the vacuole fusion defect indicating that both proteins share a common task on vacuoles. This is particularly surprising since vacuoles appear normal in the *yup1*^{ts} mutant (not shown). On the other hand, Vam7 could not substitute for Yup1 arguing for a greater functional competence of Yup1, including a specific role on EE. It might also be possible that Yup1 additionally functions as a component of a second SNARE membrane complex mediating fusion of endocytic vesicles with the vacuole.

3.3 *Yup1*- mediated endocytosis

The localisation on EE and the predicted function as a t-SNARE (Wedlich-Söldner et al., 2000) suggest that Yup1 acts during fusion of incoming vesicles with their target - the EE in *U. maydis*. Two cargos that are transported in this pathway are the pheromone receptor Pra1 and the myosin chitinsynthase Mcs1. In *yup1*^{ts} cells Pra1-GFP and GFP_3-Mcs1 are internalised but accumulate in small, very likely primary endocytic vesicles within the cytoplasm and are not found in the vacuole. A similar phenotype was reported in *rcy1*Δ cells of *S. cerevisiae*, where an accumulation of the pheromone receptor Ste2 was found in an uncharacterised endocytic compartment (Wiederkehr et al., 2000). The observations imply that Yup1 mediates the fusion of the incoming primary endocytic vesicles with EE and that it determines further sorting of Pra1 and Mcs1 into the degradation pathway. Although it has not yet been characterised whether *U. maydis* possesses an endocytic recycling compartment (compare to Fig. 1), the lack of input into EE might also affect recycling either directly from EE or from an endocytic recycling compartment (Fig. 30).

3.4 Endocytosis of the pheromone receptor Pra1

The second main focus of this work, after providing additional proof for the existence of endocytosis, was to elucidate the role of endocytosis for pathogenic development of *U. maydis*. The temperature sensitive *yup1*^{ts} mutant, which had been confirmed for a function on EE, was used as a tool in this characterisation. *Yup1*^{ts} cells were applied in assays testing for cell-cell recognition, conjugation tube formation, cell-cell fusion and host plant infection and invasion.

It was determined that *yup1*-mediated endocytosis is already crucial for the initial steps of cell-cell recognition that depend on pheromone perception. Key player during pheromone perception is the G-protein coupled transmembrane receptor Pra1 (Bölker et al., 1992). Similar to the yeast pheromone receptors Ste2 and Ste3 (Davis et al., 1993; Kaksonen et al., 2003), Pra1-GFP is constitutively endocytosed in the absence of pheromone ligand. Upon pheromone stimulation, the expression of Pra1-GFP is upregulated (Urban et al., 1996a) and the fusion protein is concentrated at the tip of conjugation hyphae that are formed in response to pheromone signalling. Pra1 is endocytosed in a *yup1*-mediated fashion but internalisation of Pra1 is not necessary for a function in pheromone signalling.

The data suggest that Pra1-GFP very likely cycles between early endosomes and the plasma membrane. A significant amount of Pra1-GFP is recycled during conjugation hyphae formation ($P<0.0001$). Nevertheless, the amount of the recycled receptor (about 40% of the total amount) seems to be relatively small in comparison to the whole amount of Pra1-GFP that is present at the tip of conjugation hyphae. The *S. cerevisiae* ABC-transporter Ste6 has a similar recycling behaviour (Losko et al., 2001). It is mainly routed to the vacuole while only a minor part recycles back to the plasma membrane. Considering the artificial experimental setup additional experiments will strengthen this evidence for Pra1 recycling.

Based on these findings it is suggested that a functional relation between endocytic recycling of Pra1 and pheromone perception exists in *U. maydis* (Fig. 30). In the absence of functional *yup1*-mediated endocytosis the accumulation of Pra1-GFP in primary endocytic vesicles leads to the depletion of the pheromone receptor molecules from the plasma membrane early during pheromone ligand binding. Ligand bound Pra1-GFP is not sorted into EE and can neither be degraded nor undergo recycling. At the same time secretion of the pheromone receptor is not sufficient to recognize the partner pheromone, which is the reason for the pheromone perception defect of the *yup1*^{ts} mutant. This conclusion is supported by the observation that high levels of additional Pra1 can rescue the pheromone perception defect of the *yup1*^{ts} mutant.

Thus, recycling of the pheromone receptor might ensure a certain level of receptor at the plasma membrane, which seems to be crucial for cell-cell recognition during initial pheromone perception. It might be that recycling becomes less important in the course of pheromone perception, which would explain why less than half of the receptor

molecules are recycled in conjugation hyphae (see above). However, *U. maydis* needs a continuously high pheromone stimulation otherwise it reverts to the haploid growth form similar to the situation in *S. cerevisiae* (Jenness and Spatrick, 1986). The closest homologue of Pra1 in *S. cerevisiae*, Ste3, is also constitutively endocytosed and after ligand-induced endocytosis recycles back to the plasma membrane (Chen and Davis, 2000). This mechanism allows the cell to reuse the receptor. In addition, the transport back to the site of ligand binding would allow the cell to polarise the receptor molecules in the direction of the pheromone source (Chen and Davis, 2000). Recycling would therefore ensure continuous growth in a pheromone gradient towards the partner cell (Snetselaar et al., 1996). This polarized growth, including the polarized receptor cap, is seen in confrontation assays (not shown) but, surprisingly, also exists in *in vitro* assays with synthetic pheromone present from all directions. Therefore, polarized growth seems to be a default program elicited by the fungus. It questions whether endocytosis occurs explicitly at the hyphal tip or whether it takes place over the whole cell periphery.

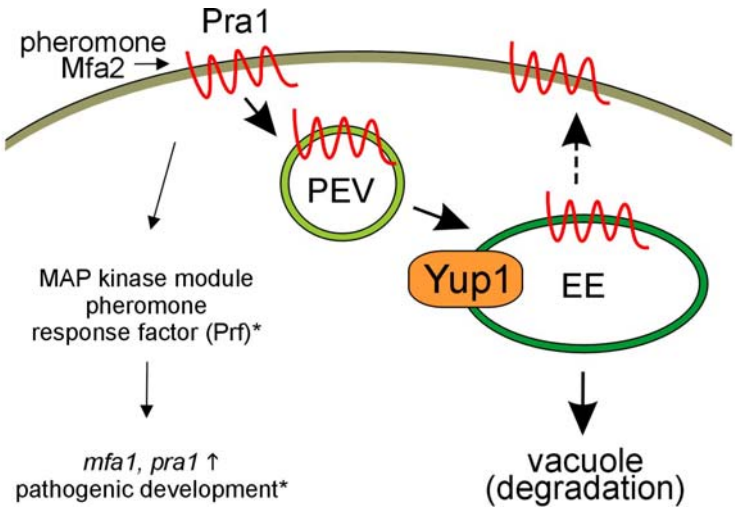

Figure 30. Present view of Yup1 function during Pra1 endocytosis in *U. maydis.*

After pheromone binding, ligand bound pheromone receptor is internalised in primary endocytic vesicles (PEV). Yup1 functions during fusion of incoming PEVs with early endosomes (EE). Pra1 is recycled from EE and transported back to the plasma membrane. It has not yet been determined whether an endosomal sorting compartment and an endosomal recycling compartment (both belong to early endosomes, compare to Figure 1) exist in *U.maydis*. The additional role of Yup1 on vacuoles is not included. * Summarised by Kahmann and Kämper, 2004).

3.5 Additional roles for yup1-mediated endocytosis

The data summarized here suggests that endocytosis is already crucial during the first step required for the initiation of pathogenic development in *U. maydis*. However, it cannot be concluded directly that the lack of pheromone perception finally leads to the loss of virulence. Therefore the requirement for endocytosis beyond pheromone perception has been elucidated.

The first attempt in this direction was a cross of compatible *yup1*^{ts} cells with increased pheromone receptor levels. This was based on the assumption that Pra1 and Pra2 undergo endocytosis using similar *yup1*-dependend pathways. Consistently, overexpression of Pra1 and Pra2 restored pheromone perception and induced the formation of conjugation hyphae (only shown for Pra1 in Fig. 23A). However, it was a clear indication that several other defects must follow pheromone perception since complemented *yup1*^{ts} cells were still non-pathogenic and also the use of a solopathogenic *Ustilago* strain (Bölker et al., 1995) carrying the *yup1*^{ts} mutation (data not shown) did not restore pathogenicity.

The loss of pathogenicity in *yup1*^{ts} mutants could in the end be determined as the sum of the requirement for *yup1*-mediated endocytosis in cell-cell fusion, spore formation and spore germination (Fig. 31). Plant infection and colonisation were not affected in *yup1*^{ts} mutants although microscopic observation during all developmental processes, very clearly indicated the morphological defects that were previously described for haploid cells and dikaryotic filaments of the *yup1*^{ts} mutant (Wedlich-Söldner et al., 2000). Presently, it can only be speculated on the cargos or components that are not sufficiently endocytosed or recycled during these developmental steps. Several components required for cell fusion have been identified in the yeast *S. cerevisiae* (summarized in White and Rose, 2001), It remains to be elucidated whether these compounds are present in *Ustilago* and if so, whether they are endocytosed and recycled in a *yup1*-dependent fashion. One possible candidate would be the yeast alpha factor transporter Ste6, which undergoes endocytic recycling (Kelm et al., 2004; Schmitz et al., 2005) and has additional roles in cell-cell fusion (Elia and Marsh, 1996). A homologue of Ste6 is present in *Ustilago maydis*. Moreover, chitin synthases that are mediators of cell wall formation and integrity are important candidates to be further elucidated. They undergo endocytosis and recycling in *S. cerevisiae* (Ziman et al., 1996; Ziman et al., 1998) and are required for maturation of ascospores of

Schizosaccharomyces pombe (Arellano et al., 2000). Preliminary results on endocytosis of the myosin chitin synthase Mcs1 already indicate a similar situation in *U. maydis*. Finally, the observations that teliospore germination in *U. maydis* depends on endocytosis are supported by experiments in *Magnaporthe grisea* germlings, where it was shown that FM4-64 is actively taken up during germination of conidia (Atkinson et al., 2002). Nevertheless, it remains to be seen whether the analysed components of the *yup1*-mediated endocytic pathway and/or several others lead to the observed phenotypes.

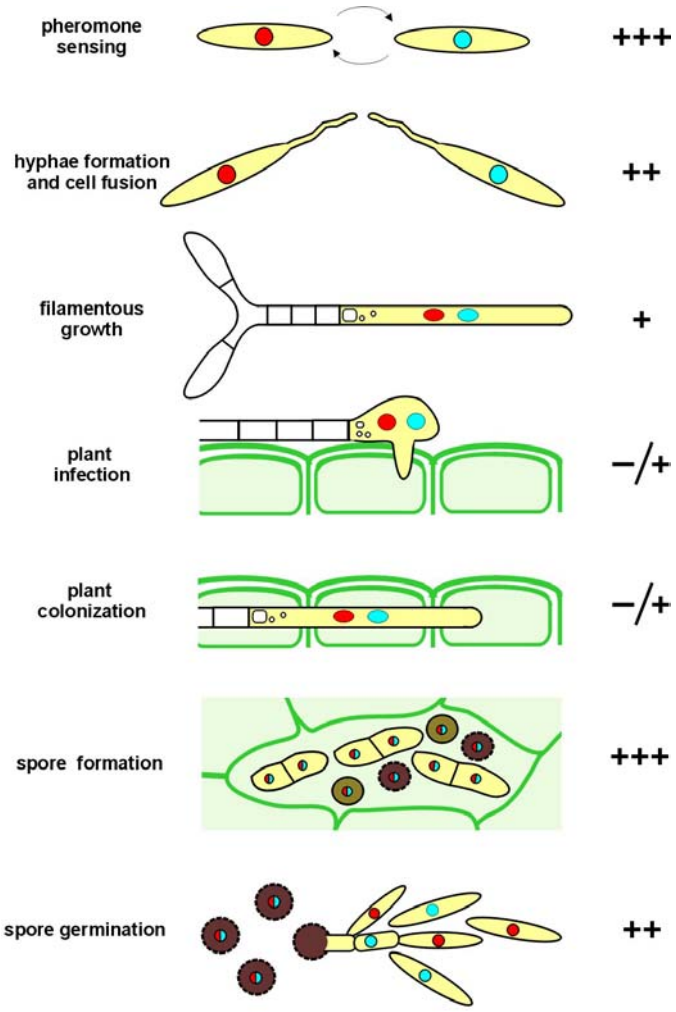

Figure 31. Importance of *yup1*-mediated endocytosis during life cycle and pathogenic development of *Ustilago maydis*.

Pathogenic development of *Ustilago maydis* is initiated by pheromone sensing of two compatible mating partner cells. During this initial step, which is the basis for initiation of the pathogenic program, endocytosis is of essential importance (+++). However, if pheromone perception is functional subsequent formation of conjugation tubes is possible even in the absence of endocytosis while endocytosis is crucial for cell fusion (++). Growth of dikaryotic hyphae relies only to a small extent on endocytosis. Similarly penetration of the plant and growth inside the plant is possible in the absence of endocytosis (+) while again endocytosis becomes necessary again for the formation (+++) and for germination of teliospores (++). (+ and – indicate the relevance of endocytosis during the different developmental steps. +++ indicates great relevance, -/+ indicates little relevance (Figure in cooperation with G. Steinberg).

3.6 Mcs1 is an endocytic cargo in *U. maydis*

The third important aim of the study was to identify endocytic cargos that are essential for growth and pathogenicity of *U. maydis*. As already described above Pra1 is one such essential cargo that requires endocytic recycling after *yup1*-dependent endocytosis in *U. maydis*. Preliminary results from studies of the myosin chitin synthase 1 (Mcs1) suggest another candidate cargo of the *yup1*-mediated endocytic pathway. Very much like for Pra1, localisation and processing of Mcs1 were altered upon shift in *yup1*^{ts} cells to restrictive conditions. This is similar to *S. cerevisiase*, where it was shown that the endocytic t-SNARE Tlg1 mediates trafficking of chitin synthase III (Holthuis et al., 1998). In analogy to Yup1, Tlg1 locates at the intersection between the endocytic and the secretory pathways and is required for delivery of chitin synthase III to the polar growth sites. All together this implies that the accumulation of Mcs1 at the poles of *yup1*^{ts} cells may also consist of primary endocytic vesicles. Similarly to Pra1-containing PEVs, they should stain with FM4-64. To further analyse Mcs1 endocytosis a *yup1*^{ts} strain is currently constructed that expresses both Pra1 and Mcs1 fused to GFP and RFP, respectively. It is the aim to elucidate whether both endocytic cargos are endocytosed in the same primary endocytic vesicles or whether they use independent endocytosis pathways. It will also be interesting to determine whether Mcs1 undergoes recycling. In addition, it needs to be elucidated whether Mcs1, which is especially important during plant invasion (Weber et al., 2006), is related to any of the phenotypes during *U. maydis* pathogenic development.

3.7 Summary and Outlook

The presented work contributes to extend the knowledge on the role of endocytosis in filamentous fungi in general and for pathogenic development of *U. maydis* in particular. Through blast search analysis it was found that basically all important and regulatory components of the endocytic machinery, known from other eukaryotic systems, are present in the *Ustilago* genome. Furthermore, using the mutant of the endocytic t-SNARE Yup1, it could be determined that endocytosis and endocytic recycling are important during pheromone sensing, cell- cell fusion, formation and germination of teliospores. Filamentous growth and plant colonisation are only slightly affected in the absence of endocytosis (Fig. 31). The pheromone receptor Pra1 and the myosin chitin

synthase Mcs1 have been identified as endocytic cargos. However, additional endocytosis mutants are needed to distinguish and to confirm the pleiotrophic phenotype observed with the *yup1*^{ts} mutant.

Therefore, it should also be attempted to characterise the different endocytic compartments in *U. maydis*. At present the overall view of the participating components and cargos is derived from studies in higher eukaryotes and yeast (summarized in Mukherjee et al., 1997; Maxfield and McGraw, 2004). Although very common concepts have been identified (Geli and Riezman, 1998), endocytosis in yeast mainly relies on the actin cytoskeleton while both actin and microtubules (Wedlich-Söldner et al., 2002) participate in endocytosis of *U. maydis*. This suggests a closer relation of endocytosis in *U. maydis* to the endocytic pathways of higher mammalian systems (Oda et al., 1995; Bananis et al., 2000; Bananis et al., 2004). Preliminary observations on the long distance transport of EE in *U. maydis* hyphae also indicate their active transport from the hyphal tip close to the nucleus (G. Fink, personal communication). From that one can also speculate on additional roles of endocytosis for cell signalling. On the one side, endocytosis regulates signalling through the removal of receptors which is a more indirect effect (summarized by Sorkin and Von Zastrow, 2002). On the other side there is a growing body of evidence indicating that endosomes directly act as intermediates in signalling between the plasma membrane and the nucleus (Miaczynska et al., 2004). This represents a whole new area of research and although Pra1 endocytosis is not required for signalling endocytosis of other cargoes might be. Analysis and characterisation of the endosomal compartments, e.g. isolation and purification of endocytic vesicles, will in the end allow the advanced search for additional endocytic cargos. In this respect, it should be of particular interest to identify receptors for plant signals or nutrients that are active during plant invasion of *U. maydis.*

4 Materials and Methods

4.1 Supplies and Source of Supplies

4.1.1 Chemicals, Buffers and Solutions, Enzymes, Kits

All chemicals used in this study were obtained from Fluka, Merck, Molecular Probes (Invitrogen), Roth and Sigma.

Restriction enzymes and the Phusion Taq-Polymerase as well as the Quick Ligase were obtained from New England Biolabs (NEB) and were used as recommended. Standard buffers and solutions were made after (Ausubel et al., 1987; Sambrooke et al., 1989). Specific buffers are listed with the corresponding method.

The following kits were used regularly and as recommended by the supplier: JetQuick PCR Purification Kit (Genomed) for purification of PCR products. JETquick DNA clean-up kit (Genomed) for purification of plasmids. The TOPO TA Cloning Kit (Invitrogen) was used to directly clone PCR products. The Quiagen MiniPrep Kit (Qiagen) was used to isolate and purify plasmid DNA before sequencing.

4.1.2 Plasmids and plasmid constructs

Table 4. Plasmids used for cloning and expression analysis

Plasmid	Description	Resistence marker	Reference
pCR®2.1-TOPO®		-	Invitrogen
pCR®4.0-TOPO®		-	Invitrogen
pSL1180		-	Pharmacia
pNEB-Ble(+)	*P*hsp70-ble-*T*trpC	B	(Brachmann, 2001)
pNEB-Ble(-)	*P*hsp70-ble-*T*trpC	B	(Brachmann, 2001)
pSL-Ble(+)	*P*hsp70-ble-*T*trpC	B	(Brachmann, 2001)
pSL-Ble(-)	*P*hsp70-ble-*T*trpC	B	(Brachmann, 2001)
pNEB-Cbx(+)	*P*ip-ip^R-*T*ip	C	(Brachmann, 2001)
pNEB-Cbx(-)	*P*ip-ip^R-*T*ip	C	(Brachmann, 2001)
pSL-Cbx(+)	*P*ip-ip^R-*T*ip	C	(Brachmann, 2001)
pSL-Cbx(-)	*P*ip-ip^R-*T*ip	C	(Brachmann, 2001)
pNEB-Nat(+)	*P*gap1-nat1-*T*cyc1	N	(Brachmann, 2001)
pNEB-Nat(-)	*P*gap1-nat1-*T*cyc1	N	(Brachmann, 2001)
pSL-Nat(+)	*P*gap1-nat1-*T*cyc1	N	(Brachmann, 2001)
pSL-Nat(-)	*P*gap1-nat1-*T*cyc1	N	(Brachmann, 2001)
pNEB-Hyg(+)	*P*hsp70-hph-*T*hsp70	H	(Brachmann, 2001)
pNEB-Hyg(-)	*P*hsp70-hph-*T*hsp70	H	(Brachmann, 2001)
pSL-Hyg(+)	*P*hsp70-hph-*T*hsp70	H	(Brachmann, 2001)
pSL-Hyg(-)	*P*hsp70-hph-*T*hsp70	H	(Brachmann, 2001)
pNEBUH	*P*hsp70-hph-*T*hsp70, Uars	H	(Weinzierl, 2001)
pRS316	URA3, CEN6	ura	(Sikorski and Hieter, 1989)
p123	*P*otef-egfp-*T*nos	C	Christian Aichinger, unpublished
pCU4	*P*otef-sgfp-*T*nos	C	(Brachmann et al., 2001)
pYup1SG2	*P*otef-yup1-sgfp-*T*nos	C	(Wedlich-Söldner et al., 2000)
poGFP$_3$Mcs1	*P*otef-3gfp-mcs1-*T*nos	C	Isabella Weber, unpublished
pmfa1GFP	*P*mfa1-egfp	C	(Spellig et al., 1996)
pPM1	P*otef-Pra1, mfa2*	C	Philip Müller
pOPra2	P*otef-Pra2*	C	Philip Müller
pPra1-GFP	*Pra1-gfp*	H	Hedwich Teunissen
potefGFPrab5a	P*otef-gfp*-rab5a-	C	Isabel Schuchardt, (Fuchs et al., 2006)
potefGFPrab5b	P*otef-gfp*-rab5b-	C	Isabel Schuchardt

Resistence marker: C, carboxin; B, Phleomycin; H, hygromycin, N, ClonNat; ble-gene of *Streptoalloteichus hindustanus*; trpC-terminator of *Aspergillus nidulans*; nat1-gene of *Streptomyces noursei*; *gap1*-promoter of *U. maydis*; *crg1*-promoter of U. maydis; *mfa1*-promoter of *U. maydis*, *cyc1*-terminator of; *hph*-gene of *E. coli*; *hsp70*-promoter from *hsp70*-Terminator of *U. maydis*; *otef*-Promoter of *U. maydis*; *Uars* autonomously replicating sequence of *U. maydis*; *URA3*-gene of *S. cerevisiae*; *CEN6* centrosome marker of *S. cerevisiae*, *Pra1* and *Pra2*-genes of *U. maydis*, *GFP*-green fluorescent protein, Mcs1, myosin chitin synthase of *U.m.*

4.1.3 Plasmids constructed during this work

All plasmid numbers correspond to the Steinberg Lab Plasmid collection.

Potef-Yup1-2RFP_cbx (#303) (Lenz et al., 2006)

This plasmid contains the Yup1 gene C-terminally tagged with a double RFP tag (RFP_2) under control of the constitutive *otef* promoter. For construction of the plasmid the RFP_2 tag was obtained from plasmid #3071 as an Nco I-Not I fragment and was ligated into the p123 vector which was previously opened with NcoI and NotI. The resulting plasmid (potef-2RFP-Tnos_cbx #300) was opened with Nco I and dephosphorylated. The Yup1 gene was PCR amplified using primers RS1 with an Nco I and RS2 with a BspH I restriction site (Wedlich-Söldner et al., 2000), partially digested accordingly and ligated into the previously opened vector.

Potef-Pra1-eGFP-Tnos_cbx (#320)

This plasmid contains the Pra1 gene C-terminally tagged with eGFP under control of the constitutive *otef* promoter. A 1474 bp BstB I-Afl II fragment of plasmid #304 and a 1532 bp BstB I-Not I fragment of pPM1 (#321) were ligated into pCU4 which had been opened with Not I and Afl II thereby the ORF of the Pra1 gene was inserted by combination of the N-terminal and the GFP-tagged C-terminal region of the gene which is terminated by the *nos*-terminator in pCU4.

pmfa_RFP_Ble (#341)

This plasmid contains the reporter construct of monomeric RFP under control of the *mfa1*-gene promoter. A 1950bp mfa-RFP fragment was generated by digestion of plasmid pmfa_RFP_cbx (#340) with Sph I and Bgl II. This fragment was inserted in pNEB Ble(+) Pmfa_eGFP (#499) which had previously been opened with Sph I and Bgl II and did not contain the pmfa-eGFP fragment anymore.

pSLYup1_2RFP_hom_hyg (#369)

This plasmid contains the Yup1 gene C-terminally tagged with RFP_2 for homologous integration in the *U. maydis* genome. For plasmid construction the Yup1-2RFP fragment of 2258 bp was cut out of potefYup1-2RFP_Hyg (#305) with BsiW I and Afl II. This fragment was ligated into pSL-yup1-RFP_Hyg (#357) which had been opened with BsiW I and Afl II and deleted for the Yup1-single RFP 1540 bp fragment.

p123otefPra1_cbx (#375)

This plasmid contains the *Pra1* – gene under control of the constitutive *otef*-promoter. A 2647 bp Hind III - EcoR I fragment containing the *otef*-promoter, the *Pra1* ORF and the *nos*-terminator was cut out of pPM1. This fragment was inserted into p123, which had been digested with Hind III and EcoR I and was deleted for the otef-eGFP-Tnos insert.

prab4-GFP_3Rab4 (#392)

This plasmid contains the Rab4 gene under control of its own promoter N-terminally fused with triple GFP. The promoter of Rab4 was PCR amplified with primers UF42 (ATCGACATGTTCGCGATAATCCTCTGGAC) and UF43 (ATTCGCGGCCGCA TCGTCGTCTTCAAACG) containing a Pci I and a Not I site, respectively, and subsequently digested with the these enzymes. The Rab4 ORF was PCR amplified using primers UF55 (TAGCCATGGCCGCAGCATACGACTT) and UF41 (CGTAGGTACCCAC GGTAACGTCGGACGGC) containing an Nde I and an Kpn I site, respectively, and digested afterwards with these enzymes. The ORF fragment was subcloned (#377) and cut out as Nde I and Acc65 I fragment. The promoter, a triple-GFP Nco I- Nde I fragment and the ORF fragment were ligated into p123, which had previously been opened with Acc65 I and Not I.

potef2RFP-tNos_Hyg (#395)

This plasmid contains a double RFP tag under control of the constitutive *otef*-promoter for cytoplasmic expression of RFP. The plasmid was generated by resistance marker exchange of p123_2RFP_cbx (#300) to hygromycin resistance. Therefore the *otef*-

2RFP-T*nos* fragment of 2656bp was cut from plasmid #300 and ligated into pSL-Hyg (+) (#19), which was opened with Acc65 I, and Hpa I.

potef3GFP_Tnos_hyg (#399)

This plasmid contains a triple GFP tag under control of the constitutive *otef*-promoter for cytoplasmic expression of GFP. The plasmid was generated by the exchange of the resistance marker gene from cbx to hyg of potef3GFP_Tnos_cbx (#325). A 3368 bp Acc65 I – BglII fragment was ligated into pSL-otef-YFP_hyg which had been opened with Acc65 I and BglII and was therby deleted for the 1934bp otef-YFP insert.

pNEBUH_otefVam7 (801)

This self-replicating plasmid contains the *S. cerevisiae* Vam7 gene under control of the constitutive *otef* Promoter. The Vam7-ORF was PCR-amplified with primers UF60 (GATCCATGGCAGCTAATTCTGTAG) and UF61 (TACGAATTCGATTCCTTTT CACCGTGGCC) thereby adding a 3` Nco I site and a 5´ EcoR I site to the sequence. The PCR product was digested with Nco I and EcoR I. This fragment and the 934 bp Hind III-Nco I *otef*-Promoter fragment of p123 were ligated into pNEBUH, which had been opened with Hind III and EcoR I.

pRS_ura3_Yup1 (803)

This plasmid is a self-replicating CEN6 plasmid containing the Yup1 gene under control of the *S. cerevisiae URA3* promoter of the gene. The Yup1-ORF was obtained as a 565 bp BamH I- Sph I fragment from pYup1SG2 (#69) and a 1015 bp Sph I-Spe I fragment from pCM54-yup2 (#66) also containing the Yup1-terminator. The URA3 promoter sequence was obtained as a Sal I-BamH I fragment of pTK209 (kindly provided by S. Brückner /AG Mösch). Both fragments were ligated into the vector pRS316 (kindly provided by S. Brückner /AG Mösch), which had been opened with Sal I and Spe I.

4.1.4 Strains

Table 5. Strains used in this study

Strains/plasmids	Genotype	reference
FB2GRab5aYup1R$_2$	a2b2/ *pOGFPRab5a / pOyup1R$_2$*	this study
FB2GRab5bYup1R$_2$	a2b2/ *pOGFPRab5b / pOyup1R$_2$*	this study
FB1G$_3$Rab4Yup1R$_2$	a1b1/ *prab4-GFP$_3$Rab4 / pOyup1R$_2$*	this study
FB1Yup1R$_2$	a2b2 yup1-rfp$_2$, hyg^R	this study
SEY6210	MATα leu 2-3, 112 ura3-52 his 3-Δ200 trp1-Δ901 lys2-801 suc2-Δ9	(Robinson et al., 1988)
⊿vam7 +vec	MATα leu 2-3, 112 ura3-52 his 3-Δ200 trp1-Δ901 lys2-801 suc2-Δ9 vam7::HIS3 / pBR316	this study
⊿vam7+YUP1	MATα leu 2-3, 112 ura3-52 his 3-Δ200 trp1-Δ901 lys2-801 suc2-Δ9 vam7::HIS3 / pBR316YUP1	this study
FB2+Vektor	a2b2 /pNEBUH	this study
FB2Yup1^{ts} + Vektor	a2b2 yup1^{ts} / *pNEBUH*	this study
FB2Yup1^{ts} + Vam7	a2b2 yup1^{ts}/ *pNEBUH_OVam7*	this study
FB1	a1b1	(Banuett and Herskowitz, 1989)
FB2	*a2b2*	(Banuett and Herskowitz, 1989)
FB1Yup1^{ts}	*a1b1 yup1^{ts}*	(Wedlich-Söldner et al., 2000)
FB2Yup1^{ts}	*a2b2 yup1^{ts}*	(Wedlich-Söldner et al., 2000)
FB1mG	*a1b1/* pmfa1GFP	(Spellig et al., 1996)
FB1Yup1^{ts}mG	*a1b1 yup1^{ts}* /pmfaGFP	this study
FB1Pra1G	*a1b1 pra1-gfp, hyg^R*	Hedwich Teunissen
FB1Pra1G Yup1R	*a1b1 pra1-gfp, hyg^R, /* pOyup1R$_2$	this study
FB1Yup1^{ts}Pra1G	*a1b1 yup1^{ts} pra1-gfp, hyg^R*	this study
FB1Yup1^{ts}oPra1G	*a1b1 yup1^{ts} pra1-gfp, hyg^R* /pOPra1GFP	this study
FB2rGTub1	*a2b2 /* P*crg-gfp-tub1*	(Steinberg et al., 2001)
FB1Yup1^{ts}mRPra1G	*a1b1 yup1^{ts} pra1-gfp, hyg^R* /pmfaRFP	this study
FB1Yup1^{ts}mRoPra1G	*a1b1 yup1^{ts} pra1-gfp, hyg^R* /pmfaRFP / pOPra1GFP	this study
FB1oPra1	*a1b1 /* pOPra1	this study
FB2oPra2	*a2b2 /* pOPra2	this study
FB1Yup1^{ts}oPra1	*a1b1 yup1^{ts}/* pOPra1	this study
FB2Yup1^{ts}oPra2	*a2b2 yup1^{ts} /* pOPra2	this study
FB1oPra1_G	*a1b1 /pOPra1/* pOGFP$_3$	this study
FB2oPra2_R	*a2b2 /pOPra2/* pORFP$_2$	this study
FB1Yup1^{ts}oPra1_G	*a1b1 yup1^{ts} /* pOPra1/pOG	this study
FB2Yup1^{ts}oPra2_R	*a2b2 yup1^{ts} /* pOPra2/pOR	this study
FB1oGMcs1 oYup1R	*a1b1 /* pOGFP$_3$Mcs1 / pOyup1R$_2$	this study
FB1Yup1^{ts}oGMcs1 Yup1R	*a1b1 yup1^{ts} /* pOGFP$_3$Mcs1 / pOyup1R$_2$	this study

a, *b*, mating type loci; P, promoter; -, fusion,; *ble^R*, phleomycine resistance; *cbx^R*, carboxin resistance; *hyg^R*, hygromycin resistance; /, ectopically integrated; *crg* inducible Ustilago promoter, *otef*, constitutive promoter; *egfp*, enhanced green fluorescent protein; *rfp*, red fluorescent protein; *pra1*, pheromone receptor 1; m, *mfa1*, mating pheromone 1; *Uars*, Ustilago autonomously replicating sequence; *yup1^{ts}*, temperature-sensitive allele of the endosomal t-SNARE *yup1; Mcs1*, myosin chitin synthase of *U.m.*

4.1.5 *E. coli* strains

For all cloning and plasmid construction *E. coli* strain DH5α (Hanahan, 1985) was used.

4.2 Genetic, microbiological and cell biology methods

4.2.1 Standard Molecular Biology Methods

All standard molecular biology methods were performed as described in (Hanahan, 1985; Sambrooke et al., 1989; Guthrie and Fink, 1991).

For Transfer and Detection of DNA (Southern Blot Analysis) the methods of Southern, (1975) were used. DNA probes were labelled using the PCR-DIG labelling mix (Roche).

4.2.2 Cultivation of *Escherichia coli*

E. coli was grown in liquid dYT medium or on YT-agarose plates (Ausubel et al., 1987; Sambrooke et al., 1989). Antibiotics were added to the medium at the following concentrations Ampicillin (100 µg/ml), Kanamycin (40 µg/ml) and X-Gal (40 µg/ml) if not stated otherwise. Liquid cultures of *E. coli* were incubated at 37°C with shaking (200 rpm) agarose plates with *E. coli* were incubated at aerob conditions at 37°C. Glycerinstocks were made from exponentially growing cultures and mixed with dYT-Glycerin at a 1:1 ratio and stored at –80°C. To grow cultures from glycerin stocks they were streaked on antibiotic containing YT agarose plates and were incubated at 37°C.

4.2.3 Cultivation of *Saccharomyces cerevisiae*

S. cerevisiae strains were grown in YPD medium (Sambrooke et al., 1989) or in Drop out medium –URA for selection.

Drop-out medium (-ura)

1,34 g Yeast nitrogen base without amino acids
0,28 g Drop-out mix (-ura, -trp, -his, - leu)
filled up to 200 ml with H_2O
4 ml of 50% (w/v) glucose (f. c. 1%) after autoclaving

4.2.4 Cultivation of *Ustilago maydis*

Ustilago maydis strains were grown at 28°C in liquid medium (see below) with shaking (200 rpm) to a density of OD_{600}= 0,5 ~ 0,6. Temperature sensitive strains (for details see Table 5) were incubated in the same medium at 22°C overnight.

For inhibition of Yup1 function, temperature sensitive $yup1^{ts}$ strains were shifted from permissive temperature (22°C) to restrictive temperature (34°C) and incubated for two hours before starting experimental set-ups.

Glycerin stocks were prepared from exponentially growing cultures and mixed with NSY-Glycerin (see below) at a 1:1 ratio and stored at –80°C. To grow cultures from glycerin stocks they were streaked on agarose plates and were incubated at 28°C.

The following media and additives were used to cultivate and store *U. maydis*:

$YEPS_{light}$ (modified after (Tsukuda et al., 1988)

10 g Yeast Extract
10 g Pepton
10 g Saccharose
filled up to 1lwith H_2O

CM Complete Medium (Holliday, 1974)

1,5 g NH_4NO_3
2,5 g casamino Acids
0,5 g DNA
1 g yeast extract
10 ml vitamin solution (see below)
62,5 ml salt solution (see below)
filled up to 980 ml with H_2O
pH to 7.0 with NaOH
20 ml of 50% (w/v) glucose (f. c. 1%)
after autoclaving

Salt- solution (Holliday, 1974)

16 g KH_2PO_4
4 g Na_2SO_4
8 g KCl
4 g $MgSO_4$ x 7 H_2O
1.32 g CaCl x 2 H_2O
8 ml trace elements solution (see below)
filled up to 1 l with H_2O, filter sterilized

Trace elements solution (Holliday, 1974)

60 mg H_3BO_3
140 mg $MnCl_2$ x 4 H_2O
400 mg $ZnCl_2$
40 mg $NaMoO_4$ x 2 H_2O
100 mg $FeCl_3$ x 6 H_2O
40 mg $CuSO_4$ x 5 H_2O
filled up to 1 l with H_2O, filter sterilized

PD Potato dextrose agar with active charcoal

24 g Potato dextrose broth
10 g charcoal
20 g Bacto Agar
filled up to 1 l with H_2O

NSY- Glycerin

8 g Bacto nutrient broth
1 g Yeast extract
5 g Sucrose
800 ml 87% glycerin
filled up to 1l with H_2O

Vitamin solution (Holliday, 1974)

100 mg Thiamine
50 mg Riboflavin
50 mg Pyridoxine
200 mg Calcium pantothenate
500 mg p-Amino benzo acid
200 mg Nicotinic acid
200 mg Choline chloride
1 g *myo*-inositol
filled up to 1 l, filter sterilized

If arabinose was required as sole carbon source in the medium 40 ml / 1 l of 25% arabinose solution was added to the media after autoclaving (f. c. 1%). For solid medium agarose was added to a final concentration of 2%. Additives to the medium were used in the following concentrations: carboxine (2 µg/ml), ClonNAT (150 µg/ml), hygromycin (200 µg/ml) and phleomycin (40 µg/ml). Phleomycin containing medium was additionally buffered with Tris-Cl, pH 8.0 to a final concentration of 100 mM to avoid inactivation of the drug due to acidification of the medium by *U. maydis*.

4.2.5 Induction of inducible promoters

The use of inducible promoters allows the controlled induction and repression of genes and alleles by a change of the cultivation medium. Inhibition of genes under the crg1 promoter occurs in CM-Glu medium where glucose is the sole carbon source. Inducible conditions are given when arabinose is the sole carbon source in CM-Ara medium in case of the *crg1* promoter. For change a medium change the cells were grown to an OD_{600} ~ 0.5 at 28°C. Cells were collected in by centrifugation at 2400 rpm for 5 min at RT. The supernatant was discarded and the cells were resuspended in new medium and transferred into clean culture flasks. Cultures were incubated again at 28°C with shaking (200 rpm).

4.2.6 Determination of cell density in *Ustilago maydis*

The cell density of liquid *U. maydis* cultures was determined using a Novosec II Photometer (Pharmacia Biotech) at an optical density of 600 nm (OD_{600}). To ensure a

linear reference the cell suspensions were diluted to a value below OD_{600} = 0.8. The corresponding culture medium was used as a reference. A culture density of OD_{600}=1 correlates to about 1-5 x 10^7 cells / ml.

4.2.7 Transformation of *Ustilago maydis*

Transformation of *U. maydis* strains was done as described previously in (Schulz et al., 1990). Briefly, *U. maydis* cells were grown overnight in $YEPS_{light}$ medium at 28°C (or 22°C for temperature sensitive strains) to a cell density of OD_{600} 0,6 – 0,8. Cells were harvested by centrifugation (10 min, 3000 rpm, RT) and washed in 25 ml SCS before resuspension in 2 ml SCS containing 3,5 mg / ml Novozyme. Cells were incubated for ~ 10 min at RT to digest the cell wall material. This process was followed under the microscope. After rounding up of the elongated *U. maydis* cells they were washed tree times with ice-cold SCS and centrifuged at 2400 rpm for 8 min at 4°C. This was followed with an additional wash with ice-cold STC. Finally, the protoplast pellet was resuspended in 0,5 ml STC and aliquots of 50 µl were used immediately or stored at -80°C. For transformation of Protoplasts, linearised DNA (5 µg) and 1 µl Heparin were added to the protoplast aliquot and the sample was incubated for 10 min on ice. Subsequently, 500 µl STC/PEG were added and the protoplast mix was incubated for another 15 min on ice. The transformation mix was plated on Regeneration-agar. Transformed colonies appeared after 3-7 days and were singled-out and grown on CM-agar plates containing the appropriate antibiotic. Single colonies were picked and saved on CM-plates.

SCS

20 mM Na-citrate, pH 5,8
1 M Sorbitol
in ddH_2O, filter sterilised

STC

10 mM Tris-Cl, pH 7,5
100 mM $CaCl_2$
1 M Sorbitol
in ddH_2O, filter sterilised

Regeneration-agar

a) Top-agar
1,5% (w/v) Bacto Agar
1M Sorbitol
in YEPS medium
b) Bottom Agar:
similar to a) plus double concentrated antibiotic.

STC/PEG

15 ml STC
10 g PEG 4000

4.2.8 DNA isolation from *Ustilago maydis*

For his method, modified from (Hoffmann and Winston, 1987), 2 ml of *Ustilago* cell suspension grown overnight in $YEPS_{Light}$ were pelleted in 2 ml Eppendorf tubes by centrifugation (1min, 13000 rpm). The supernatant was discarded and 0.3 g glass beads, 400 µl Ustilago lysis buffer and 500 µl phenol-chloroform (1:1) were added. The samples were incubated for ~ 10 min on a Vibrax-VXR shaker (IKA) with full speed. After phase separation for 15 min at 13000 rpm; 400 µl of the top phase of the supernatant were transfered to a new 1.5 µl Eppendorf tube and mixed with 1 ml 100% ethanol. Subsequently the samples were centrifuged for 2 min at 13000 rpm and the pellet was resuspended in 50 µl TE/RNAse A at 55°C and stored at –20°C. 20 µl of DNA was used for Southern Blotting.

Ustilago lysis buffer

50 mM Tris-Cl, pH 7.5
50 mM Na_2- EDTA
1% (w/v) SDS
in ddH_2O

4.2.9 Pheromone stimulation and assay for pheromone perception

The formation of conjugation hyphae was induced by the addition of 0,5 µl synthetic pheromone (a2, stock 2,5µg/µl in dimethyl sulfoxide [DMSO], final concentration $2,5 \times 10^{-3}$ µg/µl; (Szabo et al., 2002) to 500 µl cell suspension in a 2 ml reaction tube and incubation for 6 h at 22°C, 200 rpm. To assay the ability of *yup1*^{ts} mutant strains to form conjugation hyphae and to express P_{Pro}:GFP, pheromone stimulation was induced at 34°C after pre-incubation of control strains and *yup1*^{ts} strains for 2 h (or longer) at 34°C. Conjugation tube formation of FB1Pra1G and FB1Yup1^{ts}Pra1G was allowed for 2 h at permissive temperature (as described above) then strains were further incubated for 2 h at 34°C.

4.2.10 Mating on charcoal

For charcoal mating assays compatible strains were grown to a density of OD_{600} ~ 0.8 and concentrated in H_2O to an OD_{600} ~ 2. They were equally mixed and spotted on

charcoal containing potato-dextrose plates and incubated at 22°C and 34°C, respectively.

4.2.11 Confrontation assays

In order to assay growth of strains towards the mating partner they were strains were grown to a density of OD_{600} ~ 0.8 and concentrated in H_2O to an OD_{600} ~ 5. Subsequently they were spotted across from each other on 2 % water agar slides and incubated over night at 22°C or 34°C before direct observation under the light microscope (Snetselaar et al., 1996).

4.2.12 Plant infection assays and teliospore generation

Pathogenic development of wild-type and *yup1*^{ts} mutant strains were assayed by plant infections of the corn variety Early Golden Bantam (Olds Seeds, Madison,Wis.). Compatible *Ustilago maydis* strains were grown to a density of OD_{600} ~ 0.8 and concentrated in H_2O to an OD_{600} ~ 2. Subsequently they were equally mixed prior to infection. Cell suspensions were injected at the basal stem of 6 day old corn seedlings with a syringe. Infected plants were then incubated at 22°C or 34°C with 16 h light in a phyto-chamber for 14 days. All plant infection assays following the initial infection assays (Fig. 2) were done at 31°C, since the plants tolerated the heat stress better at that temperature than at 34°C. The growth phenotype of *yup1*^{ts} mutant strains was the same at 31°C and 34°C (not shown). For quantification of tumor formation plants with one or more tumors were counted, regardless of tumor size. For time course experiments wild type and *yup1*^{ts} infected plants were incubated for 1-7 days at 22°C each followed by a subsequent shift to 31°C and incubation for additional one and two days.

In order to assay the formation of teliospores or harvest teliospores, plants were incubated for 19 days and thin sections of tissue were observed under the microscope.

4.2.13 Calcofluor staining

Staining of infected plant samples with calcofluor followed the protocol delineated earlier (Weber et al., 2003). Briefly the plant samples were harvested washed in PBS

and incubated in diluted calcofluor solution 1:1000 (10 mg / ml stock in DMSO) for 30 sec and washed again in PBS before direct observation under the microscope.

4.2.14 Chlorazole Black E staining

Chlorazole Black E staining was done as described previously (Brachmann et al., 2003). In brief the plant samples were harvested and placed in 2 ml Eppendorf tubes containing 100 % EtOH and incubated over night or longer until the chlorophyll was removed. Samples were washed with H_2O and incubated in 10 % KOH at 90°C for 3 h. The KOH solution was removed and samples were washed with H_2O before incubation in chlorazole solution (1 part H_2O, 1 part lactic acid, 1 part 98% glycerin and 0.03% chlorazole black E (f. c.) for 1-2 days. The chlorazole solution was removed and samples were stored in 50% glycerin.

4.2.15 Spore germination

Spores were generated through incubation of infected plants at 22°C for about three weeks. Tumors containing spores were dried at 22°C and minced using a mortar and pestle. The tumor material was then incubated in tetracycline solution (5mg/ml stock, GERBU, Gaiberg, Germany) for 30 min before washing in water and incubation in 1.5% Copper(II)sulfate solution (Carl Roth, Karlsruhe, Germany). Samples were washed three times in water and were plated on 2% CM-Glucose containing agar slides and/or on plates with 20 µl each: tetracycline, chloramphenicol (34 mg/ml stock, Carl Roth, Karlsruhe, Germany) and ampicillin (10mg/ml stock, Carl Roth, Karlsruhe, Germany) in 25 ml agar. Slides containing the spore samples were incubated in a moist chamber at 22°C or 34°C.

4.2.16 Colocalization experiments, membrane and vacuole staining

Colocalization of fluorescently labeled proteins was done after fixation with 0.5% formaldehyde (16% stock; Polysciences, Inc., PA, USA) or after cooling of the strains to 10°C. Microscopical observation was done with a pre-cooled objective in order to be able to visualize the slowed otherwise rapidly moving molecules. The plasma membrane was stained by the addition of 1 µM of the endocytic marker dye FM4-64 (stock 16 mM, Molecular Probes, Invitrogen, Karlsruhe, Germany) and the addition of

1% formaldehyde after 20 seconds, thereby inhibiting further endocytosis of the dye. Endocytosis and accumulation of FM4-64 in strain FB1Yup1^{ts}Pra1G was observed after coincubation for 2h at 34°C (after 2 h 22°C and 2 h 34°C treatment). Vacuolar staining was done using CellTracker^{TM} Blue (CMCA) (stock 1 mM, Molecular Probes, Invitrogen, Karlsruhe, Germany) at a final concentration of 100 µM and incubation for 15 min.

Accumulation of the chitin synthase fusion protein was quantified by measuring the average region signal intensity at three different points at the cell periphery (excluding the normal localization sites at the bud periphery)

4.2.17 Inhibitor studies

For all inhibitor experiments 500 µl cell suspension were incubated in a 2-ml reaction tube and latrunculin A (LatA) at 0.1–10 µM (stock 20 mM in DMSO, kindly provided by Dr. Karen Tenney, University of California, Santa Cruz) was added for at least 45 min with gentle shaking. In control experiments the corresponding amount of the solvent DMSO was used.

For inhibition of protein biosynthesis cycloheximide (stock 5 mg/ml in H_2O, Sigma-Aldrich, Steinheim, Germany) was added to a final concentration of 100 µg/ml and cells were incubated for 45 min with gentle shaking at 22°C before addition and further incubation with DMSO or LatA.

4.2.18 Light Microscopy, image processing and quantitative data analysis

For *in vivo* observations, cells from logarithmically growing cultures were placed on a thin 1% agarose-layer and immediately observed using a Zeiss Axioplan II microscope (Zeiss, Jena, Germany). Epifluorescence was observed using filter sets for FITC (BP500/20, FT515, BP535/30) and DsRed (HQ565/30). All microscopical observations were done using a CoolSNAP-HQ CCD camera (Photometrics, Tucson, AZ, USA) controlled by the imaging software MetaMorph (Universal Imaging, Downing Town, PA, USA). All measurements and image processing, including adjustment of brightness, contrast and gamma-values and 2D-deconvolution were performed with MetaMorph and Photoshop (Adobe Systems GmbH, München, Germany). Statistical analysis by

two-tailed t-test at α: 0.05 was carried out using Prism (GraphPad). All values are given as means $\pm$ standard deviation unless otherwise stated.

4.2.19 Vesicle extraction and western blot analysis

Strains FB1Pra1G and FB1yup1^{ts} Pra1G were grown overnight at 22°C 50 ml cells were stimulated with synthetic pheromone as described above in 200ml plastic conical centrifuge tubes for 4 h at 22°C or shifted to 34°C after 2h of stimulation at 22°C. Cultures were then quickly harvested by centrifugation at 4°C for 10 min at 3000 rpm. Cells were resuspended in 10 ml extraction buffer (100 mM PIPES, pH 6,9; 2 mM $MgCl_2$, 1 mM EDTA, 1 mM EGTA) centrifuged again for 10 min at 3000 rpm and washed in 2 ml extraction buffer supplied with complete protease inhibitor (1 tablet / 10 ml buffer; Roche Applied Sciences, Penzberg, Germany), centrifuged again and resuspended in 1 pellet volume extraction buffer with complete mini. Protein extracts were obtained by disruption of the frozen cell suspensions in a mixer mill MM200 (Retsch, Haan, Germany) and centrifuged for 10 min at 16.000 rpm for veiscle observation and 8000 rpm, 4°C in a Biofuge Stratos centrifuge (Kendro, Hanau, Germany). Subsequently protein concentrations were determined using NanoDrop Analysis (Nanodrop, Wilmington, DE, USA). For analysis of Pra1 protein levels samples were supplied with SDS and Triton X-100 to a final concentration of 20% each and incubated on ice for 40 min to extract Pra1 from membranes. Protein concentrations of the supernatants were determined using a Coomassie gel. Supernatants were supplied with 6x Lämmli buffer and incubated at 65°C for 10 min before SDS gel electrophoresis. Proteins were separated in a 10% polyacrylamide gel and transferred onto a nitrocellulose membrane for 60 min at 400 mA in a wet blot chamber. The Anti-GFP antibody (Roche Applied Sciences, Penzberg, Germany) was used 1:5000 to detect GFP-tagged Pra1 fusion proteins according to standard procedures

4.2.20 Electron microscopy studies

Electron microscopy analysis was done in cooperation with Dr. Gerd Hause, University of Halle, Germany. Samples were pheromone treated for 2 h at 22°C before shifting them to 34°C as described above.

After high pressure freezing and cryosubstitution as described in (Straube et al., 2006) pheromone stimulated cells were embedded in K11M (Polysciences Europe, Eppelheim Germany). Ultra thin sections were immunolabelled with a monoclonal anti-GFP-antibody (clones 7.1 and 13.1; Roche Diagnostics, Indianapolis, U.S.A.) and a secondary antibody conjugated with 10 nm gold (G 7777; Sigma, Saint Louis, U.S.A.). The sections were post-stained with uranyl acetate and lead citrate in an EM-Stain apparatus (Leica, Bensheim, Germany) and subsequently observed with an EM 900 transmission electron microscope (Zeiss SMT, Oberkochen, Germany).

4.2.21 Bioinformatic analysis

Protein sequences were downloaded from public databases (http://www.ncbi.nlm.nih.gov/entrez/query.fcgi). For Blast search of homologous proteins to the yeast endocytic machinery components, sequences were blasted against the public *Ustilago* database http://mips.gsf.de/genre/ proj/ustilago/ for e-value determination. In a two way blast approach resulting Ustilago proteins were blasted back against the *S. cerevisiae* database http://mips.gsf.de/genre/proj/ yeast/index.jsp to confirm the obtained hits. For phylogenetic analylsis they were aligned by ClustalX (Thompson et al. 1997). Domain analysis of Rab4 proteins was done by SMART (http://smart.embl-heidelberg.de/). T-SNARE prediction was done using http://us.expasy. org/tools/scanprosite/ . Transmembrane domain prediction was done using (http://www.cbs.dtu. dk/services/TMHMM-2.0/). Phylogenetic dendrograms were constructed by the minimum evolution method (MEGA version 2.1) (Kumar et al., 2001) with a nearest-neighbour joining tree as starting point and 1000 Bootstrap replicates.

4.2.22 Accession numbers

Protein sequence data can be found in GenBank data libraries under the accession numbers: HsRab4 (E34323), HsRab5 (P20339), HsRab6 (G34323), HsRab7 (AAA86640), HsRab9 (AAM21092), HsRab11 (S47169), ScYpt6 (Q99260), ScYpt7 (P32939), ScYpt31 (NP_010948), ScYpt32 (NP_011305), ScYpt51 (P36017), ScYpt52 (NP_012939) ScYpt53 (P36019); GgRab4 (XP_419573.1), DrRab4 (XP_698896.1), DmRab4 (BAA88243.1), Pra1 (EAK83421.1); Pra2 (P31303); Yup1 (AAF62178.1);

Mfa1 (AAA99765.1). The sequence of UmRab5a was obtained from the public Ustilago database (MUMDB: http://mips.gsf.de/genre/proj/ustilago/).

5 Bibliography

Adams, A.E., Botstein, D., and Drubin, D.G. (1991). Requirement of yeast fimbrin for actin organization and morphogenesis in vivo. Nature **354,** 404-408.

Anderson, R.G., Goldstein, J.L., and Brown, M.S. (1977). A mutation that impairs the ability of lipoprotein receptors to localise in coated pits on the cell surface of human fibroblasts. Nature **270,** 695-699.

Aniento, F., Emans, N., Griffiths, G., and Gruenberg, J. (1993). Cytoplasmic dynein-dependent vesicular transport from early to late endosomes. J Cell Biol **123,** 1373-1387.

Arellano, M., Cartagena-Lirola, H., Nasser Hajibagheri, M.A., Dur inverted question markan, A., and Henar Valdivieso, M. (2000). Proper ascospore maturation requires the chs1+ chitin synthase gene in Schizosaccharomyces pombe. Mol Microbiol **35,** 79-89.

Atkinson, H.A., Daniels, A., and Read, N.D. (2002). Live-cell imaging of endocytosis during conidial germination in the rice blast fungus, Magnaporthe grisea. Fungal Genet Biol **37,** 233-244.

Ausubel, F.M., Brenz, R., Kingston, R.E., Moor, D.D., Seidmann, J.G., Smith, J.A., and Strukl, K. (1987). Current Protocolls in Molecular Biology. (John Wiley & Sons, Inc.: USA).

Ayscough, K.R., Stryker, J., Pokala, N., Sanders, M., Crews, P., and Drubin, D.G. (1997). High rates of actin filament turnover in budding yeast and roles for actin in establishment and maintenance of cell polarity revealed using the actin inhibitor latrunculin-A. J Cell Biol **137,** 399-416.

Bananis, E., Murray, J.W., Stockert, R.J., Satir, P., and Wolkoff, A.W. (2000). Microtubule and motor-dependent endocytic vesicle sorting in vitro. J Cell Biol **151,** 179-186.

Bananis, E., Murray, J.W., Stockert, R.J., Satir, P., and Wolkoff, A.W. (2003). Regulation of early endocytic vesicle motility and fission in a reconstituted system. J Cell Sci **116,** 2749-2761.

Bananis, E., Nath, S., Gordon, K., Satir, P., Stockert, R.J., Murray, J.W., and Wolkoff, A.W. (2004). Microtubule-dependent movement of late endocytic vesicles in vitro: requirements for Dynein and Kinesin. Mol Biol Cell **15,** 3688-3697.

Banuett, F., and Herskowitz, I. (1989). Different a alleles of *Ustilago maydis* are necessary for maintenance of filamentous growth but not for meiosis. Proc. Natl. Acad. Sci. U.S.A. **86,** 5878-5882.

Banuett, F., and Herskowitz, I. (1996). Discrete developmental stages during teliospore formation in the corn smut fungus, Ustilago maydis. Development **122,** 2965-2976.

Bartnicki-Garcia, S., Bartnicki, D.D., Gierz, G., Lopez-Franco, R., and Bracker, C.E. (1995). Evidence that Spitzenkörper behavior determines the shape of a fungal hypha: a test of the hyphoid model. Exp Mycol **19,** 153-159.

Behnia, R., and Munro, S. (2005). Organelle identity and the signposts for membrane traffic. Nature **438,** 597-604.

Bielli, A., Thornqvist, P.O., Hendrick, A.G., Finn, R., Fitzgerald, K., and McCaffrey, M.W. (2001). The small GTPase Rab4A interacts with the central region of cytoplasmic dynein light intermediate chain-1. Biochem Biophys Res Commun **281,** 1141-1153.

Bölker, M. (2001). Ustilago maydis - a valuable model system for the study of fungal dimorphism and virulence. Microbiology **147,** 1395-1401.

Bölker, M., Urban, M., and Kahmann, R. (1992). The a mating type locus of *U. maydis* specifies cell signaling components. Cell **68,** 441-450.

Bölker, M., Genin, S., Lehmler, C., and Kahmann, R. (1995). Genetic regulation of mating and dimorphism in *Ustilago maydis*. Can J Bot **73,** 342-352.

Bonifacino, J.S., and Lippincott-Schwartz, J. (2003). Coat proteins: shaping membrane transport. Nat Rev Mol Cell Biol **4,** 409-414.

Bottin, A., Kämper, J., and Kahmann, R. (1996). Isolation of a carbon source-regulated gene from *Ustilago maydis*. Mol Gen Genet **253,** 342-352.

Brachmann, A. (2001). Die frühe Infektionsphase von *Ustilago maydis*: Genregulation durch das bW/bE- Heterodimer. PhD dissertation (LMU, München, Germany).

Brachmann, A., Weinzierl, G., Kämper, J., and Kahmann, R. (2001). Identification of genes in the bW/bE regulatory cascade in *Ustilago maydis*. Mol Microbiol **42,** 1047-1063.

Brachmann, A., Schirawski, J., Müller, P., and Kahmann, R. (2003). An unusual MAP kinase is required for efficient penetration of the plant surface by Ustilago maydis. Embo J **22,** 2199-2210.

Bucci, C., Parton, R.G., Mather, I.H., Stunnenberg, H., Simons, K., Hoflack, B., and Zerial, M. (1992). The small GTPase rab5 functions as a regulatory factor in the early endocytic pathway. Cell **70,** 715-728.

Camacho, L., and Malho, R. (2003). Endo/exocytosis in the pollen tube apex is differentially regulated by Ca2+ and GTPases. J Exp Bot **54,** 83-92.

Carlile, M.J., and Watkinson, S.C. (1994). The Fungi. (London: Academic Press Ltd.).

Chavrier, P., Simons, K., and Zerial, M. (1992). The complexity of the Rab and Rho GTP-binding protein subfamilies revealed by a PCR cloning approach. Gene **112,** 261-264.

Chen, L., and Davis, N.G. (2000). Recycling of the yeast a-factor receptor. J Cell Biol **151,** 731-738.

Ciechanover, A., Schwartz, A.L., and Lodish, H.F. (1983). Sorting and recycling of cell surface receptors and endocytosed ligands: the asialoglycoprotein and transferrin receptors. J Cell Biochem **23,** 107-130.

Cole, L., Orlovich, D.A., and Ashford, A.E. (1998). Structure, function, and motility of vacuoles in filamentous fungi. Fungal Genet Biol **24,** 86-100.

Davis, N.G., Horecka, J.L., and Sprague, G.F., Jr. (1993). Cis- and trans-acting functions required for endocytosis of the yeast pheromone receptors. J Cell Biol **122,** 53-65.

Davis, T.N., Urdea, M.S., Masiarz, F.R., and Thorner, J. (1986). Isolation of the yeast calmodulin gene: calmodulin is an essential protein. Cell **47,** 423-431.

D'Hondt, K., Heese-Peck, A., and Riezman, H. (2000). Protein and lipid requirements for endocytosis. Annu Rev Genet **34,** 255-295.

Elia, L., and Marsh, L. (1996). Role of the ABC transporter Ste6 in cell fusion during yeast conjugation. J Cell Biol **135,** 741-751.

Ellson, C.D., Andrews, S., Stephens, L.R., and Hawkins, P.T. (2002). The PX domain: a new phosphoinositide-binding module. J Cell Sci **115,** 1099-1105.

Fischer-Parton, S., Parton, R.M., Hickey, P.C., Dijksterhuis, J., Atkinson, H.A., and Read, N.D. (2000). Confocal microscopy of FM4-64 as a tool for analysing

endocytosis and vesicle trafficking in living fungal hyphae. J Microsc **198 (Pt 3),** 246-259.

Fuchs, U., and Steinberg, G. (2005). Endocytosis in the plant-pathogenic fungus *Ustilago maydis*. Protoplasma **226,** 75-80.

Fuchs, U., Hause, G., Schuchardt, I., and Steinberg, G. (2006). Endocytosis Is Essential for Pathogenic Development in the Corn Smut Fungus Ustilago maydis. Plant Cell **18,** 1-16.

Garcia-Muse, T., Steinberg, G., and Perez-Martin, J. (2003). Pheromone-induced G2 arrest in the phytopathogenic fungus *Ustilago maydis*. Eukaryot Cell **2,** 494-500.

Geitmann, A., and Emons, A.M. (2000). The cytoskeleton in plant and fungal cell tip growth. J Microsc **198 (Pt 3),** 218-245.

Geli, M.I., and Riezman, H. (1998). Endocytic internalization in yeast and animal cells: similar and different. J Cell Sci **111 (Pt 8),** 1031-1037.

Geuze, H.J., Slot, J.W., and Schwartz, A.L. (1987). Membranes of sorting organelles display lateral heterogeneity in receptor distribution. J Cell Biol **104,** 1715-1723.

Geuze, H.J., Slot, J.W., Strous, G.J., Hasilik, A., and von Figura, K. (1985). Possible pathways for lysosomal enzyme delivery. J Cell Biol **101,** 2253-2262.

Geuze, H.J., Stoorvogel, W., Strous, G.J., Slot, J.W., Bleekemolen, J.E., and Mellman, I. (1988). Sorting of mannose 6-phosphate receptors and lysosomal membrane proteins in endocytic vesicles. J Cell Biol **107,** 2491-2501.

Gillooly, D.J., Raiborg, C., and Stenmark, H. (2003). Phosphatidylinositol 3-phosphate is found in microdomains of early endosomes. Histochem Cell Biol **120,** 445-453.

Girbardt, M. (1957). Der Spitzenkorper von *Polystictus versicolor* (L). Planta **50,** 47-59.

Goldstein, J.L., Anderson, R.G., and Brown, M.S. (1979). Coated pits, coated vesicles, and receptor-mediated endocytosis. Nature **279,** 679-685.

Goldstein, J.L., Brown, M.S., Anderson, R.G., Russell, D.W., and Schneider, W.J. (1985). Receptor-mediated endocytosis: concepts emerging from the LDL receptor system. Annu Rev Cell Biol **1,** 1-39.

Gow, N.A.R. (1995a). Tip growth and polarity. In The growing fungus, N.A.R. Gow and G.M. Gadd, eds (London ; New York: Chapman & Hall), pp. 277-299.

Guthrie, C., and Fink, G.R. (1991). Guide to Yeast Genetics and Molecular Biology. (San Diego: Academic Press).

Hanahan, D. (1985). Techniques for transformation of E. coli. In DNA cloning, a practical approach., D. Rickwood and B.D. Hames, eds (IRL Press), pp. 109-135.

Hepler, P.K., Vidali, L., and Cheung, A.Y. (2001). Polarized cell growth in higher plants. Annu Rev Cell Dev Biol **17,** 159-187.

Higuchi, Y., Nakahama, T., Shoji, J.Y., Arioka, M., and Kitamoto, K. (2006). Visualization of the endocytic pathway in the filamentous fungus Aspergillus oryzae using an EGFP-fused plasma membrane protein. Biochem Biophys Res Commun **340,** 784-791.

Hoffmann, C.S., and Winston, F. (1987). A ten-minute DNA preparation form yeast efficiently releases autonomous plasmids for transformation of *E. coli*. Gene **57,** 267-272.

Hoffmann, J., and Mendgen, K. (1998). Endocytosis and membrane turnover in the germ tube of uromyces fabae. Fungal Genet Biol **24,** 77-85.

Holliday, R. (1974). *Ustilago maydis*. The Handbook of Genetics (ed.R.C. King), R.C. King, ed (New York: Plenum Pess.

Holthuis, J.C., Nichols, B.J., and Pelham, H.R. (1998). The syntaxin Tlg1p mediates trafficking of chitin synthase III to polarized growth sites in yeast. Mol Biol Cell **9,** 3383-3397.

Hopkins, C.R. (1983). Intracellular routing of transferrin and transferrin receptors in epidermoid carcinoma A431 cells. Cell **35,** 321-330.

Huckaba, T.M., Gay, A.C., Pantalena, L.F., Yang, H.C., and Pon, L.A. (2004). Live cell imaging of the assembly, disassembly, and actin cable-dependent movement of endosomes and actin patches in the budding yeast, *Saccharomyces cerevisiae*. J Cell Biol **167,** 519-530.

Jahn, R., and Sudhof, T.C. (1999). Membrane fusion and exocytosis. Annu Rev Biochem **68,** 863-911.

Jedd, G., Mulholland, J., and Segev, N. (1997). Two new Ypt GTPases are required for exit from the yeast trans-Golgi compartment. J Cell Biol **137,** 563-580.

Jenness, D.D., and Spatrick, P. (1986). Down regulation of the alpha-factor pheromone receptor in *S. cerevisiae*. Cell **46,** 345-353.

Jiansong Xie, L.Q., Yanru Wang, Chadron M. Rose, Tao Yang, Tamako Nakamura, Sarah F. Hamm-Alvarez, Austin K. Mircheff,. (2004). Novel biphasic traffic of endocytosed EGF to recycling and degradative compartments in lacrimal gland acinar cells. Journal of Cellular Physiology **199,** 108-125.

Kahmann, R., and Kämper, J. (2004). *Ustilago maydis*: how its biology relates to pathogenic development. New Phytologist **164,** 31-42.

Kaksonen, M., Sun, Y., and Drubin, D.G. (2003). A pathway for association of receptors, adaptors, and actin during endocytic internalization. Cell **115,** 475-487.

Kämper, J., Kahmann, R., Bölker, M., L-J., M., Saville, B., Banuett, F., Kronstadt, J.W., Gold, S.E., and others, a. (in preparation). Living in pretend harmony: the genome of the biotrophic fungus *Ustilago maydis*.

Katzmann, D.J., Odorizzi, G., and Emr, S.D. (2002). Receptor downregulation and multivesicular-body sorting. Nat Rev Mol Cell Biol **3,** 893-905.

Kelm, K.B., Huyer, G., Huang, J.C., and Michaelis, S. (2004). The internalization of yeast Ste6p follows an ordered series of events involving phosphorylation, ubiquitination, recognition and endocytosis. Traffic **5,** 165-180.

Kubler, E., and Riezman, H. (1993). Actin and fimbrin are required for the internalization step of endocytosis in yeast. Embo J **12,** 2855-2862.

Kumar, S., Tamura, K., Jakobsen, I.B., and Nei, M. (2001). MEGA2: molecular evolutionary genetics analysis software. Bioinformatics **17,** 1244-1245.

Lakadamyali, M., Rust, M.J., and Zhuang, X. (2006). Ligands for clathrin-mediated endocytosis are differentially sorted into distinct populations of early endosomes. Cell **124,** 997-1009.

Lenz, J.H., Schuchardt, I., Straube, A., and Steinberg, G. (2006). A dynein loading zone for retrograde endosome motility at microtubule plus-ends. Embo J **25,** 2275-2286.

Lombardi, D., Soldati, T., Riederer, M.A., Goda, Y., Zerial, M., and Pfeffer, S.R. (1993). Rab9 functions in transport between late endosomes and the trans Golgi network. Embo J **12,** 677-682.

Losko, S., Kopp, F., Kranz, A., and Kölling, R. (2001). Uptake of the ATP-binding cassette (ABC) transporter Ste6 into the yeast vacuole is blocked in the doa4 Mutant. Mol Biol Cell **12,** 1047-1059.

Mallet, W.G., and Maxfield, F.R. (1999). Chimeric forms of furin and TGN38 are transported with the plasma membrane in the trans-Golgi network via distinct endosomal pathways. J Cell Biol **146,** 345-359.

Maxfield, F.R., and McGraw, T.E. (2004). Endocytic recycling. Nat Rev Mol Cell Biol **5,** 121-132.

Mellman, I. (1996). Endocytosis and molecular sorting. Annu Rev Cell Dev Biol **12,** 575-625.

Miaczynska, M., Christoforidis, S., Giner, A., Shevchenko, A., Uttenweiler-Joseph, S., Habermann, B., Wilm, M., Parton, R.G., and Zerial, M. (2004). APPL proteins link Rab5 to nuclear signal transduction via an endosomal compartment. Cell **116,** 445-456.

Mohrmann, K., and van der Sluijs, P. (1999). Regulation of membrane transport through the endocytic pathway by rabGTPases. Mol Membr Biol **16,** 81-87.

Mukherjee, S., Ghosh, R.N., and Maxfield, F.R. (1997). Endocytosis. Physiol Rev **77,** 759-803.

Mulholland, J., Konopka, J., Singer-Kruger, B., Zerial, M., and Botstein, D. (1999). Visualization of receptor-mediated endocytosis in yeast. Mol Biol Cell **10,** 799-817.

Munn, A.L. (2000). The yeast endocytic membrane transport system. Microsc Res Tech **51,** 547-562.

Nielsen, E., Severin, F., Backer, J.M., Hyman, A.A., and Zerial, M. (1999). Rab5 regulates motility of early endosomes on microtubules. Nat Cell Biol **1,** 376-382.

Niggli, V. (2005). Regulation of protein activities by phosphoinositide phosphates. Annu Rev Cell Dev Biol **21,** 57-79.

Oda, H., Stockert, R.J., Collins, C., Wang, H., Novikoff, P.M., Satir, P., and Wolkoff, A.W. (1995). Interaction of the microtubule cytoskeleton with endocytic vesicles and cytoplasmic dynein in cultured rat hepatocytes. J Biol Chem **270,** 15242-15249.

Ovecka, M., Lang, I., Baluska, F., Ismail, A., Illes, P., and Lichtscheidl, I.K. (2005). Endocytosis and vesicle trafficking during tip growth of root hairs. Protoplasma **226,** 39-54.

Pelham, H.R. (2002). Insights from yeast endosomes. Curr Opin Cell Biol **14,** 454-462.

Penalva, M.A. (2005). Tracing the endocytic pathway of Aspergillus nidulans with FM4-64. Fungal Genet Biol **42,** 963-975.

Pfeffer, S.R. (2001). Rab GTPases: specifying and deciphering organelle identity and function. Trends Cell Biol **11,** 487-491.

Prescianotto-Baschong, C., and Riezman, H. (1998). Morphology of the yeast endocytic pathway. Mol Biol Cell **9,** 173-189.

Read, N.D., and Kalkman, E.R. (2003). Does endocytosis occur in fungal hyphae? Fungal Genet Biol **39,** 199-203.

Reinhard, M.O. (1892). Das Wachstum der Pilzhyphen. Jahrb. Wiss. Bot. **23,** 479-566.

Riederer, M.A., Soldati, T., Shapiro, A.D., Lin, J., and Pfeffer, S.R. (1994). Lysosome biogenesis requires Rab9 function and receptor recycling from endosomes to the trans-Golgi network. J Cell Biol **125,** 573-582.

Rink, J., Ghigo, E., Kalaidzidis, Y., and Zerial, M. (2005). Rab conversion as a mechanism of progression from early to late endosomes. Cell **122,** 735-749.

Robin, J., Arffa, R., Avni, I., and Rao, N. (1986). Rapid visualization of three common fungi using fluorescein-conjugated lectins. Invest. Ophthalmol. Vis. Sci. **27,** 500-506.

Robinson, J.S., Klionsky, D.J., Banta, L.M., and Emr, S.D. (1988). Protein sorting in Saccharomyces cerevisiae: isolation of mutants defective in the delivery and processing of multiple vacuolar hydrolases. Mol Cell Biol **8,** 4936-4948.

Rohrer, J., Benedetti, H., Zanolari, B., and Riezman, H. (1993). Identification of a novel sequence mediating regulated endocytosis of the G protein-coupled alpha-pheromone receptor in yeast. Mol Biol Cell **4,** 511-521.

Roth, A.F., and Davis, N.G. (1996). Ubiquitination of the yeast a-factor receptor. J Cell Biol **134,** 661-674.

Roth, A.F., and Davis, N.G. (2000). Ubiquitination of the PEST-like endocytosis signal of the yeast a-factor receptor. J Biol Chem **275,** 8143-8153.

Roth, A.F., Sullivan, D.M., and Davis, N.G. (1998). A large PEST-like sequence directs the ubiquitination, endocytosis, and vacuolar degradation of the yeast a-factor receptor. J Cell Biol **142,** 949-961.

Rothman, J.E. (1994). Mechanisms of intracellular protein transport. Nature **372,** 55-63.

Sambrooke, J., Fritsch, E.F., and Maniatis, T. (1989). Molecular Cloning: A Laboratory Manual (Plainview, NY: Cold Spring Harbor Lab. Press.

Sato, T.K., Darsow, T., and Emr, S.D. (1998). Vam7p, a SNAP-25-like molecule, and Vam3p, a syntaxin homolog, function together in yeast vacuolar protein trafficking. Mol Cell Biol **18,** 5308-5319.

Schmitz, C., Kinner, A., and Kolling, R. (2005). The deubiquitinating enzyme Ubp1 affects sorting of the ATP-binding cassette-transporter Ste6 in the endocytic pathway. Mol Biol Cell **16,** 1319-1329.

Schulz, B., Banuett, F., Dahl, M., Schlesinger, R., Schafer, W., Martin, T., Herskowitz, I., and Kahmann, R. (1990). The b alleles of *U. maydis*, whose combinations program pathogenic development, code for polypeptides containing a homeodomain-related motif. Cell **60,** 295-306.

Sheff, D.R., Daro, E.A., Hull, M., and Mellman, I. (1999). The receptor recycling pathway contains two distinct populations of early endosomes with different sorting functions. J Cell Biol **145,** 123-139.

Sikorski, R.S., and Hieter, P. (1989). A system of shuttle vectors and yeast host strains designed for efficient manipulation of DNA in Saccharomyces cerevisiae. Genetics **122,** 19-27.

Singer-Krüger, B., Stenmark, H., Dusterhoft, A., Philippsen, P., Yoo, J.S., Gallwitz, D., and Zerial, M. (1994). Role of three rab5-like GTPases, Ypt51p, Ypt52p, and Ypt53p, in the endocytic and vacuolar protein sorting pathways of yeast. J Cell Biol **125,** 283-298.

Snetselaar, K.M., Bölker, M., and Kahmann, R. (1996). *Ustilago maydis* Mating Hyphae Orient Their Growth toward Pheromone Sources. Fungal Genet Biol **20,** 299-312.

Somsel Rodman, J., and Wandinger-Ness, A. (2000). Rab GTPases coordinate endocytosis. J Cell Sci **113 Pt 2,** 183-192.

Sönnichsen, B., De Renzis, S., Nielsen, E., Rietdorf, J., and Zerial, M. (2000). Distinct membrane domains on endosomes in the recycling pathway visualized by multicolor imaging of Rab4, Rab5, and Rab11. J Cell Biol **149,** 901-914.

Sorkin, A., and Von Zastrow, M. (2002). Signal transduction and endocytosis: close encounters of many kinds. Nat Rev Mol Cell Biol **3,** 600-614.

Southern, E.M. (1975). Detection of specific sequences among DNA fragments separated by gel electrophoresis. J Mol Biol **98,** 501-517.

Spellig, T., Bottin, A., and Kahmann, R. (1996). Green fluorescent protein (GFP) as a new vital marker in the phytopathogenic fungus *Ustilago maydis*. Mol Gen Genet **252,** 503-509.

Spellig, T., Bölker, M., Lottspeich, F., Frank, R.W., and Kahmann, R. (1994). Pheromones trigger filamentous growth in *Ustilago maydis*. Embo J **13,** 1620-1627.

Steinberg, G., Wedlich-Söldner, R., Brill, M., and Schulz, I. (2001). Microtubules in the fungal pathogen *Ustilago maydis* are highly dynamic and determine cell polarity. J Cell Sci **114,** 609-622.

Steinberg, G., Schliwa, M., Lehmler, C., Bolker, M., Kahmann, R., and McIntosh, J.R. (1998). Kinesin from the plant pathogenic fungus *Ustilago maydis* is involved in vacuole formation and cytoplasmic migration. J Cell Sci **111 (Pt 15),** 2235-2246.

Stenmark, H., Aasland, R., and Driscoll, P.C. (2002). The phosphatidylinositol 3-phosphate-binding FYVE finger. FEBS Lett **513,** 77-84.

Straube, A., Hause, G., Fink, G., and Steinberg, G. (2006). Conventional kinesin mediates microtubule-microtubule interactions in vivo. Mol Biol Cell **17,** 907-916.

Sutton, R.B., Fasshauer, D., Jahn, R., and Brunger, A.T. (1998). Crystal structure of a SNARE complex involved in synaptic exocytosis at 2.4 A resolution. Nature **395,** 347-353.

Szabo, Z., Tonnis, M., Kessler, H., and Feldbrugge, M. (2002). Structure-function analysis of lipopeptide pheromones from the plant pathogen *Ustilago maydis*. Mol Genet Genomics **268,** 362-370.

Thompson, J.D., Gibson, T.J., Plewniak, F., Jeanmougin, F., and Higgins, D.G. (1997). The CLUSTAL_X windows interface: flexible strategies for multiple sequence alignment aided by quality analysis tools. Nucleic Acids Res **25,** 4876-4882.

Torralba, S., and Heath, I.B. (2002). Analysis of three separate probes suggests the absence of endocytosis in *Neurospora crassa* hyphae. Fungal Genet Biol **37,** 221-232.

Toshima, J.Y., Toshima, J., Kaksonen, M., Martin, A.C., King, D.S., and Drubin, D.G. (2006). Spatial dynamics of receptor-mediated endocytic trafficking in

budding yeast revealed by using fluorescent alpha-factor derivatives. Proc Natl Acad Sci U S A **103,** 5793-5798.

Tsukuda, T., Carleton, S., Fotheringham, S., and Holloman, W.K. (1988). Isolation and characterization of an autonomously replicating sequence from Ustilago maydis. Mol Cell Biol **8,** 3703-3709.

Ungermann, C., and Wickner, W. (1998). Vam7p, a vacuolar SNAP-25 homolog, is required for SNARE complex integrity and vacuole docking and fusion. Embo J **17,** 3269-3276.

Urban, M., Kahmann, R., and Bölker, M. (1996a). Identification of the pheromone response element in *Ustilago maydis*. Mol Gen Genet **251,** 31-37.

Urban, M., Kahmann, R., and Bölker, M. (1996b). The biallelic a mating type locus of *Ustilago maydis*: remnants of an additional pheromone gene indicate evolution from a multiallelic ancestor. Mol Gen Genet **250,** 414-420.

Van Der Sluijs, P., Hull, M., Zahraoui, A., Tavitian, A., Goud, B., and Mellman, I. (1991). The small GTP-binding protein rab4 is associated with early endosomes. Proc Natl Acad Sci U S A **88,** 6313-6317.

van der Sluijs, P., Hull, M., Webster, P., Male, P., Goud, B., and Mellman, I. (1992). The small GTP-binding protein rab4 controls an early sorting event on the endocytic pathway. Cell **70,** 729-740.

Vetter, I.R., and Wittinghofer, A. (2001). The guanine nucleotide-binding switch in three dimensions. Science **294,** 1299-1304.

Vida, T.A., and Emr, S.D. (1995). A new vital stain for visualizing vacuolar membrane dynamics and endocytosis in yeast. J Cell Biol **128,** 779-792.

Voigt, B., Timmers, A.C., Samaj, J., Hlavacka, A., Ueda, T., Preuss, M., Nielsen, E., Mathur, J., Emans, N., Stenmark, H., Nakano, A., Baluska, F., and Menzel, D. (2005). Actin-based motility of endosomes is linked to the polar tip growth of root hairs. Eur J Cell Biol **84,** 609-621.

von Zastrow, M., and Kobilka, B. (1992). Ligand-regulated internalization and recycling of human beta 2- adrenergic receptors between the plasma membrane and endosomes containing transferrin receptors. J. Biol. Chem. **267,** 3530-3538.

Wada, Y., and Anraku, Y. (1992). Genes for directing vacuolar morphogenesis in Saccharomyces cerevisiae. II. VAM7, a gene for regulating morphogenic assembly of the vacuoles. J Biol Chem **267,** 18671-18675.

Walther, T.C., Brickner, J.H., Aguilar, P.S., Bernales, S., Pantoja, C., and Walter, P. (2006). Eisosomes mark static sites of endocytosis. Nature **439,** 998-1003.

Weber, I., Gruber, C., and Steinberg, G. (2003). A class-V myosin required for mating, hyphal growth, and pathogenicity in the dimorphic plant pathogen *Ustilago maydis*. Plant Cell **15,** 2826-2842.

Weber, I., Assmann, D., Thines, E., and Steinberg, G. (2006). Polar localizing class V myosin chitin synthases are essential during early plant infection in the plant pathogenic fungus Ustilago maydis. Plant Cell **18,** 225-242.

Wedlich-Söldner, R., Bölker, M., Kahmann, R., and Steinberg, G. (2000). A putative endosomal t-SNARE links exo- and endocytosis in the phytopathogenic fungus *Ustilago maydis*. Embo J **19,** 1974-1986.

Wedlich-Söldner, R., Straube, A., Friedrich, M.W., and Steinberg, G. (2002). A balance of KIF1A-like kinesin and dynein organizes early endosomes in the fungus *Ustilago maydis*. Embo J **21,** 2946-2957.

Weinzierl, G. (2001). Isolierung und Charakterisierung der B- vermittelten Regulationskaskade in Ustilago maydis. PhD dissertation. (Philipps University, Marburg, Germany).

Wessels, J.G.H. (1986). Cell wall synthesis in apical hyphal growth. Int. Rev. Cytol. **104,** 387-413.

White, J.M., and Rose, M.D. (2001). Yeast mating: Getting close to membrane merger. Current Biology **11,** R16-R20.

Wiederkehr, A., Avaro, S., Prescianotto-Baschong, C., Haguenauer-Tsapis, R., and Riezman, H. (2000). The F-box protein Rcy1p is involved in endocytic membrane traffic and recycling out of an early endosome in *Saccharomyces cerevisiae*. J Cell Biol **149,** 397-410.

Wilcke, M., Johannes, L., Galli, T., Mayau, V., Goud, B., and Salamero, J. (2000). Rab11 regulates the compartmentalization of early endosomes required for efficient transport from early endosomes to the trans-golgi network. J Cell Biol **151,** 1207-1220.

Wu, J.Q., Bahler, J., and Pringle, J.R. (2001). Roles of a fimbrin and an alpha-actinin-like protein in fission yeast cell polarization and cytokinesis. Mol Biol Cell **12,** 1061-1077.

Yamashiro, D.J., Tycko, B., Fluss, S.R., and Maxfield, F.R. (1984). Segregation of transferrin to a mildly acidic (pH 6.5) para-Golgi compartment in the recycling pathway. Cell **37,** 789-800.

Ziman, M., Chuang, J.S., and Schekman, R.W. (1996). Chs1p and Chs3p, two proteins involved in chitin synthesis, populate a compartment of the Saccharomyces cerevisiae endocytic pathway. Mol Biol Cell **7,** 1909-1919.

Ziman, M., Chuang, J.S., Tsung, M., Hamamoto, S., and Schekman, R. (1998). Chs6p-dependent anterograde transport of Chs3p from the chitosome to the plasma membrane in Saccharomyces cerevisiae. Mol Biol Cell **9,** 1565-1576.

Acknowledgments

Zuerst möchte ich mich bei Gero bedanken, der mich durch drei spannende Jahre Zellbiologie geleitet hat. Danke für alle Herausforderungen und die vielfältige Unterstützung zugleich; danke für konstruktive Diskussionen, gute Gespräche und die Begleitung meines Weges.

Regine Kahmann möchte ich ganz besonders danken, dass sie im Frühjahr 2003 in Asilomar die Grundsteine für die Arbeit hier am Institut gelegt hat. Vielen Dank für alle Unterstützung seitdem und die Bereitschaft meiner Prüfungskommission anzugehören.

Ich danke Michael Bölker für viele gute und konstruktive Diskussionen und Ideen, die meine Arbeit befruchtet und begleitet haben. Herzlichen Dank auch für das Zweitgutachten.

Frau Renkawitz-Pohl danke ich für die Bereitschaft, meiner Prüfungskommission anzugehören.

Für die gute Zeit in der Research School und so manches liebe Wort bedanke ich mich sehr herzlich bei Juliane.

Gerd Hause danke ich für die elektronenmikroskopische Auswertung des Yup1 Phänotyps und die angenehmen Arbeitsaufenthalte in Halle.

Allen Mitgliedern des Cytolabs sei für die gute Zusammenarbeit gedankt, es hat unheimlich viel Spaß gemacht mit Euch! Für wen soll ich jetzt Kuchen backen?

Dani und Petra gilt ein besonderer Dank für die technische Unterstützung. Isabel danke ich, dass sie immer ein offenes Ohr hat, für Laborfragen, Kino- und Musikkritik, einfach privat und generell. Danke auch für Rab5&Co. Uli, danke ich für Diskussion und Gespräch und Zeit neben dem Labor - weitermachen. Ein großes Dankeschön an Gero II für die Musik, die guten Rezepte und die geschichtlichen Anstöße. Für die gute Box-Nachbarschaft danke ich Jan Heiko und Lea. Den „alten Hasen“ Anne und Isabelle sei gedankt, dass sie mir so einen guten Start im Labor vermittelt haben.

Für das „Sorgen und Freuden“ teilen zwischen den alltäglichen Aufgaben war ich immer sehr froh; danke Kathrin, die Zusammenarbeit an der Lyophille bleibt unvergessen.

Meinen Praktikanten Rolf und Martin danke ich für die Hilfe beim Rab4 Projekt.

Für Diskussion und Unterstützung möchte ich mich bei Doris, Mauri, Thomas, Philip Müller, Kerstin, Kathi, Stefan Brückner und allen anderen Mitgliedern der Basse, Feldbrügge Kahmann, Kämper, Mösch und Schirawski Labs bedanken, Ramon, danke für das Teilen der Phytokammer!

Meinen „Doktorandenvertreter Kollegen“ Henning und Holger - danke für eine gute Zusammenarbeit.

Vor allem danke ich meiner Familie und meinen Freunden dass, sie in der Nähe und in der Ferne an mich geglaubt und mich unterstützt haben. Volle Kraft voraus – Stephan.

Curriculum vitae

Personal information	Uta Fuchs born May 17, 1979 in Radebeul, Germany
Education	1985- 1991 Primary school Radebeul 1991- 1997 Gymnasium Luisenstift Radebeul 07/1997 “Allgemeine Hochschulreife“
University studies	1997- 2001 University of Applied Sciences Dresden (FH), Germany Diploma thesis: “Virus detection in strawberries.” M. Geibel and R. Drewes-Alvares, advisors 07/2001 Diploma in Horticulture 2001- 2003 University of Delaware, DE, USA Masters thesis: “Five Hydrophobin Genes in *Fusarium verticillioides*.“ J. A. Sweigard and T.A. Evans, advisors 07/2003 MSc. Plant Science
Dissertation	2003- 2006 PhD thesis at the Max- Planck- Institute for terrestrial Microbiology Marburg, Germany Thesis Topic: “The role of endocytosis for pathogenic development of the corn smut fungus *Ustilago maydis*.” G. Steinberg, advisor